

Report
on
Climate Change Impact Assessment for
Jayakwadi Project

Study Team

B. Venkatesh, Scientist F
M.K. Jose, Scientist E
P.C.Nayak, Scientist E
S. Chandrakumar, SRA
R. Abhilash, Research Scientist



Hard Rock Regional Centre
National Institute of Hydrology
Belgaum

1.0 INTRODUCTION

The availability of freshwater resources is pivotal in daily life, as it is used to feed populations, to drive local and global economies, and to sustain terrestrial and aquatic habitats. Although water is abundant globally, much of it is not directly available for human use nor environmental needs. Freshwater resources are not evenly distributed across the globe, and the supply of freshwater can vary highly over time. Often, those areas that have a large number of economic activities or dense populations do not coincide geographically with those that are rich in freshwater resources. Despite the fact that only 10% of freshwater resources available globally are utilized, many regions are currently experiencing water scarcity; these regions are home to more than one-third of the global population (Wada et al., 2011). Climate change and socioeconomic developments are expected to increase the pressure on freshwater resources regionally and to aggravate and increase water scarcity globally (Wada et al., 2014b). The impacts of water scarcity are numerous and include crop failures, food shortages and famines, economic losses as a result of the disruption of business activities, and the degradation of terrestrial and aquatic ecosystems. This makes water scarcity one of the three global risks that are of the highest concern, and it is expected that water scarcity will be one of the most pressing global issues in the near future, both in terms of its likelihood of occurrence and impact (World Economic Forum, 2016). Therefore, in order to address water scarcity, there is an urgent need to develop effective adaptation strategies (Wada et al., 2014b). To make sound decisions, however, water managers must have insight into the factors that determine the occurrence and severity of water scarcity at both the global and regional scales (Hallegatte, 2009). They also need to comprehend the forces and mechanisms that drive water scarcity and its effects. In order to gain this insight, it is important to develop an understanding of the ability of global models to represent historical and future availability of freshwater resources and water scarcity, as well as how uncertain water scarcity estimates can be, given the broad range of possible future conditions (Bierkens, 2015).

India has experienced several devastating climate extremes during recent decades. For instance, the drought of 2016 covered about 10 states and affected about 330 million people, causing an economic loss of \$100 billion (ASSOCHAM Report 2016). Agriculture in India feeds about 17.2%

of the global population using only about 9% of the world's arable land, and more than 56% of the total agricultural area is rainfed (Rathore et al. 2014). Arable lands [1.8×10^6 km² (180 Mha)] span temperate, tropical, and subtropical climates. In India, a vast country with multifaceted geography, the effects of climate change on water resources differ substantially among different regions and river basins and cannot be generalized. Reliance on historical climate conditions will no longer be tenable since climate change generates conditions well outside past parameters for current and future planning.

The State of Maharashtra, where the agriculture is the main occupation of the rural communities and are dependent on the additional irrigation water from the reservoirs. Over last few decades, the reservoirs are receiving the designed yield due to various reasons. The same is the observation even for dams in Godavari river basin.

The Jayakwadi project is one of the largest irrigation projects in the state of Maharashtra. It is a multipurpose project. The water is mainly used to irrigate agricultural land in the drought-prone Marathwada region of the state. Other important purpose was to provide water for drinking and industrial usage to nearby towns and villages and to the municipalities and industrial areas of Aurangabad and Jalna. The 80% of water of dam is meant for irrigation, 5-7% for drinking water and the rest for industrial purposes. A numerous medium and large dams came up on the River Godavari upstream of Jayakwadi dam in last 2-3 decades. These dams are intercepting the flows leading to lower yield at Jayakwadi reservoir. Over the years, it is observed that, the reservoir is not getting adequate amount of water to cater to its planned uses. These factors coupled with the threat of the impending climate change may worsen the situation in the area. Under this background it is necessary to carryout an investigation to understand the impact of these changes on water availability at Jayakwadi reservoir.

It is therefore imperative that a comprehensive analysis be carried out for assessment of impact of climate change and water storage structure on the water availability at Jayakwadi reservoir. This analysis will be carried out using the present database and also investigate the future scenario under climate change for the development of appropriate mitigation and adaptation measures. Keeping in view of these issues, the study was initiated with the following objectives;

1. Evaluate the possible change in water availability and extreme hydrological events due to climate change upto yr. 2100 in Jayakwadi catchment using a river basin hydrological model:
2. Assessment of influence of anthropogenic intervention (construction of small and medium irrigation structure and diversion weirs) on water availability at various project in the Jayakwadi catchment

To achieve these objectives, it is proposed to carryout the following ;

1. Based on the climate change projections for the future, an investigation is necessary to detect the possibilities of climate change signals based on the observed historical datasets on weather and precipitation to understand the spatio-temporal water availability in the catchment. This is more necessary as no previous studies exist on this aspect exclusively for the study area and this objective will provide answers to the un-answered questions of possible climate change signals and its impact on water availability in the catchment.
2. As it has been reported that the construction of small and medium projects in the catchment area is influencing the reduced inflows into reservoir. There are no analysis carried out how each of these reservoirs are contributing to the reduction in the flow at reservoir or is there is any other mechanism which is responsible for the reduction. In addition to these factor, how climate change will affect the water availability at all these structures. There are no comprehensive analysis done to assess these aspects in the Jayakwadi catchment. Therefore, the analysis will provide an answer for this.

2.0 STUDY AREA

The Godavari basin is the second largest river basin of India (30.2 million ha) and partly covers six states viz., Maharashtra, Andhra Pradesh, Chhattisgarh, Madhya Pradesh, Odisha, and Karnataka. About 49% of Maharashtra's geographical area (15.26 million ha) comes under Godavari basin. In Maharashtra, the Godavari basin is divided into 27 sub-basins. The Upper Godavari sub-basin has a geographical area of 2.2 million ha and about 8.6 million population lives in 45 towns and 1883 villages. The sub-basin comprises the entire catchment of the Godavari river from its source to Jayakwadi dam including the catchment areas of the rivers Mula, Pravara and all other tributaries which joins the Godavari river in this reach. There are 17 major, 14 medium, and 558 small irrigation projects in the sub-basin with design live storage capacity of 193.5 TMC. The location of Jayakwadi basin is shown in **Figure 1**.

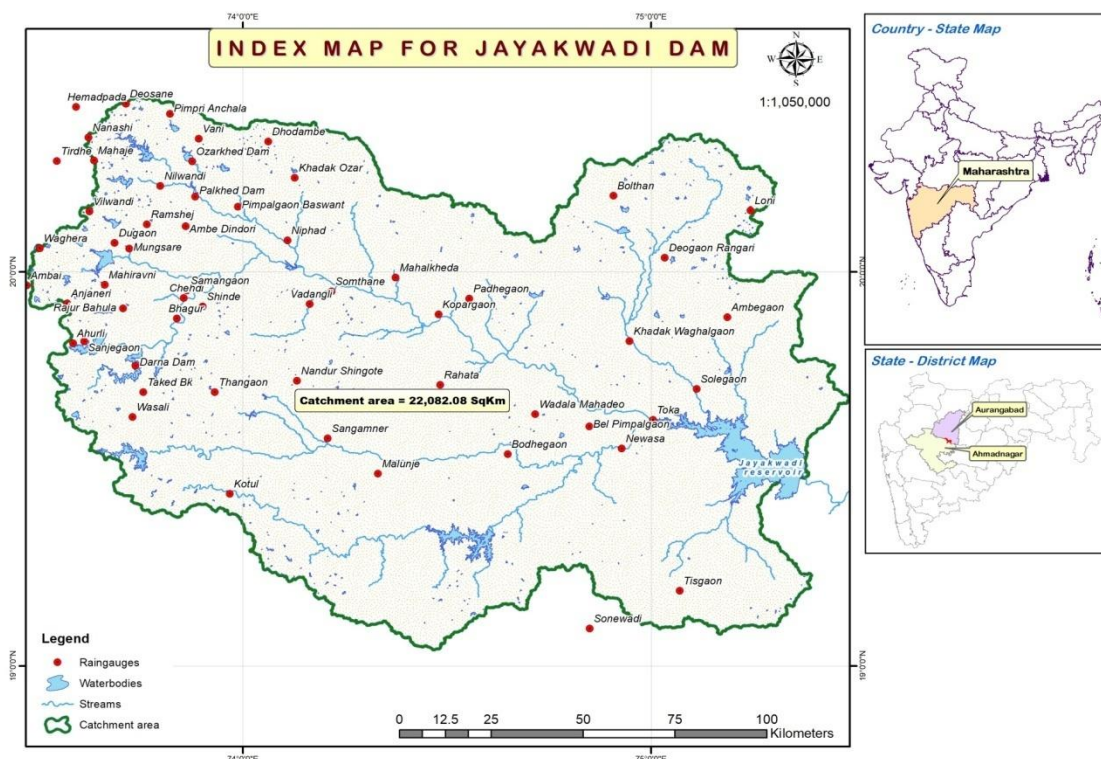


Figure 1. Location of Jayakwadi basin in Maharashtra state

The Jayakwadi irrigation project was planned in 1964 and commissioned in 1975. The designed

live storage capacity of the reservoir is 76.63 TMC and was planned to irrigate about 0.26 million ha in Marathwada region. However, since 1975 the Jayakwadi reservoir was filled to its design capacity only in 8 years. The Water Resources Department (WRD) in 2004 carried out a study to assess the sub-basin yield based on the latest hydro-meteorological data. **Table 1** shows the comparison of the virgin yield and utilization in the upstream dams as per the original planning and the revised study.

Table1. Comparison of the virgin yield and upstream utilization in the Upper Godavari sub basin as per the planning and the revised study (Kulkarni, 2016)

Parameter	As per project report (1964)	As per revised study by WRD (2004)
Annual 75% dependable virgin yield at the Jayakwadi dam (TMC)	196.56	157.155
Utilization at the upstream of Jayakwadi dam(TMC)	115.48	143.84

2.1 Data Availability

The Water Resources Department, Govt. of Maharashtra, Nashik has been monitoring and maintain a good the hydro-meteorological network in the basin (**Figure 2**). The data pertaining to this study was provided by the WRD, Nashik after validating the data using the HYMOS software. The data collected are; (i) Rainfall; (ii) Temperature; and (iii) Discharge.

Rainfall Data : There are more than 80 raingagues are installed and are being used for measurement of rainfall in the catchment. However, few stations have less than 10 years of data which are not considered for the analysis. The stations for which the longer duration data available are listed in the **Table 2 and Figure 1**. In addition to this, the rainfall and temperature data for the IMD grids (total of 47 no's grids) were obtained from the IMD and have been Tabulated in **Table 3**, which were used for analysis as well.

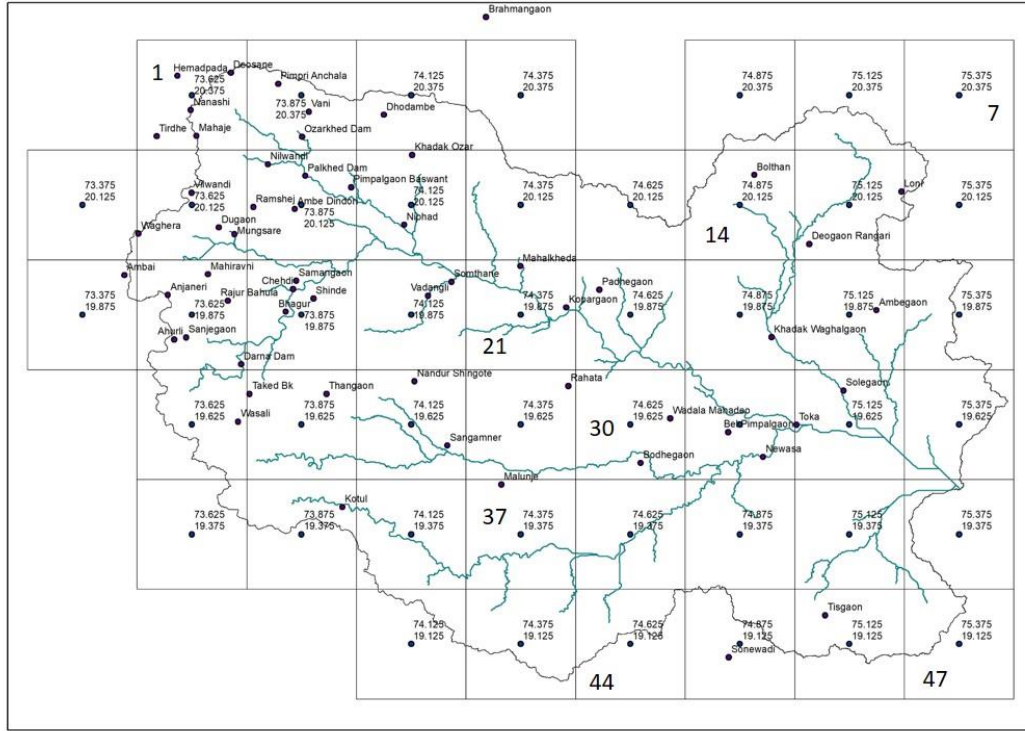


Figure 2: Layout of IMD Grid (@ 0.25° by 0.25°) in the Jayakwadi catchment with Number of Grids

Table 2: List of Rain gauge stations and the data length used for the study.

SI No	Station Name	Data Length
1	Dongarpada	1976-2016
2	Dhodambe	1976-2016
3	Deosane	1976-2016
4	Dahegaon	1976-2016
5	Chehdi	2004-2016
6	Brahmingaon	1976-2016
7	Bolthan	1976-2016
8	Ambe Dindori	1976-2016
9	Tridhe	2004-2016
10	Ranjangaon	2004-2016
11	Bel Pimpalgaon	1976-2016
12	Wadala Mahadeo	1976-2016
13	Toka	1976-2016
14	Thangaon	1976-2016
15	Rahata	1976-2016
16	Nandur Shingote	1976-2016
17	Kotul	1976-2016
18	Bhojapur	1976-2016
19	Bhavarwadi	1976-2016
20	Bhagur	1976-2016
21	Panegaon	1976-2016
22	Adhala	1976-2016
23	Padhegaon	1976-2016
24	Samangaon	1976-2016
25	Deogaon Rangari	1976-2016
26	Loni	1976-2016
27	Solegaon	1990-2016
28	Pimpalgaon Baswant (DK)	1976-2016
29	Niphad	1976-2016
30	Anjaneri	1976-2016
31	Ambai	1976-2016
32	Wasali	1997-2016
33	Taked Bk	2004-2016

34	Sanjegaon	1976-2016
35	Nanashi	1976-2016
36	Kusegaon	1976-2016
37	Indore	1976-2016
38	Aswali	1976-2016
39	Ahurli	1976-2016
40	Waghera	1976-2016
41	Vilwandi	2004-2016
42	Vani	2004-2016
43	Vadangli	2004-2016
44	Sonewadi	2004-2016
45	Somthane	1976-2016
46	Ramshej	1976-2016
47	Rajur Bahula	1976-2016
48	Palkhed Dam	2006-2016
49	Ozarkhed Dam	2004-2016
50	Nilwandi	2004-2016
51	Nalwadi	2004-2016
52	Mungsare	2004-2016
53	Mahalkheda	1976-2016
54	Khadak Ozar	1976-2015
55	Karanjkhed	1976-2016
56	Ganeshgaon	1976-2016
57	Dugaon	1976-2016
58	Deogaon	1976-2016
59	Hivarkheda	1976-2016
60	Dhondlagaon	1976-2016
61	Borvat	1976-2016
62	Phulambri	1976-2016
63	Kalanki	1976-2016
64	Kadakwada	1976-2016
65	Manjur	1976-2016
66	Mahaldevi	1976-2016
67	Nagamthan	1976-2016
68	Amblihol	1976-2016
69	Charose	1976-2016
70	Bhawali (BK)	1995-2016
71	Pishor	1976-2016
72	Kirdishate	1976-2016
73	KalagaonMal	1976-2016
74	Dorkin	1976-2016

75	Shendurwada	1999-2016
76	Usthale (Hedpada)	1985-2016
77	Hatnoor	1976-2016
78	Kopargaon	1976-2016
79	Pinpri Anchal	2008-2016

Table 3: The IMD Grids and the data length used for the study

Grid	Long	Lat	Station	Grid	Long	Lat	Station
1	73.625	20.375	Hemapada	21	74.375	19.875	Somthane
			Deosane				Mahalkheda
			Nanashi	22	74.625	19.875	Padhegaon
			Tirdhe				Kopargaon
			Mahaje	23	74.875	19.875	Khadak Waghalgaon
2	73.875	20.375	Pimpri Anchala	24	75.125	19.875	Ambegaon
			Vani	25	75.375	19.875	
			Ozarkhed dam	26	73.625	19.625	Wasali
3	74.125	20.375	Dhodambe	27	73.875	19.625	Taked BK
4	74.375	20.375					Thangaon
5	74.875	20.375		28	74.125	19.625	Sangamner
6	74.125	20.375					Nandur Shingote
7	75.375	20.375		29	74.375	19.625	Rahata
8	73.375	20.125		30	74.625	19.625	Wadala Mahdeo
							Bodhegaon
9	73.625	20.125	Vilwandi	31	74.875	19.625	Nawasa
			Dugaon				Pimplebaon
			Mungsare				Bel
			Waghera				32
10	73.875	20.125	Nilwandi				Solegaon
			Palkhed dam	33	75.375	19.625	
			Pimplagaon Baswant	34	73.625	19.375	
			Ramshej	35	73.875	19.375	
			Ambe Dindori	36	74.125	19.375	
11	74.125	20.125	Khadak ozar	37	74.375	19.375	Malunje
			Niphad	38	74.625	19.375	
12	74.375	20.125		39	74.875	19.375	
13	74.625	20.125		40	75.125	19.375	
14	74.875	20.125	Bolthan	41	75.375	19.375	
15	75.125	20.125	Deogaon Rangari	42	74.125	19.125	
16	75.375	20.125		43	74.375	19.125	
17	73.375	19.875	Ambai	44	74.625	19.125	
18	73.625	19.875	Anjaneri	45	74.875	19.125	Sonewadi
			Ahurli	46	75.125	19.125	Tisgaon
			Sanjegaon	47	75.375	19.125	
			Rajur Bahula	20	74.125	19.875	Vadangali
			Mahiravni				Vadangli
			Darna Dam				
19	73.875	19.875	Chahdi				
			Shinde				
			Bhagur				

Discharge : There are about Fifteen stations at which the discharge being measured at daily time scale on different streams. The data is available for varying time period. The list of discharge measuring stations along with the data length is provided in Table 4.

Table 4: List of Discharge Gauging stations and the data length used for the study.

Sl No.	Gauging Site	Stream	Catchment Area (Km ²)	Data Length
1	Bhagur			1989-2003
2	Diksal			1984-2016
3	Kopargaon			1990-2016
4	Mahaladevi			1977-2014
5	Nagmathan			1987-2016
6	Nashik			1987-2016
7	Newasa			1987-2015
8	Niphad			1988-2008
9	Panegaon			1989-2010
10	Samangaon			1990-2012
11	Sangamner			1976-2017
12	Usthale			1984-2016
13	Chass			1972-1997
14	Ghargaon			1989-2006
15	Pachegaon			1983-2015

Temperature : There are five full climatic station (FCS) are operative in the basin. The data is available for varying time period. The list of stations along with the data length is provided in Table 5. And the Temperature data from IMD Grids was also downloaded (**Table 6**)

Table 5: List of Full-climatic stations (FCS) and the data length used for the study.

Sl No.	Gauging Site	Data Length
1	Aurangabad	2003-2016
2	Bhagur	2008-2016

3	Mahaladevi	2011-2016
4	Nagmathan	2011-2016
5	Samangaon	2011-2016

3.0 OVER ALL METHODOLOGY ADOPTED

The methodology adopted shall include the following. (a) The investigation shall be carried out to detect the climate change signals in the present climate based on the historical datasets of precipitation, temperature and other climate datasets, land use, soil and topographical data; (b) A physically based distributed/semi-distributed hydrological model shall be setup for the study area based on the data availability and the objectives of the study and the model shall be calibrated and validated to understand the hydrology of the basin and the interaction between the various components of the water balance under the present climatic conditions; (c) Based on the global projections through General Circulation Models/Regional Climate models, the climate change induced impact assessment studies on the water resources sector shall be carried out under alternate future emission scenarios. The impact assessment studies will help to understand the scenario of water availability as well as extreme events like floods and drought into the future time horizons; (d) The anthropogenic intervention will be introduced into the model in the form of reservoirs and their date of operation to evaluate the actual setup at present and for the future scenarios (Figure 3).

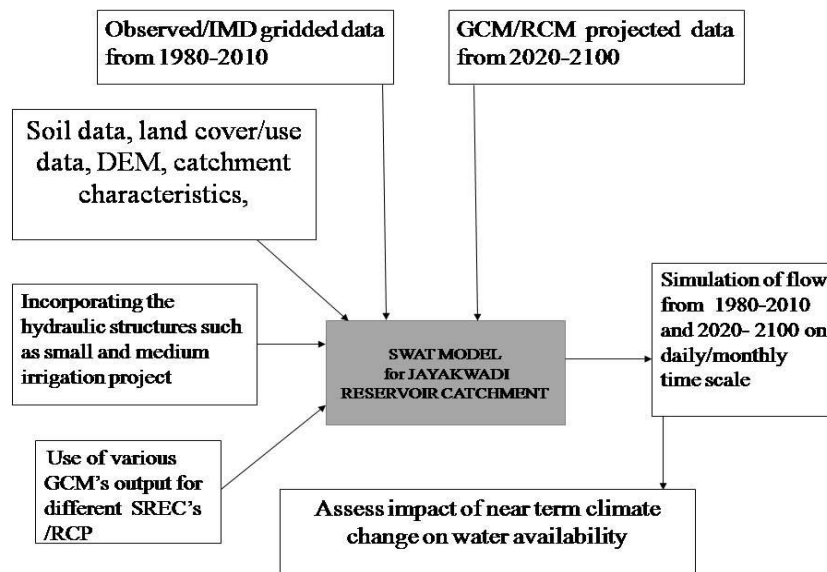


Figure 3: Schematic diagram for evaluating the impacts of climate change on inflow into Jayakwadi reservoir

In the present progress report focuses on the Data analysis such as rainfall, discharge and temperature collected from Project authorities as well as from the IMD grid data. The methodology adopted for data analysis are described in the following section;

3.1 TREND ANALYSIS

The Mann-Kendall Test (M-K test)

This M-K method tests if there is a trend in the time series data. It is a non-parametric rank based procedure, robust to the influence of extremes and suitable for application with skewed variables²⁴. More particularly, this technique can be adopted in cases with non-normally distributed data, data containing outliers and non-linear trends^{25,26}. According to this test, the null hypothesis H0 indicates that the de-seasonalised data ($X_1 \dots X_n$) is a sample of ‘n’ independent and identically distributed random variables. The alternative hypothesis is H1 of a two-sided test is that the distributions of X_k and X_j are not identical for all $K_j \leq n$ with $K \neq j$. the test statistic S is given below²⁷.

$$S = \sum_{k=1}^{n-1} \sum_{j=k+1}^n \text{sgn}(X_j - X_k) \quad (1)$$

where $\text{sgn}()$ is the signum function. The S statistic, in cases where the sample size ‘n’ is larger than 10, is assumed to be asymptotically normal, with $E(S)=0$ and

$$\text{Var}(S) = [n(n-1)(2n+5) - \sum_t t(t-1)(2t+5)]/18 \quad (2)$$

where ‘t’ refers to the extent of any given tie and \sum_t states the summation over all ties. The standard normal variate Z is computed as given below

$$Z = \begin{cases} \frac{S-1}{\sqrt{\text{Var}(S)}} & \text{if } S > 0 \\ 0 & \text{if } S = 0 \\ \frac{S+1}{\sqrt{\text{Var}(S)}} & \text{if } S < 0 \end{cases} \quad (3)$$

Therefore, in case of $|Z| \leq Z_{1-\alpha/2}$ in a two-sided test for trend, the null hypothesis H0 should be accepted at the α level of significance. A positive values of S connotes an ”upward trend”, while a negative values of S indicates a “downward trend”.

The Sen’s Estimator of Slope

This test is applied in cases the trend is assumed to be linear, depicting the quantification of change per unit time. De Lima et al(**) point out the utility of this estimator in cases there are missing values or other gaps in the data, as it remains unaffected from the outlier or gross error. The slope estimates Q_i of N pairs of data are calculated as $Q_i = (X_j - X_k)/(j - k)$ for $i = 1, \dots, N$, where X_j and X_k are data values at times j and k ($j > k$) respectively. The Sen's estimator of slope derives from the above N values of Q_i and equals to their median. When there is only one datum in each time period. Then $N = n(n-1)/2$, where 'n' corresponds to the number of time periods. The N values of slopes are ranked from the smallest to the largest and if N is odd, Sen's estimator of slope is calculated as $Q_{\text{median}} = Q_{(n-1)/2}$. On the other hand, in case that N is even, the estimator arises from $Q_{\text{median}} = [Q_{N/2} + Q_{(N+2)/2}]/2$.

3.2 TESTS FOR CHANGE POINT DETECTION

A climatic series is said to be homogeneous, if the observed variation is resulting from fluctuations in weather and climate exclusively. It is important to carry out different homogeneity tests. For example, standard normal homogeneity test (SNHT) is sensitive to change point towards the beginning and end of the data series while Buishand's and Pettitt's tests are sensitive to changes in the middle of a series.

Pettitt's Test

A number of methods can be applied to determine change point of a time series by many researcher. The pettitt's test for change detection, developed by Pettitt (1979) is a non-parametric test, which is useful for evaluating the occurrences of abrupt changes in climatic records. The pettitt's test is the most commonly used test for change point detection because of its sensitivity to breaks in the middle of any time series. The pettitt's test is a method that detects a significant change in the mean of a time series when the exact time of the change is unknown. According to Pettitt's test, if $x_1, x_2, x_3, \dots, x_n$ is the series of observed data which has a change point at t in such a way that x_1, x_2, \dots, x_t has a distribution function $F_1(x)$ which is different from the distribution function of $F_2(x)$ of the second part of the series $x_{t+1}, x_{t+2}, x_{t+3}, \dots, x_n$. The non-parametric test statistics U_t for this test may be described as below;

$$U_t = \sum_{t=1}^t \sum_{j=t+1}^n \text{sign}(x_i - x_j)$$

$$\text{sign}(x_i - x_j) = \begin{cases} 1, & \text{if } (x_i - x_j) > 0 \\ 0, & \text{if } (x_i - x_j) = 0 \\ -1, & \text{if } (x_i - x_j) < 0 \end{cases}$$

The test statistic K and the associated confidence level (ρ) for the sample length (n) may be described as;

$$K = \text{Max } |U_t|$$

$$\rho = \exp\left(\frac{-K}{n^2 + n^3}\right)$$

When ρ is smaller than the specific confidence level, the null hypothesis is rejected. The approximate significance probability (p) for a change point is defined as

$$p = 1 - \rho$$

It is obvious that where a significant change point exists, the series is segmented at the location of the change point into two subseries. The test statistic K can also be compared with the standard values at different confidence levels for detection of change point in a series.

Von Neumann Ratio Test

The adjusted partial sum (S_k), that is the cumulative deviation from mean for Kth observation of a series $x_1, x_2, x_3, \dots, x_k, \dots, x_n$ with the mean (\bar{x}) can be computed using the following equation

$$S_k = \sum_{i=1}^k (x_i - \bar{x})$$

A series may be homogeneous without any change point if $S_k \cong 0$, because in random series, the deviation from mean will be distributed on both sides of the mean of the series. The significance of shift can be evaluated by computing rescaled adjusted range \mathcal{R} using the following equation

$$R = \frac{\text{Max}(S_k) - \text{Min}(S_k)}{\bar{x}}$$

The computed value of R/\sqrt{n} is compared with the critical values given by Buishand (1982) and has been used for detection of possible changes.

Standard Normal Homogeneity (SNH) Test (Alexandersson (1986)

The test statistic (T_k) is used to compare the mean of first n observations with the mean of the remaining $(n-k)$ observations with n data point

$$T_k = kZ_1^2 + (n - k) Z_2^2$$

Where Z_1 and Z_2 computed as;

$$Z_1 = \frac{1}{k} \sum_{i=1}^k \frac{(x_i - \bar{x})}{\sigma x}$$

$$Z_2 = \frac{1}{n - k} \sum_{i=k+1}^n \frac{(x_i - \bar{x})}{\sigma x}$$

Where, (\bar{x}) and σx are the mean and standard deviation of the series. The year k can be considered as change point and consist of a break where the value of T_k attains the maximum value. To reject the null hypothesis, the test statistic should be greater than the critical values, which depends on the sample size (n).

3.3. DROUGHT ANALYSIS

The study on drought is carried out to take mitigation measure and be prepared for the impact. From the literature review observed that drought characteristics was estimated by different methods like SPI, Aridity Index, Rainfall variability Index, Regional annual Index etc. For the present study the Meteorological drought method is carried out using Station Index, Regional annual Index. The steps involved in meteorological method are

3.3.1 Rainfall variability index (δ) is calculated as

$$\delta_i = \frac{P_i - \mu}{\sigma}$$

Where δ_i is the rainfall variability index for the year i , P_i is the annual rainfall for the year, μ and σ are the mean and standard deviation of annual rainfall for the data period chosen for the study. A drought year occurs if δ_i is negative.

According to WMO (1975), rainfall time series can be classified into different climatic regimes.

$P < \mu - 2\sigma$ --- extremedry
 $\mu - 2\sigma < P < \mu - \sigma$ --- dry
 $\mu - \sigma < P < \mu + \sigma$ --- normal
 $P > \mu + \sigma$ --- wet

3.3.2 Drought Characterization

Drought intensity, duration and frequency were estimated using the conceptual model developed by Ponce et al (2000) as shown in Table 6. The conceptual approach is applicable to subtropical and mid latitude regions, and is limited to meteorological droughts lasting at least one year. In the Ponce et al (2000) methodology, the climate types, which encompass the climatic spectrum from super-arid to super-humid, are defined in terms of ratio of mean annual precipitation P_{ma} to (mean) annual global terrestrial precipitation P_{agt} . The ratio, $P_{ma}/P_{agt} = 1$ represents the middle of the climatic spectrum. This enables the division of climatic spectrum in sub-tropical and mid-latitude regions into the following eight types.

Table 6: Conceptual model of drought intensity, duration and frequency

TYPE	CLASSIFICATION
Super- arid	$P_{ma}/P_{agt} < 0.125$
Hyper-arid	$0.125 \leq P_{ma}/P_{agt} < 0.25$
Arid	$0.25 \leq P_{ma}/P_{agt} < 0.5$
Semi-arid	$0.5 \leq P_{ma}/P_{agt} < 1$
Sub-humid	$1 \leq P_{ma}/P_{agt} < 2$
Humid	$2 \leq P_{ma}/P_{agt} < 4$
Hyper-Humid	$4 \leq P_{ma}/P_{agt} < 8$
Super-Humid	$P_{ma}/P_{agt} \geq 8$

The conceptual model is also defined in terms of ratio of annual potential evapotranspiration E_{ap} to mean annual precipitation P_{ma} . The ratio $E_{ap}/P_{ma} = 2$ describes the

middle of climatic spectrum. To complement to the description, the length of rainy season L_{rs} is also indicated. The drought duration varies between 1 year at extremes of climatic spectrum and 6 year at the middle.

$$\text{Station Index (S)} = (P_{ma}-P)/P_{ma} \quad (4.2)$$

Additionally, the regional annual index RI for each year is estimated using the equation (4) which is the average of station index of all the stations during that year

$$RI = \frac{1}{N} \sum_1^N S \quad (4.3)$$

For drought events lasting more than one year, intensity is the summation of individual annual intensities. Longer drought durations are associated with higher intensities.

The dry periods (droughts) are generally followed by corresponding wet periods. Therefore recurrence interval (reciprocal of frequency) is always greater than the drought duration. Drought recurrence intervals increase from two year on the dry side of climatic spectrum (super arid) to 100 years on the wetter side (super-Humid).

For any year for which P is the annual precipitation, drought intensity is defined as the ratio of the deficit $(P_{ma}-P)$ to the mean P_{ma} . For any year an intensity of $\{(P_{ma}-P)/P_{ma}\} = 0.25$, is classified as moderate (Table II).

Classification	Type
$(P_{ma}-P)/P_{ma}=0.25$	Moderate
$(P_{ma}-P)/P_{ma}=0.50$	Severe
$(P_{ma}-P)/P_{ma}=0.75$	Extreme

4.0 DATA ANALYSIS

The Jayakwadi catchment receive majority of its rainfall during the monsoon months, i.e., June to September, July and August being the major contributing months. A well spread rainfall measurement network of more than 80 location is used for measuring the rainfall. The data of 83 stations were subjected to the preliminary statistical analysis and the results in tabulated in Table 7. The Table 7, the highest annual average rainfall is observed at Nanashi located on the catchment boundary on North-Western Part of the basin. The lowest in the central part of the catchment at Kopargoan. The Percent Standard Deviation vary from 90% at 18% in the basin.

Table 7: Basic Statistics of the observed rainfall in Jayakwadi Catchment

Sl No.	Station Name	Rainfall Statistics			Hurst Coefficient	RSD
		Length of Data	AAR	Std. Dev.		
1	Dongarpada	1976-2016	1788.20	522.29	0.48	29.21
2	Dhodambe	1976-2016	740.46	197.74	0.57	26.71
3	Deosane	1976-2016	1611.52	917.43	0.59	56.93
4	Dahegaon	1976-2016	1407.94	656.31	0.64	46.62
5	Chehdi	2004-2016	653.26	169.30	0.53	25.92
6	Brahmangaon	1976-2016	485.12	135.81	0.85	28.00
7	Bolthan	1976-2016	494.81	178.57	0.63	36.09
8	Ambe Dindori	1976-2016	468.07	189.32	0.48	40.45
9	Tridhe	2004-2016	1891.89	420.50	0.63	22.23
10	Ranjangaon	2004-2016	406.93	148.50	0.62	36.50
11	Bel Pimpalgaon	1976-2016	438.66	206.89	0.67	47.16
12	Wadala Mahadeo	1976-2016	506.88	185.37	0.66	36.57
13	Toka	1976-2016	659.53	239.53	0.55	36.32
14	Thangaon	1976-2016	584.50	212.83	0.90	36.41
15	Rahata	1976-2016	494.97	171.90	0.89	34.73
16	Nandur Shingote	1976-2016	406.00	145.45	0.76	35.83
17	Kotul	1976-2016	616.97	163.02	0.64	26.42
18	Bhojapur	1976-2016	394.24	142.63	0.73	36.18
19	Bhavarwadi	1976-2016	518.87	348.71	0.60	67.21
20	Bhagur	1976-2016	564.23	192.21	0.41	34.07
21	Panegaon	1976-2016	508.09	165.31	0.71	32.54
22	Adhala	1976-2016	431.95	154.78	0.80	35.83

23	Padhegaon	1976-2016	478.78	149.99	0.71	31.33
24	Samangaon	1976-2016	494.64	189.52	0.67	38.32
25	Deogaon Rangari	1976-2016	553.34	200.79	0.67	36.29
26	Loni	1976-2016	541.66	174.10	0.59	32.14
27	Solegaon	1990-2016	528.44	187.82	0.61	35.54
28	Pimpalgaon Baswant (DK)	1976-2016	917.76	397.81	0.51	43.35
29	Niphad	1976-2016	532.75	195.65	0.86	36.73
30	Anjaneri	1976-2016	1716.69	695.41	0.65	40.51
31	Ambai	1976-2016	2124.24	717.68	0.48	33.79
32	Wasali	1997-2016	1711.56	588.70	0.35	34.40
33	Taked Bk	2004-2016	1125.47	477.86	0.79	42.46
34	Sanjegaon	1976-2016	1681.53	708.27	0.51	42.12
35	Nanashi	1976-2016	2355.75	1244.31	0.60	52.82
36	Kusegaon	1976-2016	2122.89	749.21	0.56	35.29
37	Indore	1976-2016	1521.74	470.89	0.64	30.94
38	Aswali	1976-2016	1117.13	370.82	0.67	33.19
39	Ahurli	1976-2016	1861.78	821.03	0.67	44.10
40	Waghera	1976-2016	1613.13	615.59	0.88	38.16
41	Vilwandi	2004-2016	1596.59	467.80	0.89	29.30
42	Vani	2004-2016	1274.01	488.99	0.77	38.38
43	Vadangli	2004-2016	492.27	160.46	0.82	32.60
44	Sonewadi	2004-2016	389.61	118.97	0.83	30.54
45	Somthane	1976-2016	427.54	150.49	0.64	35.20
46	Ramshej	1976-2016	1017.46	274.67	0.70	27.00
47	Rajur Bahula	1976-2016	872.22	271.52	0.71	31.13
48	Palkhed Dam	2006-2016	537.00	284.73	0.56	53.02
49	Ozarkhed Dam	2004-2016	800.43	303.22	0.65	37.88
50	Nilwandi	2004-2016	987.92	393.81	0.67	39.86
51	Nalwadi	2004-2016	729.31	858.29	0.62	117.69
52	Mungsare	2004-2016	528.29	339.08	0.21	64.18
53	Mahalkheda	1976-2016	432.81	134.57	0.51	31.09
54	Khadak Ozar	1976-2015	426.78	177.62	0.50	41.62
55	Karanjkhed	1976-2016	1326.25	457.29	0.54	34.48
56	Ganeshgaon	1976-2016	667.85	468.47	0.55	70.15
57	Dugaon	1976-2016	441.25	159.74	0.86	36.20
58	Deogaon	1976-2016	481.43	159.39	0.68	33.11
59	Hivarkheda	1976-2016	710.16	323.21	0.82	45.51
60	Dhondlagaon	1976-2016	447.91	243.12	0.70	54.28
61	Borvat	1976-2016	1655.86	784.87	0.78	47.40
62	Phulambri	1976-2016	586.75	233.58	0.58	39.81
63	Kalanki	1976-2016	718.09	300.67	0.62	41.87
64	Kadakhwada	1976-2016	621.20	278.13	0.94	44.77

65	Manjur	1976-2016	395.16	166.34	0.72	42.10
66	Mahaldevi	1976-2016	650.24	203.65	0.58	31.32
67	Nagamthan	1976-2016	511.15	232.10	0.80	45.41
68	Amblihol	1976-2016	617.34	194.56	0.60	31.52
69	Charose	1976-2016	1495.22	466.82	0.68	31.22
70	Bhawali (BK)	1995-2016	1974.56	674.92	0.89	34.18
71	Pishor	1976-2016	616.29	244.25	0.83	39.63
72	Kirdishate	1976-2016	451.08	191.14	0.43	42.37
73	KalagaonMal	1976-2016	478.91	178.81	0.78	37.34
74	Dorkin	1976-2016	565.18	263.34	0.50	46.60
75	Shendurwada	1999-2016	542.39	180.53	0.17	33.29
76	Usthale (Hedpada)	1985-2016	1985.58	957.81	0.67	48.24
77	Hatnoor	1976-2016	608.36	180.04	0.55	29.59
78	Kopargaon	1976-2016	276.87	272.18	0.64	98.31
79	Pinpri Anchal	2008-2016	812.34	245.59		30.23
80	Darnadam	2010-2016	1089.5	178.85		16.42
81	Dupipada	2008-2016	1467.6	512.06		34.89
82	<i>Heman pada</i>	2008-2016	1777.7	329.14		18.52
83	Trimbak	2008-2016	1658.6	608.91		36.71
84	Shinde	2009-2016	1412.7	335.43		23.74
85	Tisgaon	2004-2016	523.88	306.48		58.50

The spatial representation of the Average Annual Rainfall in the catchment is shown in Figure 4, wherein it is observed that higher rainfall are concentrated on the North-Western and Western part of the catchment. However, Standard Deviation (SD) has 3-2 higher values and are spread in North-Western and in the central part of the catchment. This indicate that, rainfall decreases as moved away from the Western part towards the Eastern part of the catchment.

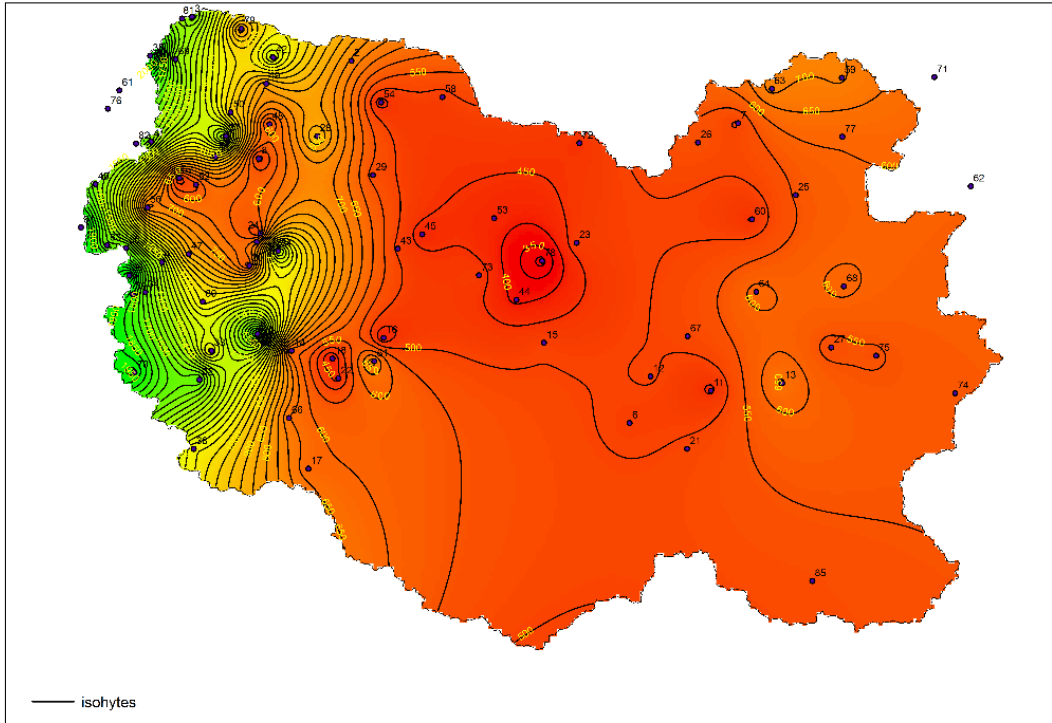


Figure 4: Mean Annual Rainfall in the study area

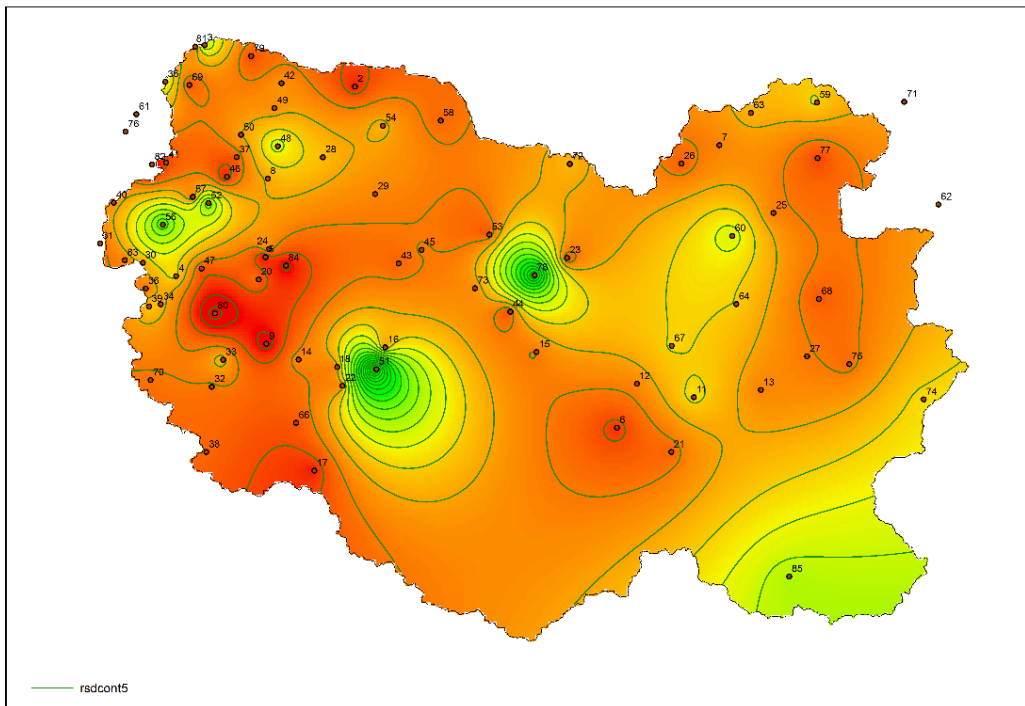


Figure 5: Variation of Relative Standard Deviation in the study area

4.1. TREND ANALYSIS

As reported earlier, about 80-85 % of annual precipitation is due to the southwestern monsoon between June and September. In order to assess the nature of the rainfall during the monsoon period, the trend analysis of the each of the monsoon month is carried out and the results is Tabulated in Table 8 and in Figure 6, Figure 7, Figure 8, Figure 9, Figure 10 and Figure 11, respectively for annual values, June, July, August, September and October.

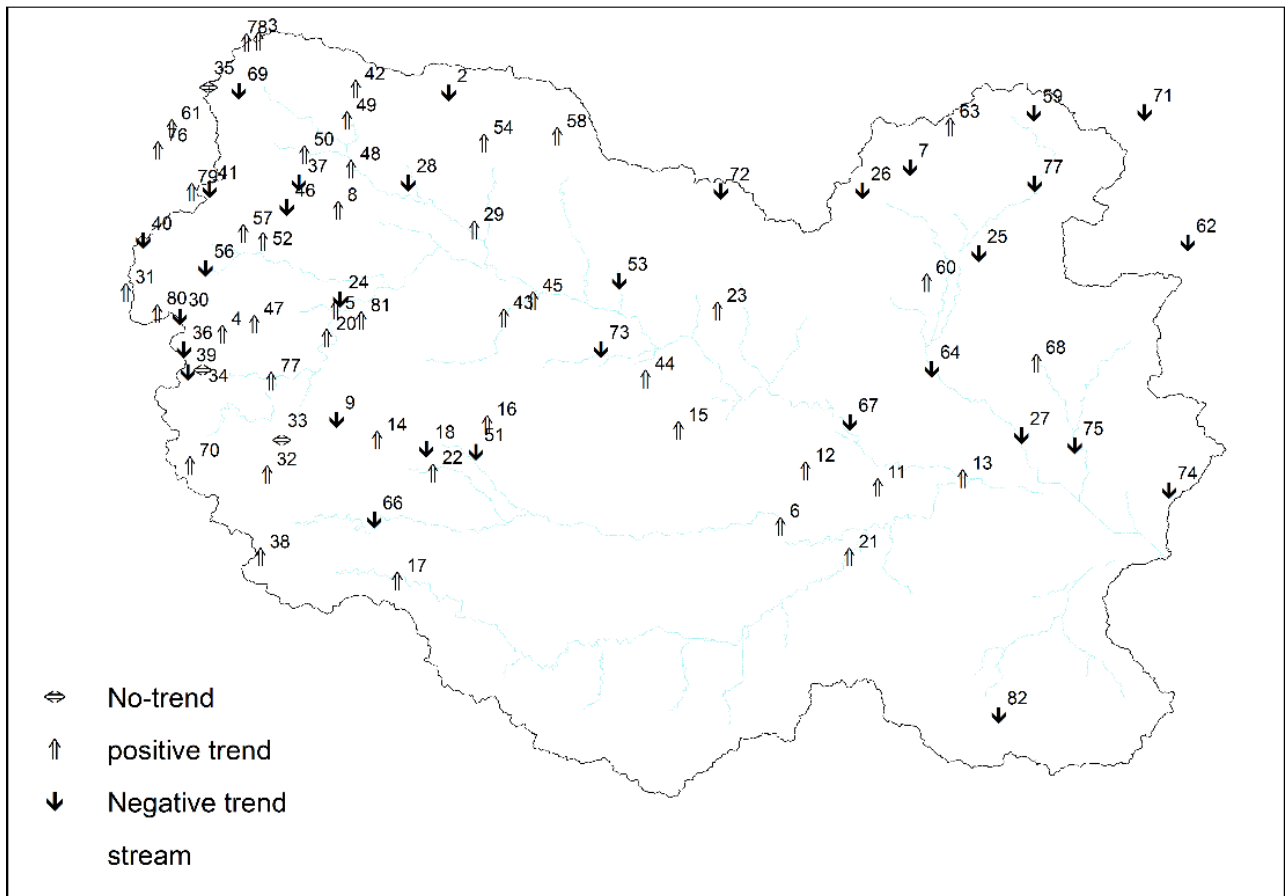


Figure 6 : Trend of Annual Rainfall in Jayakwadi catchment

The Annual rainfall (Figure 6) values show a wide spread positive trend in the basin. The positive trend is wide spread across the basin. However, there are many locations, where the negative trend is prevalent in the basin.

Table 8: Results of Sen's slope test

Station Name	Trend Analysis						Mann Kendell Test					
	June	July	Aug	Sept	Oct	Annual	June	July	Aug	Sept	Oct	Annual
Dongarpada	-0.01	2.91	-0.12	2.28	0.77	10.22	0.00	0.66	0.00	1.16	1.85	1.34
Dhodambe	-1.99	-0.59	-1.04	0.29	0.00	-4.34	-1.66	-0.53	-0.81	0.19	0.08	-1.84
Deosane	0.00	2.31	2.91	3.15	0.00	5.02	1.08	1.73	1.82	2.03	1.59	1.71
Dahegaon	-1.50	-0.46	0.12	2.91	0.54	4.41	-0.85	-0.06	0.06	1.69	0.89	0.73
Chehdi	-0.88	16.69	1.25	3.33	3.40	8.97	-0.18	1.89	0.12	0.37	0.98	0.55
Brahmangaon	-0.33	1.54	0.99	1.79	0.83	1.83	-0.42	2.10	1.28	1.74	1.39	1.19
Bolthan	-0.73	-0.06	-0.90	-0.42	0.36	-3.93	-0.65	-0.08	-1.13	-0.35	1.29	-1.63
Ambe Dindori	0.00	0.93	-0.09	0.61	0.13	3.38	0.01	1.29	-0.03	0.98	0.54	0.94
Tridhe	-16.00	13.04	-20.68	2.02	-23.87	-11.11	-1.04	0.61	-0.37	0.12	-1.23	0.00
Ranjangaon	0.00	0.00	0.34	0.01	0.00	0.00	1.27	1.83	1.93	2.26	1.42	1.01
Bel Pimpalgaon	-0.20	0.64	-0.13	-0.08	0.00	0.27	-0.49	0.82	-0.39	-0.25	0.42	0.22
Wadala Mahadeo	-0.63	1.85	1.26	1.08	0.04	1.79	-0.76	2.04	1.49	0.86	0.44	0.71
Toka	0.48	2.36	2.01	1.40	0.86	5.28	0.57	2.39	1.61	0.72	1.27	1.54
Thangaon	0.44	1.17	0.32	1.68	0.39	0.20	0.46	0.93	0.34	1.31	0.73	0.13
Rahata	-0.34	0.01	0.80	0.58	0.54	0.93	-0.43	0.01	0.97	0.62	1.32	0.34
Nandur Shingote	0.25	0.01	0.58	1.69	0.50	0.54	0.33	0.02	1.02	1.54	1.30	0.22
Kotul	0.46	-0.10	-0.92	-0.89	-0.56	4.05	0.34	-0.07	-0.81	-0.81	-2.04	1.93
Bhojapur	0.16	0.95	0.50	0.63	0.21	-0.55	0.19	1.49	0.73	0.82	0.63	-0.15
Bhavarwadi	-0.89	-0.07	0.20	0.79	0.23	-2.49	-0.90	-0.13	0.29	0.63	0.48	-0.95
Bhagur	0.57	1.22	0.42	-2.70	-0.59	0.08	0.42	1.38	0.44	-2.14	-2.08	0.03
Panegaon	-0.43	1.51	0.13	-1.41	-0.35	1.16	-0.43	2.18	0.12	-1.62	-2.13	0.48
Adhala	0.77	0.78	-0.34	-1.44	-0.45	0.87	0.95	1.13	-0.38	-1.58	-2.21	0.28
Padhegaon	-0.45	1.22	2.14	0.24	0.00	5.42	-0.21	0.75	1.05	0.28	-1.12	0.98
Samangaon	-2.26	-2.09	-0.32	-1.24	1.24	-4.90	-3.97	-4.32	-0.54	-1.45	1.79	-2.24
Deogaon Rangari	-2.00	1.32	-0.35	0.31	0.00	-2.82	-2.37	1.38	-0.25	0.26	-0.02	-0.93
Loni	-2.01	0.29	-0.46	-1.56	0.00	-4.35	-2.35	0.43	-0.54	-1.74	-0.14	-1.53
Solegaon	-4.07	-0.42	-1.33	-0.92	-1.07	-10.53	-1.87	-0.13	-0.60	-0.42	-0.88	-2.38
Pimpalgaon Baswant (DK)	-1.40	-2.62	-4.27	-2.37	-0.36	-2.93	-0.88	-1.02	-2.26	-1.61	-1.49	-0.69
Niphad	0.01	1.09	0.12	0.50	0.59	2.40	0.00	1.01	0.07	0.47	1.01	0.99
Anjaneri	2.77	-9.03	-12.42	-5.37	-0.61	-5.96	0.91	-2.89	-3.29	-3.04	-1.23	-0.71
Ambai	1.15	4.23	1.36	2.40	1.18	14.72	0.46	1.27	0.26	1.27	1.88	1.47
Wasali	0.00	17.36	11.70	4.95	-2.28	17.99	-0.23	1.56	0.65	0.75	-0.98	0.65
Taked Bk	0.00	0.00	0.00	0.04	0.00	0.00	0.42	0.34	-0.34	0.66	0.24	-0.03
Sanjegaon	-3.50	0.00	-1.40	0.80	0.05	0.00	-1.41	0.03	-0.44	0.44	0.29	0.00
Nanashi	0.00	0.00	0.00	2.75	1.12	0.00	0.49	-0.58	0.15	1.42	2.92	-0.18

Kusegaon	-2.89	-1.91	-7.21	0.96	1.17	-9.31	-0.97	-0.74	-1.57	0.31	1.56	-0.86
Indore	-1.81	0.13	-3.41	0.71	0.00	-5.30	-0.79	0.02	-1.16	0.48	0.06	-0.91
Aswali	-1.37	2.61	1.53	1.41	0.50	4.61	-0.79	1.40	0.71	0.89	0.63	0.98
Ahurli	-2.77	0.49	-3.13	-1.64	0.15	-3.90	-1.24	0.11	-0.67	-0.82	0.83	-0.34
Waghera	-2.59	-9.25	-7.41	-0.26	0.00	-21.97	-1.05	-1.85	-1.87	-0.37	0.73	-2.28
Vilwandi	-13.85	30.89	3.53	-2.69	-4.83	-8.80	-0.79	1.77	0.06	-0.43	-0.86	-0.18
Vani	0.00	3.30	1.25	1.85	0.92	6.58	1.62	2.48	2.00	2.40	3.22	2.26
Vadangli	0.88	7.93	2.72	9.58	1.14	7.70	0.25	0.73	0.49	0.86	0.37	0.24
Sonewadi	0.00	0.43	1.13	1.53	0.00	3.87	0.28	1.66	2.51	2.51	1.67	2.15
Somthane	0.21	0.69	0.68	1.32	0.00	2.36	0.39	0.99	0.75	1.24	0.34	0.98
Ramshej	-0.01	-3.70	-4.15	1.08	0.00	-8.02	-0.01	-1.79	-2.68	0.71	0.57	-2.28
Rajur Bahula	0.70	5.69	2.20	2.49	0.00	10.05	0.52	2.54	1.48	1.81	0.15	2.64
Palkhed Dam	2.50	8.00	0.00	10.90	-0.50	10.50	0.31	0.70	0.00	1.64	-0.23	0.31
Ozarkhed Dam	0.00	0.65	0.13	1.69	1.04	1.37	1.26	1.83	1.62	2.09	3.34	1.79
Nilwandi	0.00	0.66	0.00	0.80	0.28	2.18	1.78	1.86	1.99	1.98	2.87	1.69
Nalwadi	-5.33	6.37	-2.95	-5.32	-4.54	-31.77	-0.49	0.24	-0.12	-0.37	-1.10	-0.12
Mung sare	0.13	2.85	2.05	1.36	0.43	10.78	2.28	2.80	2.60	3.08	3.72	2.84
Mahalkheda	-2.01	-0.55	-0.55	0.57	-0.03	-4.04	-2.41	-0.65	-0.71	0.42	-0.68	-1.66
Khadak Ozar	0.00	2.17	-0.25	0.12	0.20	0.93	-0.19	1.91	-0.30	0.21	1.42	0.39
Karanjkhed	-1.50	3.90	-0.50	2.09	0.24	3.28	-0.69	1.47	-0.21	1.85	0.75	0.84
Ganeshgaon	-6.03	-2.35	-19.03	-7.75	0.00	-24.16	-1.59	-0.31	-1.16	-0.67	-0.19	-0.79
Dugaon	-0.03	0.23	-0.24	0.81	0.43	0.06	-0.19	0.33	-0.35	0.97	1.98	0.00
Deogaon	-0.63	0.38	0.55	2.25	0.54	2.49	-0.84	0.45	0.85	2.28	1.15	1.04
Hivarkheda	0.00	0.24	0.10	0.78	0.00	-2.11	0.00	0.22	0.13	0.78	0.54	-0.43
Dhondlagaon	0.91	2.33	1.77	0.00	0.00	2.98	1.01	2.44	2.31	0.00	1.08	0.71
Borvat	-2.20	2.59	4.37	3.66	1.73	13.17	-0.45	0.39	0.78	1.07	1.61	1.23
Phulambri	-1.31	1.00	0.52	0.16	0.00	-3.01	-1.44	0.84	0.36	0.19	-0.58	-1.02
Kalanki	-1.72	0.46	0.73	2.23	0.00	1.43	-1.73	0.40	0.57	1.15	0.59	0.46
Kadakwada	-3.31	-0.14	-0.28	-0.61	-0.81	-8.30	-2.81	-0.28	-0.33	-0.54	-1.73	-2.06
Manjur	-0.50	0.69	0.71	0.20	0.00	0.11	-0.74	0.86	0.85	0.24	0.16	0.03
Mahaldevi	-0.95	0.78	0.98	0.92	-0.18	-0.96	-0.85	0.52	0.72	0.99	-0.54	-0.40
Nagamthan	-1.08	0.94	0.72	0.92	0.00	-0.12	-1.19	1.18	0.82	0.89	-0.15	-0.07
Amblihol	-1.28	1.79	1.97	1.66	0.29	0.91	-1.22	1.88	1.92	1.62	0.52	0.44
Charose	0.26	-1.51	-3.33	2.18	0.76	-1.84	0.11	-0.51	-1.07	1.49	1.26	-0.44
Bhawali (BK)	-4.53	13.31	-0.18	4.60	-0.64	16.11	-0.28	0.76	-0.06	0.45	-0.34	0.85
Pishor	-1.15	-1.36	1.15	1.42	0.00	-2.85	-1.57	-1.25	1.08	1.20	-0.68	-0.82
Kirdishate	-0.05	0.00	0.13	0.58	0.00	-2.07	-0.17	0.03	0.19	0.56	0.32	-0.60
KalagaonMal	0.00	0.69	1.53	1.26	0.78	2.76	0.00	0.97	1.82	1.43	1.32	1.38
Dorkin	-1.28	0.84	0.13	-1.31	-0.53	-9.00	-1.50	0.62	0.06	-0.98	-1.14	-2.77
Shendurwada	-2.08	1.00	-4.70	-2.82	0.00	-7.50	-0.65	0.08	-1.33	-0.57	0.00	-0.80
Usthale (Hedpada)	-0.24	4.75	7.02	6.90	1.39	21.88	-0.23	0.93	1.22	2.19	1.65	1.54
Hatnoor	-1.55	-0.36	0.97	-0.12	0.00	-4.18	-1.49	-0.49	0.76	-0.20	-0.85	-1.24

Darnadam	-15.20	34.50	25.00	7.75	-3.20	37.67						
Dupipada	5.88	30.27	-24.42	-0.21	-19.16	7.88						
Heman pada	6.92	13.28	-20.76	-3.21	-8.32	9.51						
Trimbak	-4.97	36.13	-40.93	-18.89	8.64	41.84						
Shinde	2.69	47.00	4.80	-4.26	5.18	111.51						
Tisgaon	-0.30	5.47	-12.55	0.17	-2.71	-22.66						

The result of trend analysis June month rainfall (Figure 7) values show a wide spread negative trend in the basin. The negative trend is wide spread across the basin.

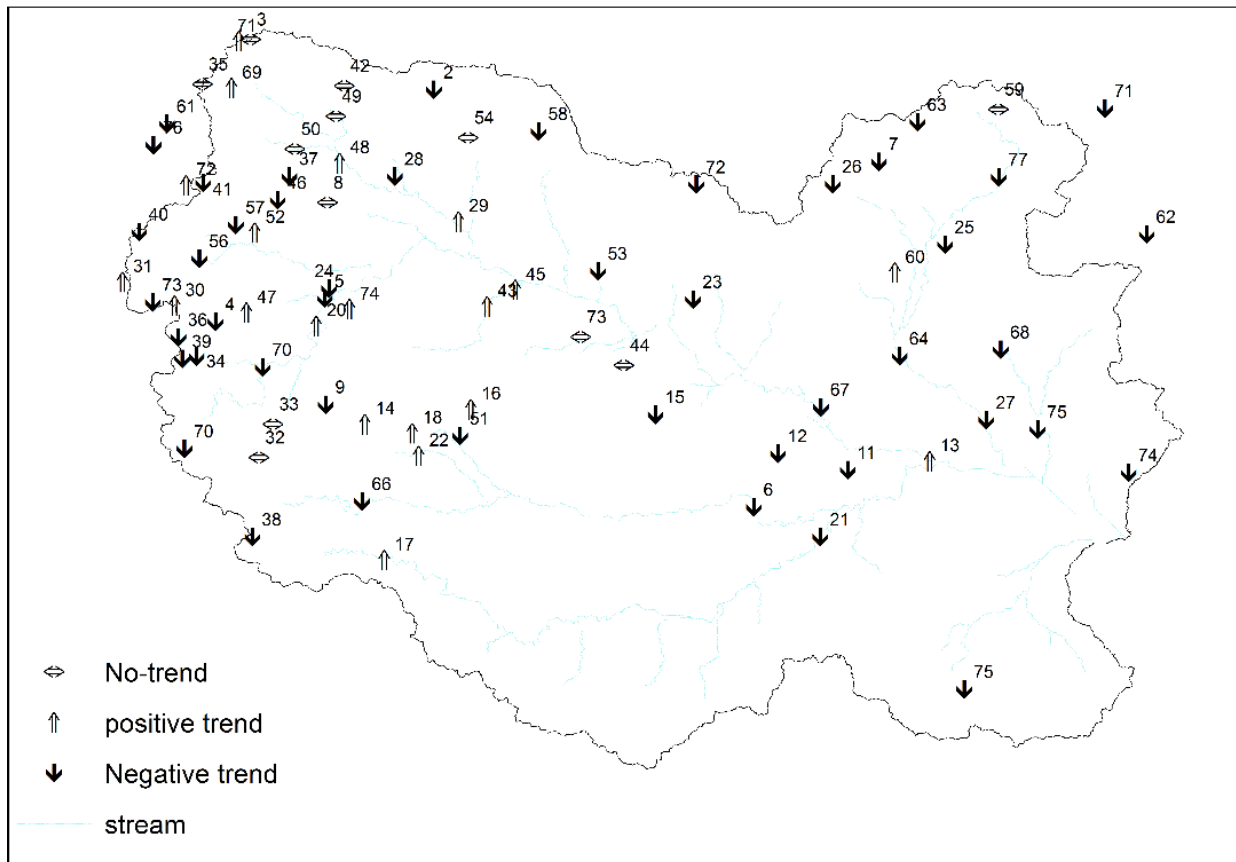


Figure 7 : Rainfall trend for the month of June in Jayakwadi catchment

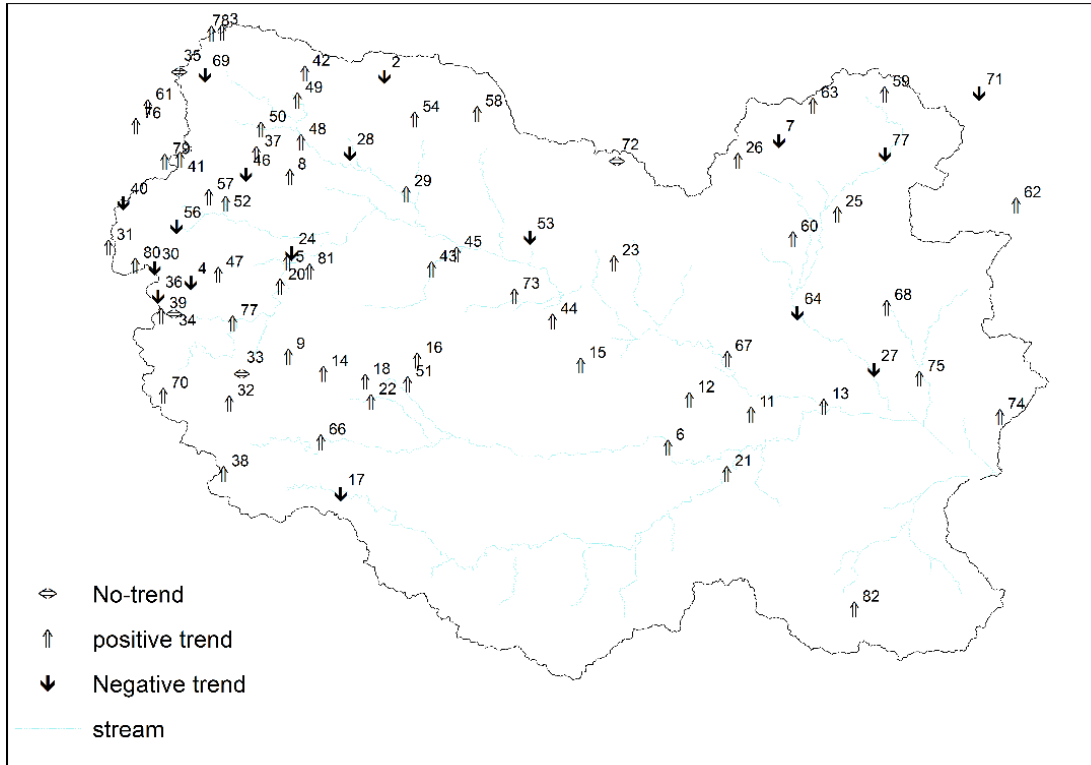


Figure 8 : Rainfall trend for the month of July in Jayakwadi catchment

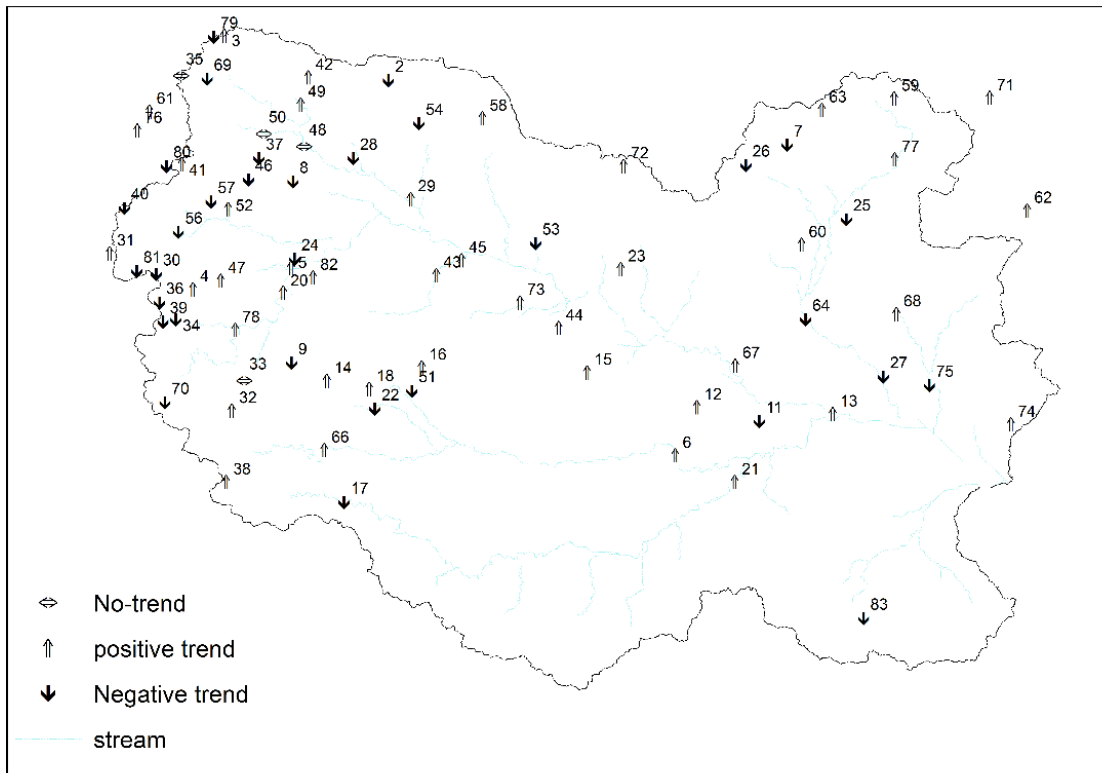


Figure 9: Rainfall trend for the month of Aug in Jayakwadi catchment

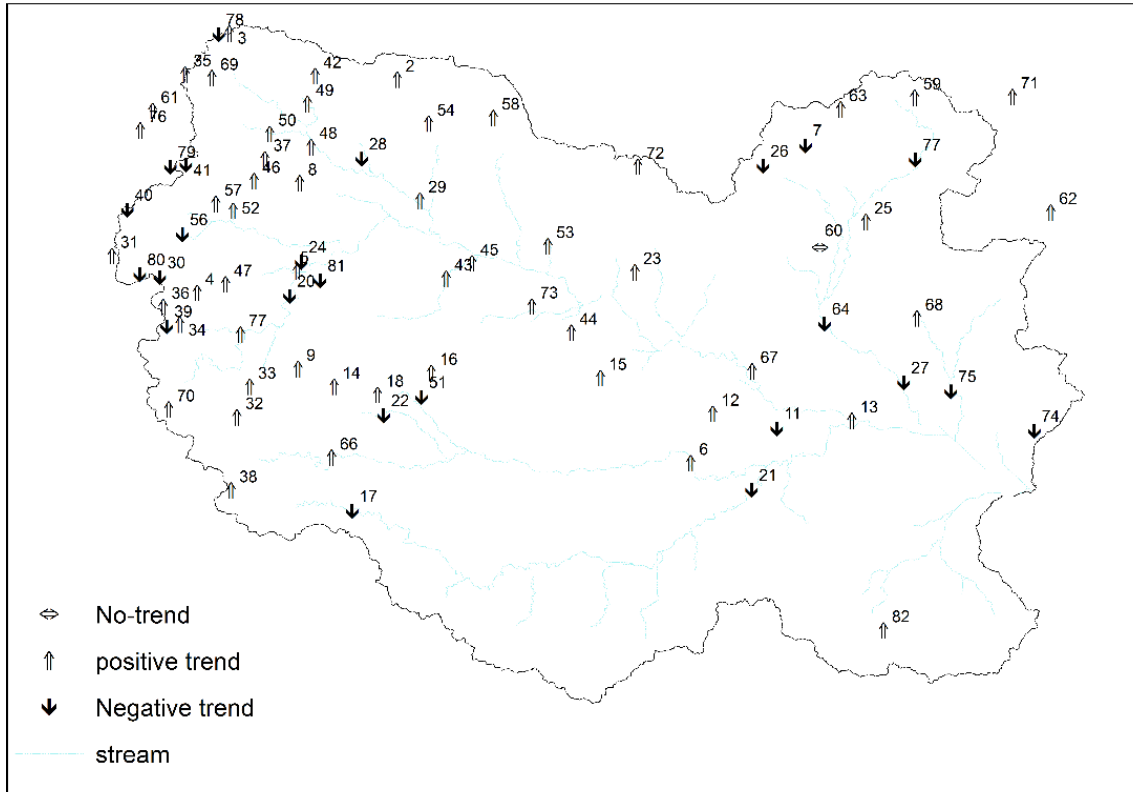


Figure 10 : Rainfall trend for the month of Sept in Jayakwadi catchment

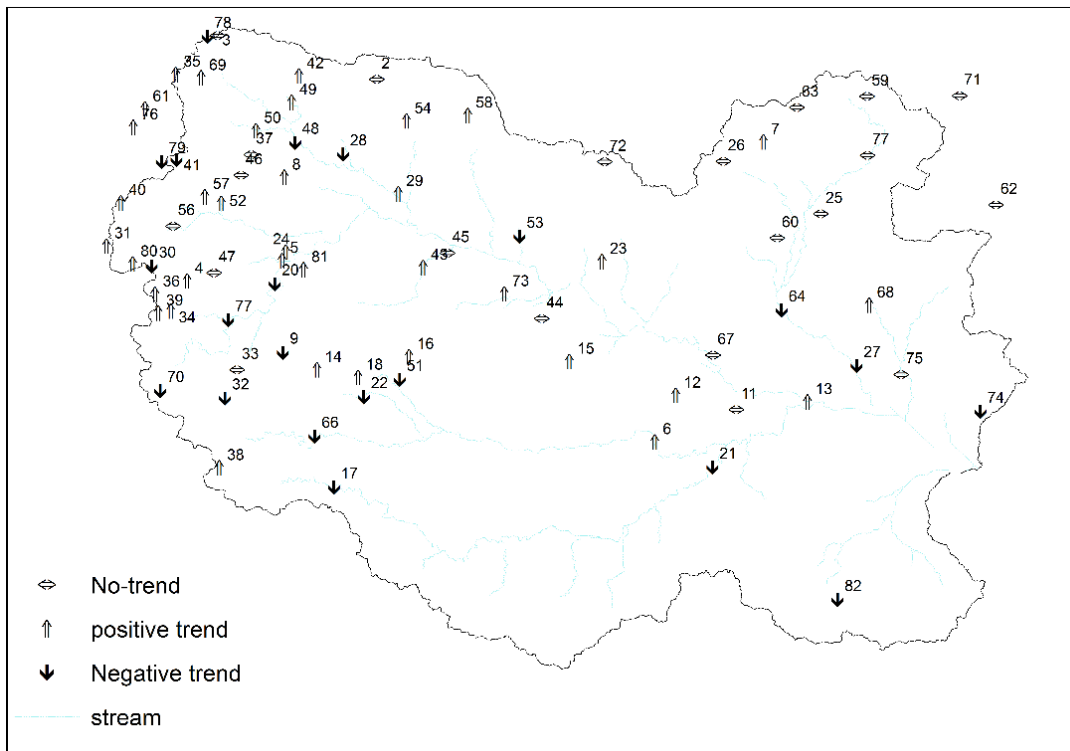


Figure 11: Rainfall trend for the month of Oct in Jayakwadi catchment

The month of July and October show more of a positive trend (Figure 8 and Figure 11), where as the month of August and September show more of negative trend in the upper catchment and close to the Jayakwadi reservoir. However, overall it is noticed in all the monsoon months, the dominant positive trend is observed.

4.2. Homogeneity Test

For carrying out change detection analysis, The rainfall values of point raingagues (observed rainfall values of all the stations in the catchment) of June, July, August, September, October and Annual totals have been analyzed with the help of Pettitt's test, SNH test and Buishand range test with 1% significant level. The test statistic of various tests and acceptance or rejection of null hypothesis for rainfall has been presented in Table 9 to Table 14, for June, July August, Sept, Oct and Annual respectively.

Table 9: The Results of Homogeneity Test for the month of June

Station	Pettitt's Test			Standard Normal Homogeneity Test (SNHT)			Buishand Test		
	K	t	Trend	To	t	Trend	Q	t	Trend
Adhala	169.00	1997	Ho	10.89	1977	Ho	5.21	1997	Ho
Ahruli	99.00	2001	Ho	2.17	2006	Ho	4.08	2006	Ho
Ambai	116.00	2001	Ho	4.52	2001	Ho	6.64	2001	Ho
Ambedindori	130.00	2007	Ho	5.63	1976	Ho	4.56	1998	Ho
Amblihol	133.00	1992	Ho	3.10	1992	Ho	5.63	1992	Ho
Anjaneri	150.00	2001	Ho	8.26	2015	Ho	6.48	2001	Ho
Aswali	117.00	2005	Ho	8.61	1976	Ho	4.70	2005	Ho
Belpimp	96.00	2006	Ho	2.22	1988	Ho	4.52	2002	Ho
Bhagur	56.00	1992	Ho	1.12	2015	Ho	2.62	1985	Ho
Bhavarwadi	114.00	1992	Ho	3.32	1991	Ho	5.76	1991	Ho
Bhawali	20.00	1995	Ho	2.38	1995	Ho	1.72	2006	Ho
Bhojapur	102.00	1995	Ho	8.83	1977	Ho	4.47	2007	Ho
Bholtan	116.00	2007	Ho	3.74	2014	Ho	3.93	1992	Ho
Borvat	101.00	2006	Ho	4.51	2006	Ho	5.62	2006	Ho
Brahmangaon	118.00	2007	Ho	3.55	2013	Ho	4.95	2007	Ho
Charose	110.00	1990	Ho	5.16	1977	Ho	3.94	2007	Ho
Dahegaon	170.00	2006	Ho	4.58	2006	Ho	6.10	2005	Ho
Deogaon	124.00	2007	Ho	3.07	2010	Ho	4.63	2007	Ho
Deogaon-Rangeri	214.00	1992	Ho	7.47	1992	Ho	8.73	1992	Ho

Dokrin	166.00	2002	Ho	4.63	1992	Ho	6.88	1992	Ho
Dodambe	143.00	2007	Ho	5.05	2007	Ho	6.01	2007	Ho
Dondlagoan	34.00	2014	Ho	4.50	2003	Ho	1.36	2014	Ho
Dugaon	96.00	1978	Ho	7.54	1976	Ho	3.72	1978	Ho
Hatnoor	126.00	2007	Ho	3.22	2007	Ho	5.10	1992	Ho
Hivarkhed	120.00	2007	Ho	2.56	2007	Ho	4.27	2007	Ho
Indore	119.00	2005	Ho	4.82	1976	Ho	5.02	2007	Ho
Kadakoar	89.00	1998	Ho	7.42	1976	Ho	3.93	1978	Ho
Kadakhwagh	236.00	1994	Ha(D)	9.00	1994	Ho	9.56	1994	Ha(D)
Kalanki	178.00	2003	Ho	5.18	2003	Ho	7.03	2001	Ho
KalgoanMal	106.00	2007	Ho	2.25	1985	Ho	4.26	1988	Ho
Karankhed	148.00	2007	Ho	4.47	2007	Ho	5.68	2007	Ho
Kirdisheta	92.00	1989	Ho	2.53	1976	Ho	4.54	2002	Ho
Kushigaon	144.00	1980	Ho	7.56	1980	Ho	5.83	1980	Ho
Loni	218.00	2002	Ho	7.53	2002	Ho	8.43	2002	Ho
Mahaladevi	112.00	2007	Ho	13.72	1976	Ho	4.32	2007	Ho
Mahalkhed	181.00	2007	Ho	10.95	1977	Ho	6.58	2007	Ho
Manjur	123.00	2002	Ho	5.20	1977	Ho	4.75	2002	Ho
Nagmathan	172.00	2007	Ho	6.46	2007	Ho	6.82	2007	Ho
Nandur-Shingote	118.00	1995	Ho	7.41	1977	Ho	4.62	1980	Ho
Niphad	104.00	1990	Ho	2.36	1990	Ho	4.79	1990	Ho
Padhegaon	53.00	1982	Ho	1.79	1982	Ho	3.06	1982	Ho
Panegaon	66.00	1994	Ho	1.64	1977	Ho	2.72	1992	Ho
Phulambri	166.00	1993	Ho	3.40	1992	Ho	5.91	1993	Ho
Pimplegaon	162.00	2007	Ho	5.06	2011	Ho	5.81	2006	Ho
Pishor	140.00	2004	Ho	3.84	2010	Ho	5.41	2004	Ho
Rahata	105.00	2003	Ho	2.51	1977	Ho	3.65	2003	Ho
Rajur-Bhaua	101.00	1990	Ho	3.06	1999	Ho	5.58	1999	Ho
Ramshej	109.00	1998	Ho	4.08	1977	Ho	4.85	2007	Ho
Samangaon	122.00	1991	Ho	2.21	2010	Ho	3.92	2007	Ho
Shendurwada	42.00	2002	Ho	5.48	2002	Ho	4.25	2002	Ho
Solegaon	84.00	2003	Ho	5.24	2003	Ho	6.06	2003	Ho
Somthan	121.00	2007	Ho	3.96	2010	Ho	5.14	2007	Ho
Thangoan	114.00	1990	Ho	6.09	1977	Ho	3.81	1980	Ho
Toka	106.00	1997	Ho	1.88	1990	Ho	4.29	1990	Ho
Usthale	70.00	2006	Ho	2.93	2006	Ho	4.56	2006	Ho
Wadalamahadeva	95.00	2007	Ho	3.27	1978	Ho	4.54	2007	Ho
Wasali	24.00	2006	Ho	3.19	1997	Ho	2.97	2006	Ho

Table 10: The Results of Homogeneity Test for the month of July

Station	Pettitt's Test			Standard Normal Homogeneity Test (SNHT)			Buishand Test		
	K	t	Trend	To	t	Trend	Q	t	Trend
Adhala	123.00	2005	Ho	6.17	1976	Ho	5.15	2005	Ho
Ahruli	122.00	2004	Ho	1.90	2010	Ho	3.76	2004	Ho
Ambai	196.00	2004	Ho	7.38	2005	Ho	7.80	2005	Ho
Ambedindori	140.00	1992	Ho	3.51	2004	Ho	5.52	2004	Ho
Amblihol	181.00	2002	Ho	6.88	2002	Ho	8.06	2002	Ho
Anjaneri	206.00	1995	Ho	8.40	1983	Ho	8.39	1995	Ho
Aswali	136.00	2004	Ho	9.87	1976	Ho	4.23	2011	Ho
Belpimp	104.00	2008	Ho	4.35	2008	Ho	5.34	2008	Ho
Bhagur	73.00	2003	Ho	1.41	2003	Ho	3.58	2003	Ho
Bhavarwadi	73.00	1999	Ho	3.05	1984	Ho	4.74	1993	Ho
Bhawali	60.00	2005	Ho	4.09	2005	Ho	4.74	2005	Ho
Bhojapur	168.00	1992	Ho	5.68	1992	Ho	7.61	1992	Ho
Bholtan	74.00	1993	Ho	3.52	2015	Ho	3.41	1993	Ho
Borvat	70.00	2004	Ho	2.39	2004	Ho	4.27	2004	Ho
Brahmangaon	165.00	1988	Ho	6.33	2005	Ho	7.22	2005	Ho
Charose	110.00	1996	Ho	4.17	1976	Ho	4.38	1989	Ho
Dahegaon	128.00	2006	Ho	2.94	2006	Ho	4.75	2006	Ho
Deogaon	55.00	1991	Ho	1.50	2005	Ho	3.33	1991	Ho
Deogaon-Rangeri	190.00	2002	Ho	6.12	2002	Ho	7.61	2002	Ho
Dokrin	110.00	1983	Ho	3.13	1983	Ho	4.83	1986	Ho
Dodambe	111.00	2005	Ho	4.81	1981	Ho	4.65	1981	Ho
Dondlagoan	0.00	1978	Ho	8.74	2003	Ho	0.00	1978	Ho
Dugaon	89.00	1988	Ho	1.81	1988	Ho	4.06	1988	Ho
Hatnoor	78.00	2010	Ho	2.84	2011	Ho	3.36	2010	Ho
Hivarkhed	82.00	1989	Ho	3.93	2015	Ho	3.36	1989	Ho
Indore	84.00	1980	Ho	3.71	1976	Ho	2.65	1980	Ho
Kadakojar	158.00	2005	Ho	7.49	2005	Ho	7.86	2002	Ho
Kadakhwagh	98.00	1997	Ho	2.23	2008	Ho	3.82	2008	Ho
Kalanki	87.00	1987	Ho	1.75	2015	Ho	3.76	1987	Ho
KalgoanMal	116.00	1987	Ho	2.87	1987	Ho	4.99	1987	Ho
Karanjkhed	140.00	1992	Ho	7.66	1976	Ho	4.62	2004	Ho
Kirdisheta	79.00	1990	Ho	1.51	1988	Ho	3.80	1990	Ho
Kushigaon	122.00	1984	Ho	3.97	1976	Ho	5.18	1994	Ho
Loni	116.00	2003	Ho	3.41	2005	Ho	5.30	2005	Ho
Mahaladevi	144.00	1987	Ho	11.29	1976	Ho	3.63	1987	Ho
Mahalkhed	116.00	2007	Ho	3.65	2009	Ho	4.97	2007	Ho
Manjur	116.00	1987	Ho	8.32	2015	Ho	5.16	1987	Ho

Nagmathan	140.00	1990	Ho	3.70	1990	Ho	6.09	1992	Ho
Nandur-Shingote	70.00	2008	Ho	2.55	2015	Ho	3.16	1994	Ho
Niphad	110.00	1987	Ho	3.28	2015	Ho	5.13	2002	Ho
Padhegaon	45.00	1987	Ho	1.77	1987	Ho	3.39	1987	Ho
Panegaon	141.00	2002	Ho	5.28	2015	Ho	6.01	2003	Ho
Phulambri	150.00	2001	Ho	4.69	2015	Ho	5.01	2001	Ho
Pimplegaon	160.00	2006	Ho	6.28	2009	Ho	6.58	2006	Ho
Pishor	130.00	1989	Ho	4.99	1977	Ho	5.71	1989	Ho
Rahata	90.00	1987	Ho	2.28	1987	Ho	4.46	1987	Ho
Rajur-Bhaua	174.00	1987	Ho	5.07	1976	Ho	6.42	2004	Ho
Ramshej	222.00	1994	Ho	7.64	2015	Ho	7.93	1994	Ho
Samangaon	162.00	1999	Ho	3.98	1999	Ho	6.37	1999	Ho
Shendurwada	19.00	2011	Ho	1.41	2015	Ho	2.16	2003	Ho
Solegaon	46.00	1998	Ho	2.80	1990	Ho	2.38	1998	Ho
Somthan	117.00	2002	Ho	8.15	2015	Ho	5.39	2002	Ho
Thangoan	186.00	1987	Ho	5.72	1987	Ho	7.06	1987	Ho
Toka	244.00	2002	Ho	12.29	2008	Ho	10.50	2002	Ho
Usthale	80.00	2002	Ho	2.53	2005	Ho	4.34	2005	Ho
Wadalamahadeva	168.00	2001	Ho	5.41	2008	Ho	6.87	2001	Ho
Wasali	49.00	2011	Ho	3.45	2004	Ho	4.17	2004	Ho

Table 11: The Results of Homogeneity Test for the month of Aug

Station	Pettitt's Test			Standard Normal Homogeneity Test (SNHT)			Buishand Test		
	K	t	Trend	To	t	Trend	Q	t	Trend
Adhala	96.00	1996	Ho	3.58	1980	Ho	4.01	1980	Ho
Ahruli	90.00	1990	Ho	6.51	2003	Ho	7.66	2003	Ho
Ambai	138.00	2005	Ho	7.20	2005	Ho	7.71	2005	Ho
Ambedindori	84.00	1996	Ho	4.55	2015	Ho	5.55	2003	Ho
Amblihol	165.00	1986	Ho	4.31	1986	Ho	5.96	1986	Ho
Anjaneri	258.00	2008	Ho	12.60	1983	Ha(D)	9.12	1983	Ho
Aswali	136.00	2001	Ho	7.21	2003	Ho	8.10	2003	Ho
Belpimp	70.00	1996	Ho	1.31	2011	Ho	2.50	1986	Ho
Bhagur	148.00	1986	Ho	4.42	1986	Ho	6.04	1986	Ho
Bhavarwadi	80.00	2007	Ho	2.28	1984	Ho	4.05	1984	Ho
Bhawali	46.00	2002	Ho	2.69	2002	Ho	3.74	2002	Ho
Bhojapur	130.00	1996	Ho	7.96	1980	Ho	5.98	1980	Ho
Bholtan	138.00	2002	Ho	3.66	2002	Ho	5.88	2002	Ho
Borvat	90.00	2002	Ho	3.75	2003	Ho	5.40	2003	Ho
Brahmangaon	142.00	1991	Ho	2.71	1991	Ho	5.21	1991	Ho
Charose	138.00	1990	Ho	3.38	2015	Ho	4.03	1990	Ho

Dahegaon	80.00	1984	Ho	3.30	2003	Ho	5.45	2003	Ho
Deogaon	52.00	1982	Ho	5.83	1999	Ho	2.34	1982	Ho
Deogaon-Rangeri	126.00	2011	Ho	3.86	2011	Ho	4.17	2011	Ho
Dokrin	146.00	1983	Ho	5.16	1983	Ho	5.84	1983	Ho
Dodambe	83.00	1981	Ho	4.41	1980	Ho	4.03	1980	Ho
Dondlagoan	146.00	1995	Ho	4.34	2008	Ho	5.43	1997	Ho
Dugaon	110.00	1981	Ho	1.23	1981	Ho	2.55	1981	Ho
Hatnoor	50.00	2006	Ho	3.10	1985	Ho	1.85	2011	Ho
Hivarkhed	60.00	1983	Ho	1.20	2011	Ho	2.31	2011	Ho
Indore	184.00	1986	Ho	7.89	1986	Ho	8.07	1986	Ho
Kadakojar	96.00	1981	Ho	1.46	2007	Ho	3.24	2007	Ho
Kadakhgh	100.00	1998	Ho	1.40	1998	Ho	3.78	1998	Ho
Kalanki	116.00	2001	Ho	1.73	1989	Ho	4.05	1989	Ho
KalgaonMal	170.00	1991	Ho	8.48	2005	Ho	8.36	2005	Ho
Karankhed	74.00	2002	Ho	3.38	2003	Ho	5.54	2003	Ho
Kirdisheta	88.00	2011	Ho	3.20	2011	Ho	3.79	2011	Ho
Kushigaon	172.00	1984	Ho	2.77	2003	Ho	5.02	2003	Ho
Loni	80.00	2002	Ho	3.52	2014	Ho	2.96	2011	Ho
Mahaladevi	144.00	2001	Ho	5.97	2003	Ho	7.37	2003	Ho
Mahalkhed	109.00	2009	Ho	3.07	1980	Ho	4.07	2008	Ho
Manjur	142.00	1991	Ho	4.16	1991	Ho	6.45	1991	Ho
Nagmathan	180.00	1991	Ho	6.30	1989	Ho	7.77	1991	Ho
Nandur-Shingote	141.00	1996	Ho	1.78	2005	Ho	3.83	2005	Ho
Niphad	74.00	2003	Ho	2.94	2015	Ho	4.74	2003	Ho
Padhegaon	74.00	1991	Ho	5.39	1993	Ho	5.58	1991	Ho
Panegaon	122.00	1999	Ho	2.94	1999	Ho	5.47	1999	Ho
Phulambri	84.00	2000	Ho	2.31	2008	Ho	3.90	2008	Ho
Pimplegaon	212.00	2008	Ho	9.96	2008	Ho	8.11	2008	Ho
Pishor	138.00	2000	Ho	2.19	1986	Ho	4.25	1986	Ho
Rahata	168.00	1985	Ho	5.48	1985	Ho	6.54	1986	Ho
Rajur-Bhauia	187.00	1995	Ho	7.03	2003	Ho	8.39	1996	Ho
Ramshej	218.00	1988	Ho	8.95	1988	Ho	9.32	1992	Ho
Samangaon	110.00	1986	Ho	2.30	1983	Ho	3.90	1983	Ho
Shendurwada	40.00	2011	Ho	3.16	2011	Ho	3.47	2011	Ho
Solegaon	53.00	2011	Ho	3.13	2011	Ho	3.64	2011	Ho
Somthan	110.00	2005	Ho	3.24	2005	Ho	5.17	2005	Ho
Thangoan	100.00	2003	Ho	4.68	2015	Ho	5.31	2003	Ho
Toka	194.00	1986	Ho	6.55	1986	Ho	7.35	1986	Ho
Usthale	131.00	1999	Ho	5.80	2001	Ho	6.91	2001	Ho
Wadalamahadeva	144.00	1994	Ho	4.14	1986	Ho	5.84	1986	Ho
Wasali	47.00	2003	Ho	2.81	2003	Ho	3.67	2003	Ho

Table 12: The Results of Homogeneity Test for the month of Sept

Station	Pettitt's Test			Standard Normal Homogeneity Test (SNHT)			Buishand Test		
	K	t	Trend	To	t	Trend	Q	t	Trend
Adhala	254.00	2008	Ho	9.35	2008	Ho	7.85	2008	Ho
Ahruli	152.00	1996	Ho	3.08	2007	Ho	4.71	2007	Ho
Ambai	172.00	2002	Ho	7.25	2004	Ho	7.94	2004	Ho
Ambedindori	156.00	1991	Ho	2.91	1992	Ho	5.45	1992	Ho
Amblihol	141.00	2003	Ho	2.60	1978	Ho	3.91	2003	Ho
Anjaneri	250.00	2008	Ho	11.31	2008	Ho	8.64	2008	Ho
Aswali	174.00	2004	Ho	6.32	2004	Ho	7.41	2004	Ho
Belpimp	76.00	1989	Ho	3.24	1989	Ho	5.40	1989	Ho
Bhagur	78.00	1987	Ho	3.02	1978	Ho	3.27	1987	Ho
Bhavarwadi	90.00	1978	Ho	3.62	1978	Ho	3.21	1978	Ho
Bhawali	66.00	2004	Ho	5.67	2004	Ho	5.58	2004	Ho
Bhojapur	112.00	1994	Ho	2.95	2002	Ho	5.28	2002	Ho
Bholtan	74.00	1984	Ho	1.50	1984	Ho	3.29	1984	Ho
Borvat	68.00	2003	Ho	2.27	2003	Ho	4.21	2003	Ho
Brahmangaon	148.00	1994	Ho	3.42	1978	Ho	5.34	1994	Ho
Charose	156.00	1991	Ho	4.91	1987	Ho	6.53	1987	Ho
Dahegaon	143.00	1991	Ho	4.26	2004	Ho	6.06	2004	Ho
Deogaon	8.00	1984	Ho	3.62	2003	Ho	0.59	1988	Ho
Deogaon-Rangeri	138.00	2002	Ho	2.05	1978	Ho	4.36	1989	Ho
Dokrin	124.00	1989	Ho	6.64	1989	Ho	7.92	1989	Ho
Dodambe	96.00	2000	Ho	3.11	2014	Ho	4.81	2000	Ho
Dondlagoan	144.00	1984	Ho	9.03	1979	Ho	6.45	1984	Ho
Dugaon	125.00	1987	Ho	3.18	1977	Ho	5.26	2003	Ho
Hatnoor	68.00	1984	Ho	2.43	2014	Ho	3.49	1988	Ho
Hivarkhed	70.00	1983	Ho	4.29	1983	Ho	4.73	1983	Ho
Indore	125.00	2002	Ho	2.48	2010	Ho	4.67	2002	Ho
Kadakoazar	103.00	1993	Ho	2.43	2008	Ho	4.01	2008	Ho
Kadawkagh	95.00	2001	Ho	3.59	1984	Ho	5.07	1989	Ho
Kalanki	151.00	1995	Ho	2.73	1995	Ho	5.36	1995	Ho
KalgoanMal	138.00	1994	Ho	4.97	1978	Ho	5.41	1994	Ho
Karanjkhed	178.00	1991	Ho	5.86	1987	Ho	7.14	1987	Ho
Kirdisheta	90.00	1987	Ho	2.59	1978	Ho	2.76	2008	Ho
Kushigaon	138.00	2004	Ho	4.88	2004	Ho	6.52	2004	Ho
Loni	152.00	1984	Ho	6.49	1984	Ho	6.84	1984	Ho
Mahaladevi	122.00	2000	Ho	1.80	2000	Ho	4.24	2000	Ho
Mahalkhed	105.00	2008	Ho	2.75	2008	Ho	4.26	2008	Ho
Manjur	78.00	2002	Ho	1.71	1978	Ho	2.87	2002	Ho

Nagmathan	118.00	1994	Ho	1.79	1996	Ho	4.33	1996	Ho
Nandur-Shingote	160.00	2002	Ho	6.05	2002	Ho	7.56	2002	Ho
Niphad	86.00	1992	Ho	2.30	1978	Ho	2.70	2008	Ho
Padhegaon	30.00	1981	Ho	1.29	1977	Ho	1.83	1989	Ho
Panegaon	170.00	1997	Ho	3.87	2003	Ho	5.98	1997	Ho
Phulambri	122.00	2000	Ho	4.06	1983	Ho	5.52	1988	Ho
Pimplegaon	235.00	2008	Ho	12.00	2009	Ho	8.71	2008	Ho
Pishor	136.00	2002	Ho	1.88	1978	Ho	3.84	2002	Ho
Rahata	116.00	1994	Ho	1.89	1987	Ho	4.26	1994	Ho
Rajur-Bhauila	170.00	2003	Ho	5.01	2003	Ho	6.75	2003	Ho
Ramshej	102.00	1978	Ho	4.40	1978	Ho	3.83	1987	Ho
Samangaon	82.00	2010	Ho	2.43	2010	Ho	4.16	1990	Ho
Shendurwada	33.00	2007	Ho	2.67	2007	Ho	3.57	2007	Ho
Solegaon	38.00	2008	Ho	1.54	2013	Ho	2.76	2008	Ho
Somthan	146.00	2003	Ho	5.43	2003	Ho	7.03	2003	Ho
Thangoan	164.00	1991	Ho	3.55	1991	Ho	5.96	1991	Ho
Toka	78.00	1994	Ho	2.14	1977	Ho	2.28	1978	Ho
Usthale	124.00	1997	Ho	4.88	1997	Ho	6.23	1997	Ho
Wadalamahadeva	102.00	2005	Ho	2.76	2005	Ho	4.77	2005	Ho
Wasali	44.00	2007	Ho	1.93	2007	Ho	3.17	2007	Ho

Table 13: The Results of Homogeneity Test for the month of Oct

Station	Pettitt's Test			Standard Normal Homogeneity Test (SNHT)			Buishand Test		
	K	t	Trend	To	t	Trend	Q	t	Trend
Adhala	245.00	2001	Ha(D)	6.29	2001	Ho	7.83	2001	Ho
Ahruli	108.00	1989	Ho	2.18	1989	Ho	4.54	1989	Ho
Ambai	186.00	1992	Ho	6.49	1992	Ho	8.13	1992	Ha(I)
Ambedindori	84.00	1981	Ho	1.98	1981	Ho	3.64	2000	Ho
Amblihol	92.00	1992	Ho	2.00	1989	Ho	4.35	1989	Ho
Anjaneri	224.00	2009	Ho	6.92	2009	Ho	6.42	2009	Ho
Aswali	102.00	2001	Ho	2.58	1989	Ho	4.95	2001	Ho
Belpimp	87.00	2006	Ho	2.55	1989	Ho	4.79	1989	Ho
Bhagur	116.00	1992	Ho	3.07	1986	Ho	5.34	2001	Ho
Bhavarwadi	150.00	1992	Ho	3.08	1989	Ho	5.40	1989	Ho
Bhawali	44.00	2007	Ho	1.80	2007	Ho	3.06	2007	Ho
Bhojapur	96.00	1980	Ho	2.76	1983	Ho	5.03	1989	Ho
Bholtan	159.00	1995	Ho	3.00	1992	Ho	5.53	1992	Ho
Borvat	92.00	1996	Ho	3.57	1991	Ho	4.25	1996	Ho
Brahmangaon	185.00	1991	Ho	5.20	1992	Ho	7.29	1992	Ho
Charose	136.00	2007	Ho	3.64	2007	Ho	5.12	2007	Ho

Dahegaon	106.00	1982	Ho	2.45	1982	Ho	4.19	1989	Ho
Deogaon	23.00	1999	Ho	2.92	1992	Ho	2.02	1999	Ho
Deogaon-Rangeri	62.00	2001	Ho	1.54	1983	Ho	3.27	1999	Ho
Dokrin	149.00	2001	Ho	4.15	2001	Ho	6.36	2001	Ho
Dodambe	63.00	2009	Ho	1.34	1980	Ho	3.31	1999	Ho
Dondlagoan	144.00	1984	Ho	9.03	1979	Ho	6.45	1984	Ho
Dugaon	210.00	1989	Ho	5.47	1989	Ho	7.19	1989	Ho
Hatnoor	124.00	1999	Ho	3.50	1999	Ho	5.82	1999	Ho
Hivarkhed	84.00	2001	Ho	2.61	1982	Ho	2.63	2001	Ho
Indore	64.00	2001	Ho	2.10	2001	Ho	4.53	2001	Ho
Kadakojar	138.00	1989	Ho	3.62	1989	Ho	5.85	1989	Ho
Kadakhwagh	231.00	2000	Ho	5.99	2000	Ho	7.68	2000	Ho
Kalanki	111.00	2000	Ho	3.04	1986	Ho	5.01	1986	Ho
KalgaonMal	177.00	1992	Ho	6.65	1992	Ho	8.23	1992	Ho
Karankhed	139.00	1981	Ho	4.80	1980	Ho	5.01	1981	Ho
Kirdisheta	95.00	1983	Ho	3.11	1987	Ho	5.25	1989	Ho
Kushigaon	141.00	1992	Ho	4.44	1989	Ho	6.69	1992	Ho
Loni	80.00	2001	Ho	2.27	2013	Ho	4.51	2001	Ho
Mahaladevi	131.00	2001	Ho	3.42	2001	Ho	5.88	1999	Ho
Mahalkhed	125.00	2001	Ho	1.76	2001	Ho	4.14	2001	Ho
Manjur	128.00	1999	Ho	2.82	1999	Ho	5.36	1999	Ho
Nagmathan	115.00	2001	Ho	4.03	1989	Ho	6.17	1989	Ho
Nandur-Shingote	154.00	1992	Ho	4.60	1989	Ho	6.60	1989	Ho
Niphad	123.00	1989	Ho	4.24	1989	Ho	6.33	1989	Ho
Padhegaon	76.00	1993	Ho	4.35	1993	Ho	4.78	1993	Ho
Panegaon	120.00	1992	Ho	3.36	1989	Ho	5.63	1989	Ho
Phulambri	92.00	1990	Ho	3.90	1993	Ho	6.35	1993	Ho
Pimplegaon	210.00	2009	Ho	4.31	2009	Ho	6.25	2001	Ho
Pishor	93.00	2010	Ho	2.17	1999	Ho	4.70	1999	Ho
Rahata	161.00	1986	Ho	4.42	1984	Ho	6.21	1992	Ho
Rajur-Bhauia	98.00	1982	Ho	2.10	1982	Ho	4.29	1999	Ho
Ramshej	160.00	1992	Ho	4.31	1992	Ho	6.63	1992	Ho
Samangaon	144.00	2002	Ho	3.74	2002	Ho	6.00	2001	Ho
Shendurwada	22.00	2006	Ho	1.43	2001	Ho	2.39	2006	Ho
Solegaon	76.00	1999	Ho	11.58	1990	Ho	5.92	1999	Ho
Somthan	66.00	1993	Ho	1.42	1978	Ho	2.69	1993	Ho
Thangoan	78.00	2007	Ho	2.19	1983	Ho	4.31	1992	Ho
Toka	180.00	1994	Ho	3.66	1989	Ho	5.88	1989	Ho
Usthale	124.00	2003	Ho	3.54	1996	Ho	5.24	1996	Ho
Wadalamahadeva	102.00	1992	Ho	2.41	1989	Ho	4.78	1989	Ho
Wasali	43.00	2001	Ho	5.73	2001	Ho	4.76	2001	Ho

Table 14: The Results of Homogeneity Test for the Annual values

Station	Pettitt's Test			Standard Normal Homogeneity Test (SNHT)			Buishand Test		
	K	t	Trend	To	t	Trend	Q	t	Trend
Adhala	148.00	1996	Ha(D)	4.20	1980	Ho	4.76	1996	Ho
Ahruli	115.00	2003	Ho	3.19	2003	Ho	5.36	2003	Ho
Ambai	216.00	2002	Ho	10.09	2004	Ho	9.76	2002	Ha(l)
Ambedindori	162.00	1996	Ho	4.90	1996	Ho	7.17	1996	Ho
Amblihol	85.00	2005	Ho	1.81	1986	Ho	3.73	1986	Ho
Anjaneri	174.00	1983	Ho	11.18	1981	Ho	8.30	1983	Ho
Aswali	138.00	2003	Ho	9.33	1976	Ho	5.01	2003	Ho
Belpimp	107.00	1987	Ho	2.24	2006	Ho	4.15	2006	Ho
Bhagur	114.00	1986	Ho	2.97	1986	Ho	4.95	1986	Ho
Bhavarwadi	90.00	1999	Ho	1.81	1999	Ho	4.30	1999	Ho
Bhawali	68.00	2002	Ho	5.08	2005	Ho	5.28	2005	Ho
Bhojapur	124.00	1980	Ho	6.29	1980	Ho	5.32	1980	Ho
Bholtan	172.00	2000	Ho	4.43	2007	Ho	5.86	2000	Ho
Borvat	79.00	2003	Ho	2.19	2003	Ho	4.14	2003	Ho
Brahmangaon	194.00	1987	Ho	6.94	1987	Ho	7.77	1987	Ho
Charose	88.00	2002	Ho	4.79	1976	Ho	3.57	1994	Ho
Dahegaon	139.00	1989	Ho	2.78	2006	Ho	5.14	1992	Ho
Deogaon	48.00	2008	Ho	3.45	1979	Ho	1.85	2008	Ho
Deogaon-Rangeri	138.00	1992	Ho	6.20	2011	Ho	5.28	2011	Ho
Dokrin	254.00	1996	Ha(D)	10.51	1996	Ho	10.51	1996	Ha(D)
Dodambe	129.00	1981	Ho	6.38	1981	Ho	5.35	1981	Ho
Dondlagoan	36.00	1980	Ho	2.76	1987	Ho	1.58	1980	Ho
Dugaon	123.00	1987	Ho	3.42	1987	Ho	5.48	1989	Ho
Hatnoor	128.00	2006	Ho	5.23	2006	Ho	6.10	2006	Ho
Hivarkhed	110.00	1991	Ho	2.70	2013	Ho	4.38	2007	Ho
Indore	130.00	1986	Ho	4.43	1986	Ho	6.04	1986	Ho
Kadakojar	94.00	1995	Ho	1.90	1995	Ho	4.47	1995	Ho
Kadakhwagh	212.00	1994	Ho	10.25	2000	Ho	10.04	2000	Ha(D)
Kalanki	142.00	1986	Ho	2.74	1986	Ho	4.75	1986	Ho
KalgoanMal	192.00	1987	Ho	6.69	1986	Ho	7.59	1987	Ho
Karanjkhed	138.00	1989	Ho	6.24	1976	Ho	4.12	1989	Ho
Kirdisheta	120.00	1988	Ho	4.63	2013	Ho	5.03	2001	Ho
Kushigaon	168.00	1984	Ho	6.32	1981	Ho	5.76	1981	Ho
Loni	140.00	2000	Ho	10.52	2014	Ho	5.90	2000	Ho
Mahaladevi	118.00	2008	Ho	9.72	1976	Ho	5.04	1981	Ho
Mahalkhed	178.00	2008	Ho	11.48	2008	Ha(D)	8.70	2008	Ho
Manjur	106.00	1986	Ho	2.02	1986	Ho	4.35	1992	Ho

Nagmathan	130.00	2007	Ho	4.50	2010	Ho	4.86	2010	Ho
Nandur-Shingote	117.00	1989	Ho	3.24	1977	Ho	4.75	1989	Ho
Niphad	156.00	1989	Ho	2.22	1989	Ho	4.58	1989	Ho
Padhegaon	58.00	1986	Ho	4.54	1995	Ho	4.45	1987	Ho
Panegaon	86.00	1987	Ho	1.56	1987	Ho	3.68	1987	Ho
Phulambri	176.00	1993	Ho	6.52	1993	Ho	8.22	1993	Ho
Pimplegaon	144.00	2008	Ho	9.99	2011	Ho	7.62	2008	Ho
Pishor	108.00	1993	Ho	2.76	2011	Ho	4.09	1993	Ho
Rahata	168.00	1987	Ho	3.75	1987	Ho	5.71	1987	Ho
Rajur-Bhaula	230.00	1992	Ha(l)	4.88	2004	Ho	6.94	1996	Ho
Ramshej	222.00	1994	Ho	6.84	1994	Ho	8.46	1994	Ho
Samangaon	180.00	2000	Ho	7.15	2011	Ho	7.22	2000	Ho
Shendurwada	32.00	2011	Ho	2.15	2011	Ho	3.08	2007	Ho
Solegaon	108.00	2001	Ho	6.54	2014	Ho	6.64	2001	Ho
Somthan	122.00	1987	Ho	2.15	1987	Ho	4.33	1987	Ho
Thangoan	128.00	1987	Ho	3.78	1987	Ho	5.73	1987	Ho
Toka	170.00	1987	Ho	5.05	1987	Ho	6.75	1989	Ho
Usthale	130.00	2001	Ho	4.92	2001	Ho	6.36	2001	Ho
Wadalamahadeva	116.00	1986	Ho	2.56	1986	Ho	4.60	1986	Ho
Wasali	33.00	2003	Ho	1.90	2003	Ho		2003	Ho

The change point analysis for Monsoon months (June, July, August, September and October) reveals that, the time series (Rainfall values) are more or less homogeneous and no change in the rainfall mean observed. However, on annual time scale (Table 14), there are many stations which have recorded change in the mean annual rainfall, for example, Adhala and Dorkin recoded decreasing mean rainfall since 1996, similarly, the decreasing mean rainfall observed at Kadakwagh and Mahalkhed respectively from the year 2000 and 2008. However, there are few stations which have recorded the increasing mean rainfall at Ambai and Rajur-Bhaula respectively from 2002 and 1992. Leaving these stations, the data observed at other stations are found to be homogeneous.

4.3 Drought Analysis

These homogeneous rainfall series have been used to assess the drought condition in the catchment. The method described in section 3.3 has been used for analysis. The statistics of drought events such as intensity, duration and severity index were computed and are presented in Table 15.

Table 15: Statistics of Drought events in Jayakwadi Catchment

SI No	Station Name	Intensity	Duration	SI	SI No	Station Name	Intensity	Duration	SI
1	Deogaon	0.54	2.20	1.19	41	Nandur Shingote	0.60	2.20	1.33
2	Hivrakheda	0.72	2.43	1.74	42	Mahalkhed	0.65	2.25	1.47
3	Ganeshgaon	0.83	2.29	1.89	43	Whagera	0.95	4.00	3.78
4	Dhondalgaon	0.90	2.38	2.13	44	Toka	0.47	1.77	0.83
5	Deosane	0.48	1.86	0.90	45	Wadalamahadev	0.54	2.09	1.12
6	Dahegaon	0.85	3.71	3.14	46	Thangaon	0.68	2.22	1.51
7	Borvat	0.57	2.30	1.30	47	Somthan	0.60	2.20	1.31
8	Belpimp	0.52	1.91	1.00	48	Ramshej	0.41	2.67	1.10
9	Ahruli	0.70	2.75	1.92	49	KhanjarKhed	0.62	2.50	1.55
10	Nanashi	0.44	1.63	0.72	50	Khadak Ozar	0.64	1.70	1.08
11	Phulambri	0.70	2.25	1.57	51	Kirdisathe	1.00	3.14	3.14
12	Sanjegaon	0.65	2.75	1.79	52	Kalgaon_mal	0.79	3.29	2.59
13	Kalanki	0.56	2.30	1.29	53	Kushigaon	0.62	2.24	1.40
14	Khadakwada	0.50	1.55	0.78	54	Loni(Kh)	0.70	2.71	1.89
15	Adhala	0.67	2.33	1.56	55	Dodambe	0.55	3.00	1.66
16	Ambi	0.61	2.67	1.62	56	Dorkin	0.62	2.27	1.42
17	Anjaneri	0.81	3.43	2.78	57	Dongrapada	0.46	1.73	0.80
18	Bhagur	0.52	2.00	1.03	58	Dugaon	0.54	1.91	1.02
19	Kotul	0.49	2.56	1.26	59	Indore	0.56	2.11	1.18
20	Manjur	0.70	2.78	1.95	60	Hatnoor	0.46	2.30	1.06
21	Mahaladevi	0.44	2.22	0.99	61	Kopragaon	0.56	2.11	1.18
22	Nagamthan	0.67	2.67	1.79	62	Chehadi	0.27	1.60	0.43
23	Niphad	0.57	2.75	1.58	63	Mungusare	1.13	4.00	4.53
24	Panegaon	0.47	1.83	0.86	64	Nalwadi	0.72	2.00	1.44
25	Padhegaon	0.47	2.09	0.99	65	Nilwandi	0.89	3.00	2.68
26	Pimplegaon	0.62	2.50	1.54	66	Ozarkhed Dam	1.83	9.00	16.43
27	Samngaon	0.60	2.18	1.31	67	Palkhed Dam	2.18	7.00	15.23
28	Salegaon	0.52	1.86	0.97	68	Pimpri Anchal	0.30	1.33	0.40
29	Aswali	0.55	2.67	1.47	69	Shedurwada	0.45	1.60	0.72
30	Amblehol	0.50	2.10	1.06	70	Sonewadi	0.37	1.75	0.65
31	Ambedindori	0.84	2.63	2.21	71	tirdhe	0.37	1.50	0.55
32	Deogaon Rangari	1.02	3.33	3.38	72	Usthale	1.23	5.25	6.43
33	Charose	0.58	3.00	1.75	73	Vadangali	0.55	2.00	1.10
34	Bharamangaon	0.46	2.00	0.93	74	Vani	0.60	3.00	1.79
35	Bolthan	0.59	2.00	1.18	75	Vilvandi	0.34	1.75	0.59
36	Bhojapur	0.67	2.22	1.48	76	Ranjangaon	0.47	1.75	0.82
37	RajurBhula	0.65	2.75	1.78	77	Wasli	0.70	2.75	1.93
38	Rahata	0.64	2.00	1.27	78	Taked	0.88	4.00	3.53
39	Bhawali (BK)	0.46	1.17	0.53	79	Bharvarwadi	0.84	2.89	2.43
40	Pishor	0.53	1.54	0.81					

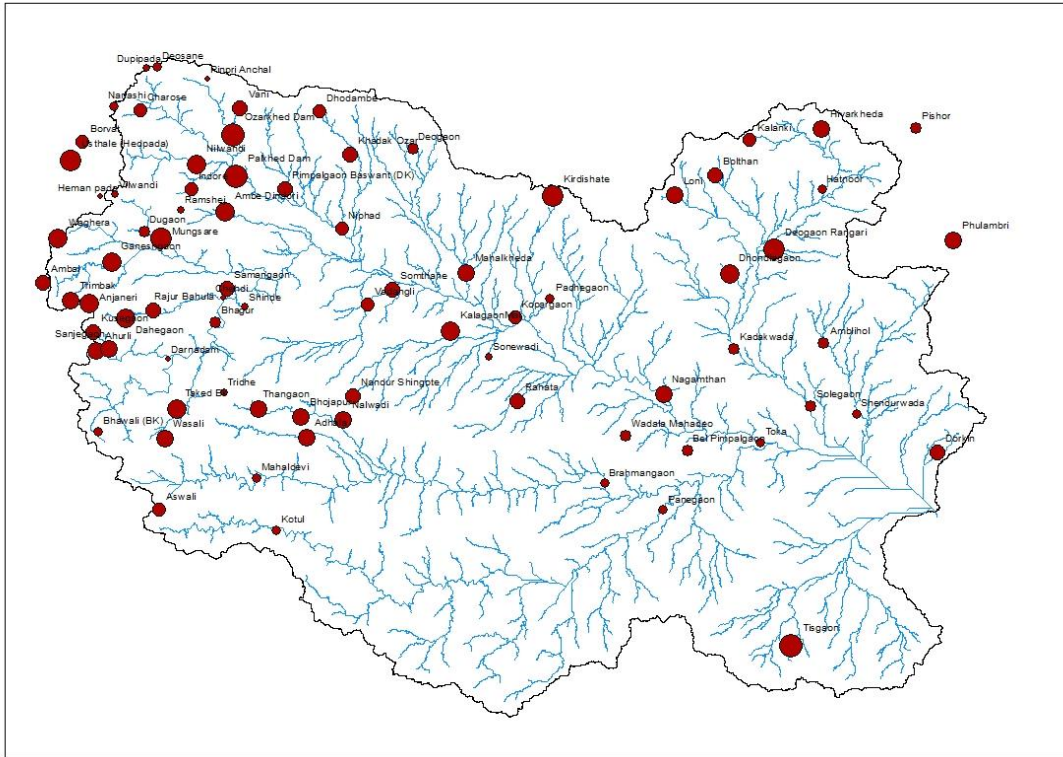


Figure : Spatial Distribution of Drought Intensity in Jayakwadi

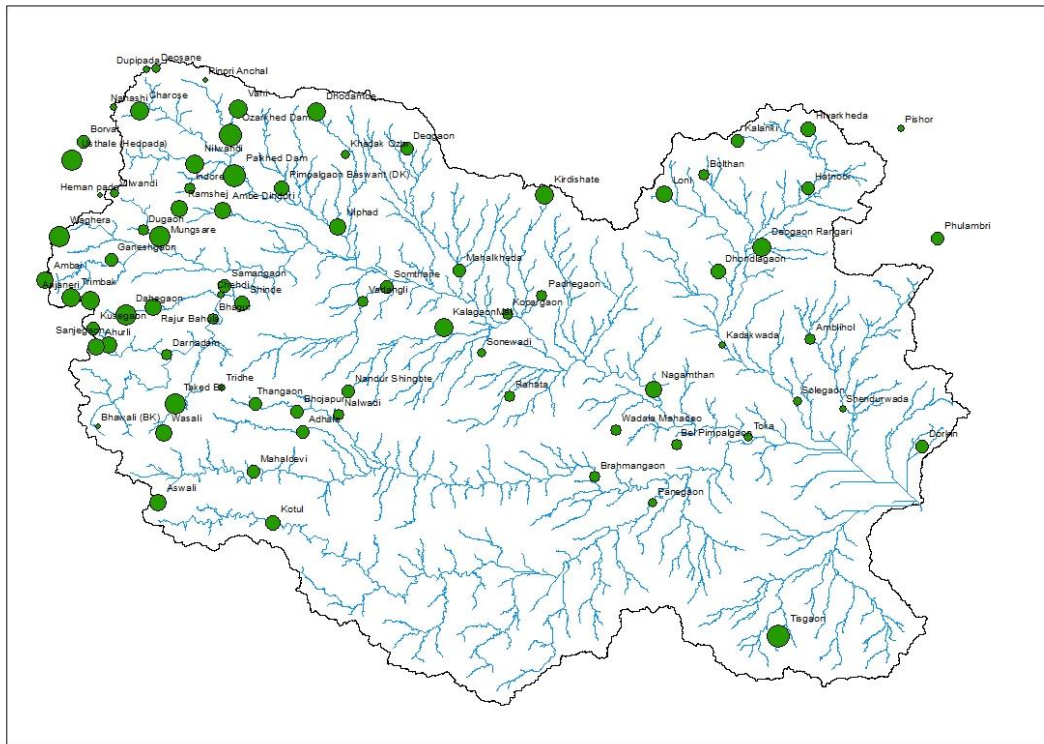


Figure : Spatial Distribution of Drought Duration in Jayakwadi

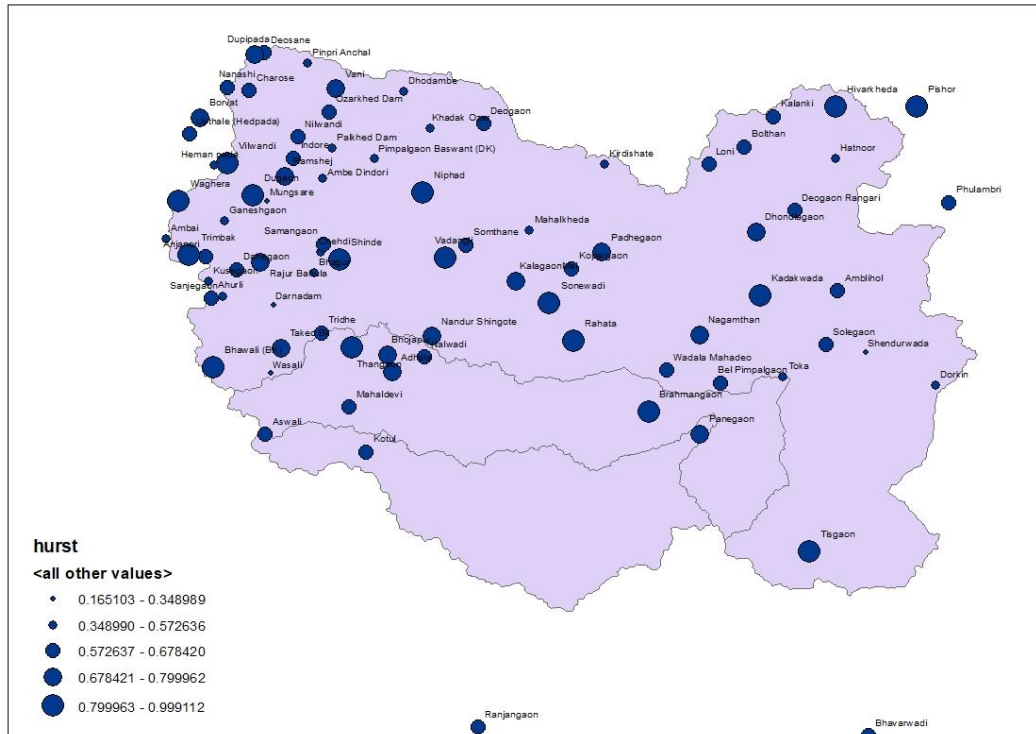


Figure : Spatial Distribution of Hurst Coefficient in Jayakwadi

The maximum computed Drought intensity is 2.13 with an average intensity of 0.62 with an average drought duration of 2.53 years. The maximum drought duration is recorded at Usthale station with 5 year duration. The Usthale station has recorded the higher drought intensity and higher drought duration, thereby the higher drought severity.

4.4 Analysis of Rainfall Values of IMD Grids

As state in the Table 3, the rainfall data for the Grids in which the filed observation is existing is considered for the analysis. The Grid data were obtained from the IMD website for a period of 1901 to 2018. The analysis procedure adopted earlier has been adopted for the analysis. The results obtained for the month of June, July, August, September, October and for Annual data are Tabulated in Table 16, Table 17, Table 18, Table 19, Table 20 and Table 21 respectively.

Table 16: The Results of Homogeneity Test for the June values

Grid No	Pettitt's Test			Standard Normal Homogeneity Test (SNHT)			Buishand Test		
	K	t	Trend	To	t	Trend	Q	t	Trend
1	490.00	1960	Ho	4.90	1901	Ho	10.23	1960	Ho
2	918.00	2002	Ho	52.09	2016	Ho	17.46	2003	Ha (I)
3	1214.00	1944	Ha (I)	9.77	1944	Ho	16.53	1944	Ha (I)
4	390.00	1970	Ho	3.81	1905	Ho	5.82	1961	Ho
5	477.00	1965	Ho	1.99	2007	Ho	6.27	1964	Ho
6	1014.00	1961	Ha (I)	10.20	2002	Ho	15.94	1961	Ha (I)
7	406.00	1970	Ho	2.89	1905	Ho	4.87	2003	Ho
8	908.00	1932	Ho	5.49	1932	Ho	11.37	1932	Ho
9	1022.00	1960	Ha(D)	6.59	2004	Ho	12.29	1970	Ho
10	980.00	1988	Ha (I)	15.89	2004	Ha (I)	14.74	2002	Ha (I)
11	1044.00	1992	Ha (I)	11.22	2003	Ho	13.24	1992	Ho
12	714.00	1970	Ho	3.71	1905	Ho	9.89	1970	Ho
13	363.00	1983	Ho	3.02	1905	Ho	5.61	1985	Ho
14	408.00	1964	Ho	2.31	2007	Ho	4.82	2007	Ho
15	604.00	1970	Ho	3.74	2007	Ho	6.55	2003	Ho
16	330.00	1908	Ho	2.49	1908	Ho	5.44	1985	Ho
17	998.00	1932	Ho	7.34	1932	Ho	13.14	1932	Ho
18	520.00	1970	Ho	7.63	1901	Ho	7.88	1960	Ho
19	1068.00	2003	Ha (I)	31.14	2004	Ha (I)	20.42	2003	Ha (I)
20	888.00	2003	Ho	18.35	2004	Ha (I)	15.84	2003	Ha (I)
21	792.00	1944	Ho	3.41	1906	Ho	9.52	1944	Ho
22	1074.00	1944	Ha (I)	5.38	1944	Ho	12.27	1944	Ho
23	538.00	1992	Ho	2.86	2007	Ho	7.33	1992	Ho
24	748.00	1992	Ho	6.00	2002	Ho	9.93	1992	Ho
25	493.00	1955	Ho	3.18	2007	Ho	6.46	1955	Ho
26	688.00	1930	Ho	8.18	1901	Ho	10.31	1930	Ho
27	3236.00	1959	Ha (I)	69.31	1960	Ha (I)	45.60	1960	Ha (I)
28	968.00	2003	Ho	24.01	2004	Ha (I)	17.90	2003	Ha (I)
29	902.00	1944	Ho	5.21	2004	Ho	11.47	1944	Ho
30	1208.00	1944	Ha (I)	6.12	1944	Ho	13.05	1944	Ho
31	698.00	1970	Ho	2.81	2002	Ho	6.74	1970	Ho
32	626.00	1954	Ho	1.72	2002	Ho	4.90	2002	Ho
33	924.00	1992	Ho	9.36	2007	Ho	12.41	1992	Ho
34	1366.00	1988	Ha (I)	20.40	2002	Ha (I)	20.52	1988	Ha (I)
35	1325.00	1953	Ha(D)	17.41	2004	Ha (I)	14.72	2004	Ha (I)
36	1538.00	1965	Ha (I)	19.83	2004	Ha (I)	21.51	1965	Ha (I)
37	984.00	1944	Ho	2.82	1944	Ho	8.88	1944	Ho

38	483.00	1935	Ho	5.38	2003	Ho	9.24	1988	Ho
39	581.00	1943	Ho	4.06	1998	Ho	9.70	1986	Ho
40	600.00	1954	Ho	2.93	1943	Ho	9.22	1954	Ho
41	668.00	1992	Ho	5.10	2002	Ho	8.83	1992	Ho
42	1338.00	1961	Ha (I)	10.83	2005	Ho	11.74	1988	Ha (I)
43	1072.00	1954	Ha (I)	5.83	2005	Ho	8.54	2004	Ho
44	1278.00	1959	Ho	5.77	2005	Ho	8.48	2005	Ho
45	551.00	1961	Ho	6.44	1998	Ho	11.10	1987	Ho
46	421.00	1955	Ho	4.81	1997	Ho	9.15	1997	Ho

Table 17: The Results of Homogeneity Test for the July values

Grid No	Pettitt's Test			Standard Normal Homogeneity Test (SNHT)			Buishand Test		
	K	t	Trend	To	t	Trend	Q	t	Trend
1	598.00	1979	Ho	4.30	1995	Ho	9.12	1995	Ho
2	864.00	1944	Ho	10.36	2017	Ho	12.36	1944	Ho
3	902.00	1987	Ho	5.98	1924	Ho	11.84	1944	Ho
4	942.00	1953	Ho	2.99	1953	Ho	9.41	1953	Ho
5	748.00	1966	Ho	5.36	1966	Ho	12.54	1966	Ho
6	936.00	1958	Ho	5.27	1958	Ho	12.57	1958	Ho
7	707.00	1969	Ho	4.48	1969	Ho	11.38	1969	Ho
8	628.00	1926	Ho	6.51	2016	Ho	10.03	1969	Ho
9	954.00	1974	Ho	6.72	1974	Ho	13.79	1973	Ho
10	758.00	1953	Ho	4.47	1954	Ho	11.54	1954	Ho
11	1000.00	1987	Ha(I)	7.78	1994	Ho	13.07	1987	Ho
12	628.00	1994	Ho	4.78	1994	Ho	9.76	1994	Ho
13	497.00	1969	Ho	2.04	1966	Ho	7.74	1966	Ho
14	954.00	1936	Ho	6.63	1936	Ho	12.93	1936	Ho
15	725.00	1969	Ho	4.58	1969	Ho	11.51	1969	Ho
16	831.00	1969	Ho	4.64	1969	Ho	11.58	1969	Ho
17	1753.00	1959	Ha(D)	22.76	1959	Ha(D)	26.02	1959	Ha(D)
18	760.00	1974	Ho	4.62	1974	Ho	11.42	1974	Ho
19	964.00	1930	Ho	12.50	2004	Ha(I)	14.77	1954	Ha(I)
20	1012.00	1930	Ha(I)	8.23	1924	Ho	13.54	1930	Ho
21	856.00	1987	Ho	8.12	1994	Ho	12.72	1994	Ho
22	866.00	1987	Ho	5.53	1994	Ho	11.64	1954	Ho
23	590.00	1930	Ho	2.25	1969	Ho	8.07	1969	Ho
24	1075.00	1969	Ha(D)	7.89	1969	Ho	15.10	1969	Ha(D)
25	999.00	1969	Ha(D)	6.94	1969	Ho	14.16	1969	Ha(D)

26	734.00	1938	Ho	5.48	1916	Ho	11.11	1931	Ho
27	3008.00	1959	Ha(I)	52.90	1959	Ha(I)	39.84	1959	Ha(I)
28	902.00	1930	Ho	13.88	2004	Ha(I)	14.27	1992	Ha(I)
29	986.00	1942	Ho	11.27	2005	Ha(I)	14.11	1994	Ha(I)
30	1134.00	1946	Ha(I)	11.51	1994	Ha(I)	15.16	1958	Ha(I)
31	553.00	1969	Ho	3.15	1969	Ho	9.55	1969	Ho
32	619.00	1969	Ho	3.51	1969	Ho	10.08	1969	Ho
33	737.00	1969	Ho	6.70	2013	Ho	9.65	1969	Ho
34	3362.00	1959	Ha(D)	77.19	1959	Ha(D)	48.12	1959	Ha(D)
35	1373.00	1951	Ha(D)	11.67	1951	Ha(D)	18.46	1951	Ha(D)
36	558.00	1959	Ho	2.19	2004	Ho	7.97	1959	Ho
37	546.00	1995	Ho	5.96	2005	Ho	8.61	2005	Ho
38	423.00	1975	Ho	2.89	1975	Ho	8.92	1975	Ho
39	382.00	1936	Ho	1.92	1916	Ho	5.19	1999	Ho
40	599.00	1969	Ho	3.17	1969	Ho	9.56	1969	Ho
41	904.00	1950	Ho	5.02	1936	Ho	11.81	1950	Ho
42	398.00	2004	Ho	7.12	2005	Ho	9.42	2005	Ho
43	400.00	1995	Ho	7.95	2005	Ho	9.95	2005	Ho
44	606.00	1988	Ho	9.92	2005	Ho	11.11	2005	Ho
45	422.00	1946	Ho	5.27	2004	Ho	9.12	1997	Ho
46	514.00	1936	Ho	1.59	2013	Ho	5.92	1936	Ho

Table 18: The Results of Homogeneity Test for the August values

Grid No	Pettitt's Test			Standard Normal Homogeneity Test (SNHT)			Buishand Test		
	K	t	Trend	To	t	Trend	Q	t	Trend
1	752.00	1914	Ho	8.69	1914	Ho	10.41	1914	Ho
2	754.00	1914	Ho	7.92	1914	Ho	9.93	1914	Ho
3	681.00	1914	Ho	6.13	1914	Ho	8.74	1914	Ho
4	1040.00	1979	Ha(I)	10.76	1979	Ha(I)	16.98	1979	Ha(I)
5	1314.00	1954	Ha(I)	11.33	1954		18.29	1954	Ha(I)
6	1100.00	1979	Ha(I)	12.47	1979	Ha(I)	18.27	1979	Ha(I)
7	978.00	1952	Ha(I)	7.31	1952	Ho	14.67	1953	Ha(I)
8	513.00	1943	Ho	3.45	1906	Ho	6.65	1943	Ho
9	702.00	1914	Ho	7.19	1914	Ho	9.47	1914	Ho
10	654.00	1914	Ho	6.00	1914	Ho	9.77	1971	Ho
11	764.00	1914	Ho	6.85	1914	Ho	9.24	1914	Ho
12	1344.00	1954	Ha(I)	15.23	1954	Ha(I)	21.29	1954	Ha(I)

13	910.00	1954	Ho	5.66	1954	Ho	12.93	1954	Ho
14	1362.00	1952	Ha(I)	11.57	1954		18.49	1954	Ha(I)
15	1492.00	1950	Ha(I)	15.52	1952	Ha(I)	21.34	1952	Ha(I)
16	1332.00	1954	Ha(I)	11.63	1954	Ha(I)	18.53	1954	Ha(I)
17	2105.00	1959	Ha(D)	30.22	1959	Ha(D)	29.98	1959	Ho
18	718.00	1962	Ho	7.10	1914	Ho	9.59	1962	Ho
19	696.00	1914	Ho	6.70	1914	Ho	9.63	1995	Ho
20	692.00	1995	Ho	4.55	1914	Ho	9.13	1995	Ho
21	453.00	1914	Ho	3.65	1914	Ho	6.74	1914	Ho
22	554.00	1914	Ho	5.22	1914	Ho	8.16	1915	Ho
23	1255.00	1953	Ha(I)	11.84	1954	Ha(I)	18.70	1954	Ha(I)
24	940.00	1952	Ho	7.20	1954	Ho	14.58	1954	Ho
25	1130.00	1954	Ha(I)	8.85	1954	Ho	16.17	1954	Ha(I)
26	804.00	1914	Ho	8.94	1914	Ho	10.55	1914	Ho
27	914.00	1988	Ho	9.65	1998	Ho	14.69	1971	Ha(I)
28	696.00	1996	Ho	6.50	1998	Ho	10.93	1996	Ho
29	568.00	1996	Ho	4.18	1914	Ho	7.76	1996	Ho
30	650.00	1914	Ho	6.04	1999	Ho	9.85	1999	Ho
31	1086.00	1986	Ha(I)	10.64	1986	Ha(I)	15.82	1986	Ha(I)
32	892.00	1986	Ho	6.52	1986	Ho	12.83	1954	Ho
33	874.00	1954	Ho	7.82	1954	Ho	15.20	1954	Ho
34	3524.00	1959	Ha(D)	77.21	1959	Ha(D)	48.13	1959	Ha(D)
35	610.00	1996	Ho	5.36	1998	Ho	9.48	1998	Ho
36	1436.00	1945	Ha(I)	19.36	1996	Ha(I)	21.21	1967	Ha(I)
37	1820.00	1967	Ha(I)	24.64	1967	Ha(I)	26.97	1967	Ha(I)
38	1002.00	1944	Ha(I)	8.39	1944	Ho	15.28	1944	Ha(I)
39	926.00	1954	Ho	8.62	1997	Ho	14.76	1954	Ha(I)
40	754.00	1986	Ho	6.03	1986	Ho	13.03	1954	Ho
41	1486.00	1954	Ha(I)	16.58	1954	Ha(I)	22.13	1954	Ha(I)
42	1866.00	1952	Ha(I)	16.00	1967	Ho	21.73	1967	Ha(I)
43	1766.00	1955	Ha(I)	15.47	1967	Ho	21.37	1967	Ha(I)
44	1922.00	1954	Ha(I)	17.72	1967	Ho	22.88	1967	Ha(I)
45	935.00	1953	Ho	12.19	2004	Ho	12.96	1997	Ha(I)
46	916.00	1954	Ho	10.09	1999	Ho	14.80	1954	Ho

Table 19: The Results of Homogeneity Test for the September values

Grid No	Pettitt's Test			Standard Normal Homogeneity Test (SNHT)			Buishand Test		
	K	t	Trend	To	t	Trend	Q	t	Trend
1	712.00	1965	Ho	6.78	1952	Ho	14.15	1952	Ho
2	715.00	1965	Ho	3.98	1952	Ho	10.84	1952	Ho
3	612.00	1965	Ho	3.26	1965	Ho	9.84	1965	Ho
4	3002.00	1959	Ha(D)	51.83	1959	Ha(D)	39.43	1959	Ha(D)
5	882.00	1950	Ho	5.51	1950	Ho	12.65	1950	Ho
6	2926.00	1959	Ha(D)	48.32	1959	Ha(D)	38.08	1959	Ha(D)
7	800.00	1956	Ho	5.00	1956	Ho	12.18	1956	Ho
8	535.00	1913	Ho	5.02	1912	Ho	8.44	1977	Ho
9	888.00	1965	Ho	6.88	1965	Ho	14.31	1965	Ha(D)
10	534.00	1952	Ho	2.76	1952	Ho	9.02	1952	Ho
11	506.00	1965	Ho	2.89	1930	Ho	8.70	1957	Ho
12	2944.00	1959	Ha(D)	50.68	1957	Ha(D)	38.96	1957	Ha(D)
13	437.00	1913	Ho	3.69	1913	Ho	6.56	1913	Ho
14	523.00	1913	Ho	4.69	1913	Ho	7.40	1913	Ho
15	680.00	1956	Ho	3.23	1956	Ho	9.79	1956	Ho
16	602.00	1956	Ho	2.09	2017	Ho	6.64	1956	Ho
17	1252.00	1964	Ha(D)	10.02	1964	Ho	17.21	1964	Ha(D)
18	716.00	1965	Ho	3.62	1952	Ho	10.33	1952	Ho
19	390.00	1930	Ho	1.97	1930	Ho	6.87	1957	Ho
20	436.00	1965	Ho	2.77	1957	Ho	9.12	1957	Ho
21	747.00	1965	Ho	5.62	1952	Ho	12.88	1952	Ho
22	686.00	1999	Ho	6.61	1999	Ho	13.10	1952	Ho
23	487.00	1913	Ho	3.99	1913	Ho	6.82	1913	Ho
24	586.00	1956	Ho	1.47	1956	Ho	6.61	1956	Ho
25	496.00	1950	Ho	1.36	2017	Ho	4.95	1950	Ho
26	862.00	1983	Ho	5.66	1952	Ho	12.93	1952	Ho
27	806.00	1965	Ho	4.28	1960	Ho	11.33	1960	Ho
28	549.00	1965	Ho	4.02	1957	Ho	10.97	1957	Ho
29	601.00	1965	Ho	4.82	1999	Ho	10.73	1957	Ho
30	675.00	1983	Ho	5.35	1999	Ho	9.28	1999	Ho
31	570.00	1956	Ho	3.47	1913	Ho	8.41	1956	Ho
32	858.00	1956	Ho	4.01	1956	Ho	10.91	1956	Ho

33	715.00	1989	Ho	5.61	1989	Ho	11.13	1989	Ho
34	3500.00	1959	Ha(D)	71.95	1959	Ha(D)	46.46	1959	Ha(D)
35	911.00	1965	Ho	7.67	1964	Ho	15.05	1964	Ho
36	2786.00	1959	Ho	48.15	1956	Ho	37.94	1956	Ho
37	2802.00	1957	Ha(D)	49.81	1956	Ha(D)	38.59	1956	Ha(D)
38	467.00	1913	Ho	4.10	2003	Ho	7.73	1997	Ho
39	394.00	1914	Ho	4.05	1998	Ho	8.23	1998	Ho
40	798.00	1964	Ho	4.76	1964	Ho	11.86	1964	Ho
41	768.00	1956	Ho	3.40	1956	Ho	10.04	1956	Ho
42	2718.00	1959	Ha(D)	47.76	1956	Ha(D)	37.79	1956	Ha(D)
43	2746.00	1957	Ha(D)	47.47	1956	Ha(D)	37.67	1956	Ha(D)
44	2822.00	1957	Ha(D)	50.80	1956	Ha(D)	38.99	1957	Ha(D)
45	364.00	1950	Ho	6.12	1998	Ho	10.12	1998	Ho
46	624.00	1964	Ho	2.71	1913	Ho	5.62	1913	Ho

Table 20: The Results of Homogeneity Test for the October values

Grid No	Pettitt's Test			Standard Normal Homogeneity Test (SNHT)			Buishand Test		
	K	t	Trend	To	t	Trend	Q	t	Trend
1	395.00	1911	Ho	2.83	1980	Ho	8.64	1980	Ho
2	402.00	1946	Ho	2.56	1980	Ho	8.23	1980	Ho
3	440.00	1911	Ho	3.59	2009	Ho	5.76	2009	Ho
4	2028.00	1959	Ha(D)	16.79	1959	Ha(D)	22.44	1959	Ha(D)
5	520.00	1926		2.34	1926	Ho	7.08	1930	Ho
6	2050.00	1959	Ha(D)	18.53	1959	Ha(D)	23.58	1959	Ha(D)
7	659.00	1973	Ho	1.90	1926	Ho	6.23	1926	Ho
8	496.00	1926	Ho	3.01	1961	Ho	9.46	1961	Ho
9	642.00	1981	Ho	3.91	1980	Ho	10.17	1980	Ho
10	350.00	1945	Ho	3.80	2009	Ho	5.92	2009	Ho
11	352.00	1911	Ho	5.38	2009	Ho	7.05	2009	Ho
12	2126.00	1959	Ha(D)	15.57	1959	Ha(D)	21.61	1959	Ha(D)
13	544.00	1926	Ho	3.58	1926	Ho	8.55	1926	
14	489.00	1926	Ho	2.49	1926	Ho	7.17	1986	Ho
15	462.00	1980	Ho	2.92	2016	Ho	7.11	1926	Ho
16	748.00	1972	Ho	3.37	1926	Ho	8.34	1927	Ho
17	1190.00	1926	Ha(I)	5.00	1930	Ho	10.62	1930	Ho
18	568.00	1981	Ho	1.95	1980	Ho	7.19	1980	Ho

19	443.00	1981	Ho	4.34	2009	Ho	7.14	1946	Ho
20	452.00	1981	Ho	3.79	2009	Ho	6.83	1945	Ho
21	480.00	1981	Ho	2.81	2009	Ho	6.15	1945	Ho
22	535.00	1981	Ho	3.14	2009	Ho	7.20	1945	Ho
23	582.00	1926	Ho	3.71	1926	Ho	8.71	1926	Ho
24	596.00	1926	Ho	3.86	1926	Ho	8.88	1926	Ho
25	694.00	1972	Ho	3.51	1926	Ho	8.83	1973	Ho
26	592.00	1981	Ho	4.12	2009	Ho	6.17	2009	Ho
27	688.00	1981	Ho	2.41	1980	Ho	8.22	1952	Ho
28	434.00	1981	Ho	2.59	2009	Ho	7.41	1945	Ho
29	556.00	1981	Ho	2.00	2009	Ho	7.45	1945	Ho
30	675.00	1983	Ho	5.35	1999	Ho	9.28	1999	Ho
31	646.00	1926	Ho	3.80	1926	Ho	8.81	1926	Ho
32	641.00	1926	Ho	5.06	1989	Ho	10.57	1989	Ho
33	537.00	1926	Ho	2.80	1926		7.56	1926	Ho
34	2818.00	1959	Ha(D)	26.06	1959	Ha(D)	27.96	1959	Ha(D)
35	697.00	1981	Ho	3.46	2009	Ho	6.13	1945	Ho
36	2382.00	1959	Ha(D)	21.73	1957	Ha(D)	25.51	1957	Ha(D)
37	2178.00	1959	Ha(D)	18.70	1959	Ha(D)	23.69	1959	Ha(D)
38	899.00	1926	Ho	5.91	1926	Ho	10.99	1926	Ho
39	674.00	1926	Ho	4.35	1926	Ho	9.44	1927	Ho
40	855.00	1983	Ho	7.36	1989	Ho	13.10	1983	Ho
41	616.00	1926	Ho	2.92	1926	Ho	7.73	1926	Ho
42	2358.00	1959	Ha(D)	24.04	1957	Ha(D)	26.83	1957	Ha(D)
43	2112.00	1959	Ha(D)	19.27	1959	Ha(D)	24.04	1959	Ha(D)
44	2206.00	1959	Ha(D)	20.33	1959	Ha(D)	24.70	1959	Ha(D)
45	641.00	1927	Ho	3.91	1927	Ho	9.06	1927	Ho
46	751.00	1992	Ho	5.47	1992	Ho	11.30	1983	Ho

Table 21: The Results of Homogeneity Test for the Annual values

Grid No	Pettitt's Test			Standard Normal Homogeneity Test (SNHT)			Buishand Test		
	K	t	Trend	To	t	Trend	Q	t	Trend
1	1100.00	1960	Ha (D)	11.33	1901	Ho	13.92	1960	Ho
2	992.00	1927	Ha (I)	40.95	2016	Ho	18.07	2002	Ha (I)
3	1066.00	1927	Ha (I)	10.76	1910	Ha (I)	14.91	1927	Ha (I)
4	614.00	1926	Ho	3.37	1909	Ho	6.82	1926	Ho
5	758.00	1966	Ho	4.61	1970	Ho	11.56	1966	Ho
6	946.00	1926	Ho	7.47	2004	Ho	11.83	1926	Ho

7	738.00	1970	Ho	4.18	1970	Ho	10.95	1970	Ho
8	910.00	1929	Ho	8.22	1929	Ho	13.29	1929	Ho
9	1322.00	1960	Ha (D)	11.24	1901	Ho	15.31	1960	Ha (D)
10	994.00	1968	Ha (I)	13.37	2003	Ho	14.14	1997	Ha (I)
11	1052.00	1993	Ha (I)	12.02	1996	Ho	15.00	1996	Ha (I)
12	696.00	1926	Ho	6.36	2004	Ho	11.40	1993	Ho
13	630.00	1926	Ho	2.58	1908	Ho	7.11	1926	Ho
14	995.00	1929	Ha (I)	7.99	1926	Ho	13.00	1929	Ho
15	942.00	1930	Ho	8.57	1930	Ho	13.90	1930	Ho
16	648.00	1930	Ho	4.64	1925	Ho	10.20	1930	Ho
17	1081.00	1929	Ha (I)	10.95	1929	Ha (I)	15.54	1929	Ha (I)
18	824.00	1930	Ho	14.26	1901	Ho	14.26	1901	Ho
19	1224.00	1930	Ha (I)	30.19	2004	Ha (I)	20.18	2003	Ha (I)
20	1106.00	1927	Ha (I)	16.48	2004	Ho	15.82	1996	Ha (I)
21	820.00	1927	Ho	6.18	1901	Ho	10.14	1988	Ho
22	862.00	1927	Ho	8.19	1901	Ho	11.17	1927	Ho
23	874.00	1926	Ho	7.14	1926	Ho	12.08	1926	Ho
24	778.00	1967	Ho	2.46	1997	Ho	7.44	1967	Ho
25	540.00	1930	Ho	3.80	2010	Ho	8.86	1930	Ho
26	1370.00	1930	Ha (I)	16.55	1930	Ha (I)	19.35	1930	Ha (I)
27	3394.00	1960	Ha (I)	81.29	1960	Ha (I)	49.38	1960	Ha (I)
28	1148.00	1996	Ha (I)	20.33	2004	Ho	16.48	1996	Ha (I)
29	982.00	1927	Ha (I)	9.09	2004	Ho	11.40	1996	Ho
30	1005.00	1927	Ha (I)	9.39	2005	Ho	12.61	1943	Ho
31	602.00	1926	Ho	3.52	1926	Ho	8.48	1926	Ho
32	749.00	1969	Ho	1.99	1926	Ho	6.67	1969	Ho
33	808.00	1990	Ho	11.28	2010	Ho	11.51	1990	Ho
34	3170.00	1959	Ha (D)	69.76	1959	Ha (D)	45.55	1959	Ha (D)
35	1791.00	1951	Ha (D)	15.67	2004	Ha (I)	15.60	1951	Ha (I)
36	1320.00	1942	Ha (I)	15.86	2004	Ho	15.65	1993	Ha (I)
37	500.00	1926	Ho	6.58	2004	Ho	9.33	2004	Ho
38	748.00	1926	Ho	5.44	2003	Ho	10.18	1987	Ho
39	592.00	1926	Ho	4.38	1997	Ho	9.37	1986	Ho
40	701.00	1967	Ho	4.27	1967	Ho	11.17	1967	Ho
41	844.00	1926	Ho	6.04	1926	Ho	11.11	1926	Ho
42	1398.00	1945	Ha (I)	9.00	2005	Ho	10.88	2004	Ho
43	374.00	1913	Ho	6.06	2005	Ho	8.94	2004	Ho
44	388.00	1913	Ho	6.32	2005	Ho	9.05	2004	Ho
45	488.00	1926	Ho	6.64	1997	Ho	10.75	1997	Ho
46	476.00	1926	Ho	4.73	1995	Ho	9.40	1995	Ho

The Grid based analysis indicate that the annual total rainfall are showing greater change in the mean annual rainfall across majority of the grids at different time period (Table 21). However, the changes are most towards the increasing trend. On the other hand, the change in the mean annual rainfall is not evident in respect of the point rainfall measurement.

Comparison of Results of Point Rainfall and IMD Gridded Data

A comparison of the results obtained through the analysis of Homogeneity, trend and change in magnitude of rainfall across all IMD gridded data and the point observed data are presented in Table *** for homogeneity, Table ** for trend and Table *** for change in magnitude of rainfall as percent of their mean rainfall.

Table *** : Comparison of the Homogeneity

Grid	Station	June		July		August		Sept		Oct		Annual	
		IMD Grid	Station	IMD Grid	Station	IMD Grid	Station	IMD Grid	Station	IMD Grid	Station	IMD Grid	Station
1	Hemapada	Ho	Ho	Ho	Ho	Ho	Ho	Ho	Ho	Ho	Ho	Ho	Ho
	Deosane		Ho		Ho		Ho		Ho		Ho		
	Nanashi		Ho		Ho		Ho		Ho		Ho		
	Tirdhe		Ho		Ho		Ho		Ho		Ho		
	Mahaje		Ho		Ho		Ho		Ho		Ho		
2	Pimpri Anchala	Ha (I)	Ho	Ho	Ho	Ho	Ho	Ho	Ho	Ho	Ho	Ho	Ho
	Vani		Ho		Ho		Ho		Ho				
	Ozarkhed dam		Ho		Ho		Ho		Ho		Ha (I)		Ho
3	Dhodambe	Ha (I)	Ho		Ho	Ho	Ho	Ho	Ho	Ho	Ho	Ha (I)	Ho
4		Ho		Ho		Ha(I)		Ha(D)		Ha(D)		Ho	
5		Ho		Ho		Ha(I)		Ho		Ho		Ho	
6		Ha (I)		Ho		Ha(I)		Ha(D)		Ha(D)		Ho	
7		Ho		Ho		Ha(I)		Ho		Ho		Ho	
8		Ho		Ho		Ho		Ho		Ho		Ho	
9	Vilwandi	Ho	Ho	Ho	Ho	Ho	Ho	Ha(D)	Ho	Ho	Ho	Ho	Ho
	Dugaon		Ho		Ho		Ho		Ho				
	Mungsare		Ho		Ho		Ho		Ho				
	Waghera		Ho		Ho		Ho		Ho				
10	Nilwandi	Ha (I)	Ho	Ho	Ho	Ho	Ho	Ho	Ho	Ho	Ho	Ho	Ho
	Palkhed dam		Ho		Ho		Ho		Ho				
	Pimplagaon Baswant		Ho		Ho		Ho		Ho		Ho		Ha (I)

Table *** : Comparison of Trend of Rainfall at point measurement and IMD Gridded data

Grid	Station	June		July		August		Sept		Oct		Annual	
		IMD Grid	Station	IMD Grid	Station	IMD Grid	Station	IMD Grid	Station	IMD Grid	Station	IMD Grid	Station
1	Hemapada	-0.20	6.92	-0.98	13.28	-0.32	-20.76	-0.02	-3.21		-8.32	-4.70	9.51
	Deosane		0.00		2.31		2.91		3.15		0.00		5.02
	Nanashi		0.00		0.00		0.00		2.75		1.12		0.00
	Tirdhe		-16.00		13.04		-20.68		2.02		-23.87		-11.11
	Mahaje												
2	Pimpri Anchala	0.63		0.42		0.07		-0.05				1.00	
	Vani		0.00		3.30		1.25		1.85		0.92		6.58
	Ozarkhed dam		0.00		0.65		0.13		1.69		1.04		1.37
3	Dhodambe	0.49	-1.99	0.47	-0.59	0.01	-1.04	-0.03	0.29		0.00	0.84	-4.34
4													
5													
6													
7													
8													
9	Vilwandi	-1.10	-13.85	-0.92	30.89	-0.43	3.53	-0.04	-2.69		-4.83	-4.09	-8.80
	Dugaon		-0.03		0.23		-0.24		0.81		0.43		0.06

	Mungsare		0.13		2.85		2.05		1.36		0.43		10.78
	Waghera		-2.59		-9.25		-7.41		-0.26		0.00		-21.97
10	Nilwandi	0.71	0.00	0.43	0.66	0.07	0.00	-0.02	0.80		0.28	1.89	2.18
	Palkhed dam		2.50		8.00		0.00		10.90		-0.50		10.50
	Pimplagaon Baswant		-1.40		-2.62		-4.27		-2.37		-0.36		-2.93
	Ramshej		-0.01		-3.70		-4.15		1.08		0.00		-8.02
	Ambe Dindori		0.00		0.93		-0.09		0.61		0.13		3.38
11	Khadak ozar	0.39	0.00	0.49	2.17	0.10	-0.25	-0.02	0.12		0.20	0.74	0.93
	Niphad		0.01		1.09		0.12		0.50		0.59		2.40
12													
13													
14	Bolthan	-0.05	-0.73	-0.07	-0.06	0.54	-0.90	-0.35	-0.42	0.09	0.36	-0.20	-3.93
15	Deogaon Rangari	-0.20	-2.00	-0.19	1.32	0.58	-0.35	-0.48	0.31	0.10	0.00	-0.14	-2.82
16													
17	Ambai	1.03	1.15	-4.95	4.23	-4.40	1.36	-1.86	2.40	0.35	1.18	-1.94	14.72
18	Anjaneri	-0.32	2.77	-1.41	-9.03	-0.75	-12.42	-0.03	-5.37		-0.61	-3.18	-5.96
	Ahurli		-2.77		0.49		-3.13		-1.64		0.15		-3.90
	Sanjegaon		-3.50		0.00		-1.40		0.80		0.05		0.00
	Rajur Bahula		0.70		5.69		2.20		2.49		0.00		10.05
	Mahiravni												
	Darna Dam		-15.20		34.50		25.00		7.75		-3.20		37.67
19	Chahdi	0.62	-0.88	0.46	16.69	0.26	1.25	-0.04	3.33		3.40	2.11	8.97
	Shinde		2.69		47.00		4.80		-4.26		5.18		111.51
	Bhagur		0.57		1.22		0.42		-2.70		-0.59		0.08
20	Vadangali	0.24	0.88	0.39	7.93	0.20	2.72	-0.04	9.58		1.14	1.11	7.70

6														
7														
8														
9	Vilwandi	-14.81		-22.59		-22.39		-12.08		29.33		40.66	-20.94	
	Dugaon		-1.60		11.54		-10.63		29.33		40.66			0.54
	Mungsare		5.86		73.04		46.80		70.19		31.60			83.65
	Waghera		-41.82		-61.56		-61.09		-4.76		0.00			-54.86
10	Nilwandi	37.13	0.00	34.33	8.27	5.85	0.00	-4.96	17.12	25.91	13.57	25.91	9.05	
	Palkhed dam		47.83		56.41		0.00		74.47		-11.96		21.51	
	Pimplagaon Baswant		-37.61		-44.36		-91.24		-70.57		-31.00		-14.50	
	Ramshej		-0.32		-41.00		-70.74		26.25		0.00		-32.31	
	Ambe Dindori		0.00		30.86		-3.58		25.55		12.47		29.60	
11	Khadak ozar	32.97	0.00	49.58	80.84	7.74	-10.40	-5.95	5.35	12.90	23.00	12.90	8.94	
	Niphad		0.47		40.82		5.05		16.87		44.88		19.46	
12														
13														
14	Bolthan	-4.18	-32.47	-5.25	-2.46	51.20	-31.12	-24.59	-14.85	17.54	36.70	-3.32	-32.56	
15	Deogaon Rangari	-14.57	-75.10	-10.99	41.58	36.49	-11.14	-29.73	10.59	19.83	0.00	-1.81	-20.89	
16														
17	Ambai	24.88	16.80	-52.51	21.31	-70.25	8.41	-57.43	34.34	31.10	72.66	-6.94	28.42	
18	Anjaneri	-2.72	37.41	-20.35	-65.21	-28.38	-114.98	-7.08	-116.92	-10.21	-10.85	-10.21	-14.23	
	Ahurli		-51.27		3.05		-22.97		13.67		-9.52			
	Sanjegaon		-55.73		0.00		-11.02		3.18		0.00			
	Rajur Bahula		18.31		88.67		39.74		55.66		0.00		44.75	

	Mahiravni												
	Darna Dam		-66.12		66.48		58.95		25.87		-38.15	24.20	
19	Chahdi	24.68	-10.51	28.17	114.84	17.68	9.43	-11.64	28.25		71.75	23.63	17.86
	Shinde		20.57		61.01		9.27		-17.10		52.79		63.15
	Bhagur		23.93		53.55		16.81		-69.23		-31.83		0.57
20	Vadangali	20.17	12.91	42.30	104.67	15.60	32.74	-10.68	83.47		23.84	19.19	20.32
21	Somthane	24.32	11.51	46.93	34.06	-1.14	36.24	-21.79	49.45		0.00	1.69	23.21
	Mahalkheda		-96.74		-28.50		-34.56		20.96		-2.69		-39.84
22	Padhegaon	31.25	-10.58	51.34	38.44	-6.82	67.18	-24.51	5.63		0.00	3.97	29.70
	Kopargaon												
23	Khadak Waghgaon	-10.50	-105.47	-3.39	-5.68	61.49	-10.87	-16.25	-18.41	8.42	-46.80	-8.26	-58.36
24	Ambegaon	-25.90	0.00	-28.95	30.86	36.51	-3.58	-24.03	25.55	24.75	12.47	-69.81	29.60
25													
26	Wasali	8.92	0.00	4.90	66.82	-7.89	47.73	-26.16	53.11		-85.05	5.72	24.72
27	Taked BK	144.20	0.00	119.48	0.00	39.79	0.00	-31.33	0.53		0.00	118.92	0.00
	Thangaon		16.24		33.17		10.55		54.44		30.07		1.43
28	Sangamner	31.44		50.26		17.58		-16.29				17.97	
	Nandur Shingote		12.74		0.86		39.63		62.17		41.33		5.41
29	Rahata	23.96	-13.02	64.01	0.41	11.51	40.16	-21.92	22.48		35.88	10.79	8.05
30	Wadala Mahdeo	32.80	-29.42	72.64	77.12	16.78	54.51	-18.72	34.39		2.77	19.23	14.49
	Bodhegaon												
31	Nawasa	-19.71		1.49		62.61		-23.44		7.03		-15.05	
	Pimplebaon		-11.19		36.26		-7.67		-3.07		0.00		2.67

The Table ***, show that, change in the rainfall as percent of mean rainfall of grid is as high as -70% (decrease) in the month of August and 74% (increase) July across all the grids. However, month of September recorded a decreasing magnitude of rainfall across all the grids. Similarly, the point measured rainfall (at observation stations), an identical pattern has been observed, wherein as high as -91% (decreasing) and 77% increasing. Further, it is understood from the Table ***, that, there are many instances where the observed change in the rainfall magnitude (increasing/decreasing) at grid level are quite opposite to that of the observation point. For ex, the grid no 10 registered mostly the increasing magnitude, whereas the station falling within the grid no 10 have decreasing magnitude to an extent of 91%. The possible reasons for such variation could be, (i) the length of data used for the study, i.e., more than 100 year for IMD grid and around 40 years of observed data; (ii) number of stations and nature of data used for developing the IMD gridded data.

5.0 Analysis of GCM Project Rainfall and Temperature

5.1 What are GCM Models

General Circulation Models (GCMs) are a class of computer-driven models for weather forecasting, understanding climate and projecting climate change, where they are commonly called Global Climate Models. A global climate model or general circulation model aims to describe climate behavior by integrating a variety of fluid-dynamical, chemical, or even biological equations that are either derived directly from physical laws (e.g. Newton's law) or constructed by more empirical means. There are both atmospheric GCMs (AGCMs) and ocean GCMs (OGCMs). An AGCM and an OGCM can be coupled together to form an atmosphere-ocean coupled general circulation model (AOGCM). A recent trend in GCMs is to extend them to become Earth system models, that include such things as sub models for atmospheric chemistry or a carbon cycle model to better predict changes in carbon dioxide concentrations resulting from changes in emissions.

Climate models are based on well-documented physical processes to simulate the transfer of energy and materials through the climate system. Climate models, also known as general circulation models or GCMs, use mathematical equations to characterize how energy and matter interact in different parts of the ocean, atmosphere, land. Building and running a climate model is complex process of identifying and quantifying Earth system processes, representing them with mathematical equations, setting variables to represent initial conditions and subsequent changes in climate forcing, and repeatedly solving the equations using powerful supercomputers.

5.1.2 Climate Model Resolution

Climate models separate Earth's surface into a three-dimensional grid of cells. The results of processes modeled in each cell are passed to neighboring cells to model the exchange of matter and energy over time. Grid cell size defines the resolution of the model: the smaller the size of the grid cells, the higher the level of detail in the model. More detailed models have more grid cells, so they need more computing power.

Climate models also include the element of time, called a time step. Time steps can be in minutes, hours, days, or years. Like grid cell size, the smaller the time step, the more detailed the results will be. However, this higher temporal resolution requires additional computing power.

5.1.3 How are Climate Models Tested?

Once a climate model is set up, it can be tested via a process known as "hind-casting." This process runs the model from the present time backwards into the past. The model results are then compared with observed climate and weather conditions to see how well they match. This testing allows scientists to check the accuracy of the models and, if needed, revise its equations. Science teams

around the world test and compare their model outputs to observations and results from other models.

5.1.4 Using Scenarios to Predict Future Climate

Once a climate model can perform well in hind-casting tests, its results for simulating future climate are also assumed to be valid. To project climate into the future, the climate forcing is set to change according to a possible future scenario. Scenarios are possible stories about how quickly human population will grow, how land will be used, how economies will evolve, and the atmospheric conditions (and therefore, climate forcing) that would result for each storyline.

In 2000, the Intergovernmental Panel on Climate Change (IPCC) issued its Special Report on Emissions Scenarios (SRES), describing four scenario families to describe a range of possible future conditions. Referred to by letter-number combinations such as A1, A2, B1, and B2, each scenario was based on a complex relationship between the socioeconomic forces driving greenhouse gas and aerosol emissions and the levels to which those emissions would climb during the 21st century. The SRES scenarios have been in use for more than a decade, so many climate model results describe their inputs using the letter-number combinations.

In 2013, climate scientists agreed upon a new set of scenarios that focused on the level of greenhouse gases in the atmosphere in 2100. Collectively, these scenarios are known as Representative Concentration Pathways or RCPs. Each RCP indicates the amount of climate forcing, expressed in Watts per square meter, that would result from greenhouse gases in the atmosphere in 2100. The rate and trajectory of the forcing is the pathway. Like their predecessors, these values are used in setting up climate models.

5.1.5 How are the RCPs different from previous scenarios?

In preparation for the Fifth Assessment Report (AR5), researchers developed a new approach for creating and using scenarios in climate change research. This new approach was motivated by the changing information needs of policy makers. For example the increasing interest in exploring different approaches to achieving specific climate change targets (such as limiting change to 2°C), and growing interest in a “risk management” approach that combines reductions in emissions and adaptation to reduce climate change damages.

Scientific advances also dictated the need for new scenarios. Since the Fourth Assessment Report (AR4) important improvements in climate models have been made. As the climate models became more sophisticated, more detailed input was needed. Simultaneously, models that are used in the production of scenarios have improved and more advanced input can therefore be provided.

5.1.6 What is radiative forcing?

Radiative forcing, expressed as Watts per square metre, is the additional energy taken up by the Earth system due to the enhanced greenhouse effect. More precisely, it can be defined as the difference in the balance of energy that enters the atmosphere and the amount that is returned to space compared to the pre-industrial situation. Total radiative forcing is determined by both

positive forcing from greenhouse gases and negative forcing from aerosols. The dominant factor by far is the positive forcing from CO₂. As the radiative forcing increases, the global temperature rises. However, the precise relationship between these factors is not fully known.

The new approach is built around the concept of Representative Concentration Pathways (RCPs). RCPs are time and space dependent trajectories of concentrations of greenhouse gases and pollutants resulting from human activities, including changes in land use. RCPs provide a quantitative description of concentrations of the climate change pollutants in the atmosphere over time, as well as their radiative forcing in 2100 (for example, RCP 6 achieves an overall impact of 6 watts per square metre by 2100). The word “representative” signifies that each RCP provides only one of many possible scenarios that would lead to the specific radiative forcing pathway. Radiative forcing is a measure of the additional energy taken up by the Earth system due to increases in climate change pollution (see box on radiative forcing).

5.1.7 How were the RCPs developed and how are they used in climate research?

Each RCP was developed by a different modelling group. Since the RCPs had been developed with different, independent models, they are not directly comparable. By fixing the pathways for the radiative forcing and the concentrations, climate modellers could already begin with their simulations and analyse the results for the Fifth Assessment Report (published in September 2013). In a parallel process, the scenario community is developing a set of consistent socio-economic scenarios with storylines to guide mitigation, adaptation, and mitigation analysis. These are called shared socioeconomic pathways (SSPs) and will be assessed in the IPCCs AR5 Working Group 3 Report released in March 2014.

A key difference between the new RCPs and the previous scenarios is that there are no fixed sets of assumptions related to population growth, economic development, or technology associated with any RCP. Many different socio-economic futures are possible leading to the same level of radiative forcing. This enables researchers to test various permutations of climate policies and social, technological, and economic circumstances. For example, at a global scale, higher population or increased energy consumption could be compensated by a higher fraction of renewable energy. So rather than prescribing the economic development and calculate climate change, researchers could pick an RCP scenario that is compatible with the 2°C target, for example, and then assess various technology and policy options to achieve the emissions consistent with that pathway and target. In previous scenarios, for example the SRES, analysis started with a socio-economic storyline from which emission trajectories and climate impacts were assessed. This essentially ‘locked in’ the options for socioeconomic change and made such explorations difficult.

5.1.7.1 Gases and pollutants included in the RCPs

Greenhouse gases such as, CO₂, methane, Nitrous oxide, Several groups of fluorocarbons and sulphur and Hexafluoride. The Aerosols and chemically active gasses; Sulphur dioxide, Soot, Organic carbon, Carbon monoxide, Nitrogen oxides, Volatile organic compounds and Ammonia.

Another key difference is that the RCPs are spatially explicit and provide information a global grid at a resolution of approximately 60 kilometres. This gives the spatial and temporal information about the location of various emissions and land use changes. This is an important improvement as the location of some emissions affects their warming potential.

5.1.7.2 The RCPs used in AR5

The four RCPs are consistent with certain socio-economic assumptions. These will later be replaced by the Shared Socio-economic Pathways which will provide flexible descriptions of possible futures within each RCP.

RCP 8.5 – High emissions

This RCP is consistent with a future with no policy changes to reduce emissions. It was developed by the International Institute for Applied System Analysis in Austria and is characterised by increasing greenhouse gas emissions that lead to high greenhouse gas concentrations over time. Comparable SRES scenario A1 F1. This future is consistent with:

- Three times today's CO₂ emissions by 2100
- Rapid increase in methane emissions
- Increased use of croplands and grassland which is driven by an increase in population
- A world population of 12 billion by 2100
- Lower rate of technology development
- Heavy reliance on fossil fuels
- High energy intensity
- No implementation of climate policies

RCP 6 – Intermediate emissions

This RCP is developed by the National Institute for Environmental Studies in Japan. Radiative forcing is stabilised shortly after year 2100, which is consistent with the application of a range of technologies and strategies for reducing greenhouse gas emissions. Comparable SRES scenario: B2

This future is consistent with:

- Heavy reliance on fossil fuels
- Intermediate energy intensity
- Increasing use of croplands and declining use of grasslands
- Stable methane emissions
- CO₂ emissions peak in 2060 at 75 per cent above today's levels, then decline to 25 per cent above today

RCP 4.5 – Intermediate emissions

This RCP is developed by the Pacific Northwest National Laboratory in the US. Here radiative forcing is stabilised shortly after year 2100, consistent with a future with relatively ambitious emissions reductions. Comparable SRES scenario: B1

This future is consistent with:

- Lower energy intensity
- Strong reforestation programmes
- Decreasing use of croplands and grasslands due to yield increases and dietary changes

- Stringent climate policies
- Stable methane emissions
- CO₂ emissions increase only slightly before decline commences around 2040

RCP 2.6 – Low emissions

This RCP is developed by PBL Netherlands Environmental Assessment Agency. Here radiative forcing reaches 3.1 W/m² before it returns to 2.6 W/m² by 2100. In order to reach such forcing levels, ambitious greenhouse gas emissions reductions would be required over time. Comparable SRES scenario: None

This future would require:

- Declining use of oil
- Low energy intensity
- A world population of 9 billion by year 2100
- Use of croplands increase due to bio-energy production
- More intensive animal husbandry
- Methane emissions reduced by 40 per cent
- CO₂ emissions stay at today's level until 2020, then decline and become negative in 2100
- CO₂ concentrations peak around 2050, followed by a modest decline to around 400 ppm by 2100

5.2 Cordex Data

The WCRP CORDEX foster international partnership in order to produce an ensemble of high-resolution past and future climate projections at regional scale. This CORDEX dataset is comprised of downscaled climate scenarios for the South Asia region that are derived from the Atmosphere-Ocean coupled General Circulation Model (AOGCM) runs conducted under the Coupled Model Intercomparison Project Phase 5 (CMIP5) [Taylor et al. 2012] and using three of the four greenhouse gas emissions scenarios known as Representative Concentration Pathways (RCPs) [Meinshausen et al. 2011]. The CMIP5 AOGCM runs were developed in support of the Fifth Assessment Report of the Intergovernmental Panel on Climate Change (IPCC AR5). The coarser spatial resolution ranging from 1.0° to 3.8°, and systematic error (called bias) of these AOGCMs limits the examination of possible impacts of climate change and adaptation strategies on a smaller scale. The CORDEX South Asia dataset includes dynamically downscaled projections from the 10 models and scenarios for which daily scenarios were produced and distributed under CMIP5. The purpose of these datasets is to provide a set of high resolution (25 km) regional climate change projections that can be used to evaluate climate change impacts on processes that are sensitive to finer-scale climate gradients and the effects of local topography on climate conditions.

The dynamical downscaling method using high resolution limited area regional climate models (RCMs) utilizes the outputs provided by AOGCMs as lateral boundary condition to provide physically consistent spatiotemporal variations of climatic parameters at spatial scales much smaller than the AOGCMs' grid. The RCMs by resolving the topographical details, coastlines, and land-surface heterogeneities allow the reproduction of small-scale processes and information that are most useful for impact assessment and in decision making for adaptation (Flato et al. 2013). An initial assessment of the ability of the CORDEX RCMs to simulate the general characteristics of the Indian climate indicated that the geographical distribution of surface air temperature and seasonal precipitation in the present climate for land areas in South Asia is strongly affected by

the choice of the RCM and boundary conditions (i.e. driving AOGCMs), and the downscaled seasonal averages are not always improved (Sanjay et al. 2017). The data for the following models have been used in the present study (Table **).

Table *** : The RCM's considered for the present study

CORDEX South Asia RCM	RCM Description	Contributing CORDEX Modeling Center	Driving CMIP5 AOGCM (see details at https://verc.enes.org/data/enes-model-data/cmip5/resolution)	Contributing CMIP5 Modeling Center
IITM-RegCM4 (6 ensemble members)	The Abdus Salam International Centre for Theoretical Physics (ICTP) Regional Climatic Model version 4.4.5 (RegCM4; Giorgi et al., 2012)	Centre for Climate Change Research (CCCR), Indian Institute of Tropical Meteorology (IITM), India	GFDL-ESM2M	National Oceanic and Atmospheric Administration (NOAA), Geophysical Fluid Dynamics Laboratory (GFDL), USA
			MPI-ESM-MR	Max Planck Institute for Meteorology (MPI-M), Germany
			IPSL-CM5A-LR	Institut Pierre-Simon Laplace (IPSL), France
SMHI-RCA4 (10 ensemble members)	Rossby Centre regional atmospheric model version 4 (RCA4; Samuelsson et al., 2011)	Rosssy Centre, Swedish Meteorological and Hydrological Institute (SMHI), Sweden	NorESM1-M	Norwegian Climate Centre (NCC), Norway
			MPI-ESM-LR	MPI-M, Germany
			IPSL-CM5A-MR	IPSL, France
CCAM (6 ensemble members)	Commonwealth Scientific and Industrial Research Organisation (CSIRO), Conformal-Cubic Atmospheric Model (CCAM; McGregor and Dix, 2001)	CSIRO Marine and Atmospheric Research, Melbourne, Australia	ACCESS1-0	CSIRO, Australia

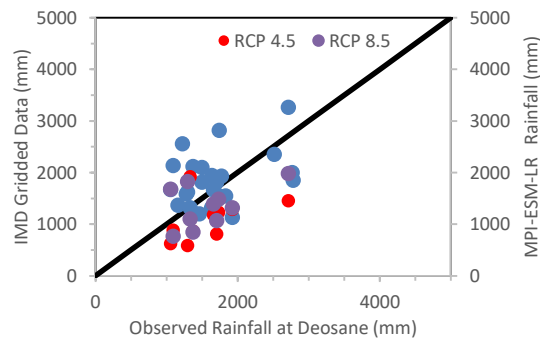
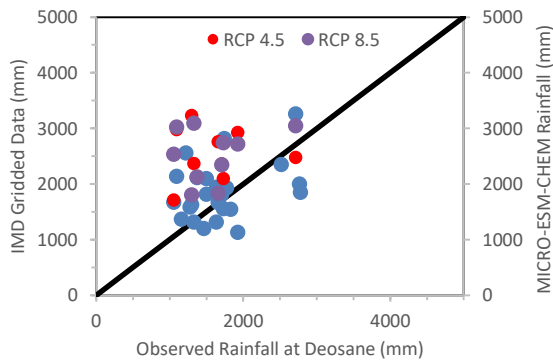
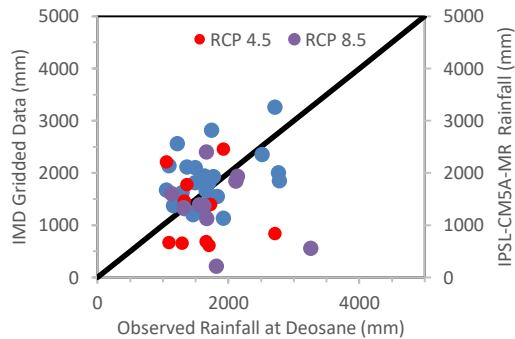
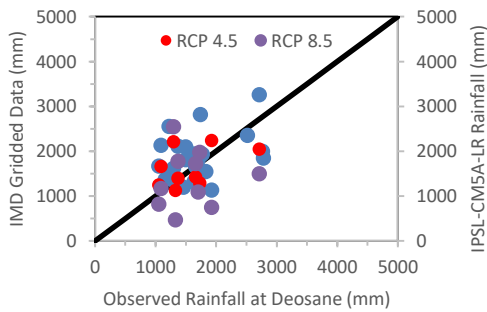
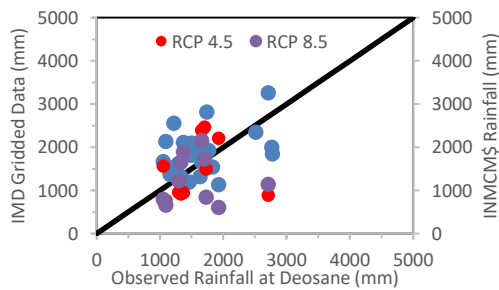
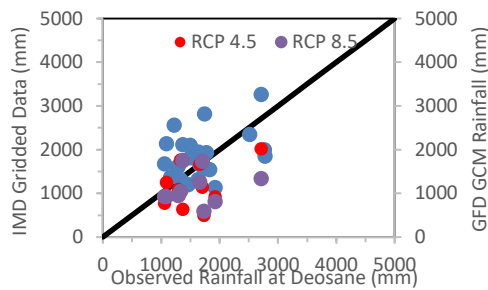
		Institute of Numerical Mathematics Climate Model Version 4 (INMCM4) coupled atmospheric-ocean general circulation model from Moscow, Russia	INMCM4	
		the Meteorological Research Institute of Japan Meteorological Agency	MRI-CGCM3	
This coupled model is comprised of 4 individual models; an atmospheric model, oceanic and sea-ice model, land surface model, and a coupling model.	the Center for Climate System Research (CCSR) at the University of Tokyo, Japan.	Interdisciplinary Research on Climate version 5 (MIROC5) Japan	MICRO-ESM-CHEM	

5.3 Spatio-Temporal variation of Future Rainfall

The Jayakwadi catchment is covered by 47 grids of CORDEX as shown in Figure (***). The daily rainfall data for these grids were downloaded from cordex website ([Centre for Climate Change Research \(tropmet.res.in\)](http://www.ccr.ac.cn/eng/center.htm)). The data was downloaded for each of these grids for a period of 2006 to 2099 along with the historical data. However, for the future analysis, the data from 2025 to 2099 was used. The results and plots obtained through the analysis has been presented below.

5.3.1 Comparison of observed rainfall with IMD and GCM Models

Before using the GCM data, normally one has to validate the rainfall/temperature (historical) values with the overlapping observed point data. This is done either using the procedure such as Bias correction. However, many researchers (*****REF*****) have proposed to use the graphical method also. In this study, we have adopted the Graphical method for verifying GCM historical values with that of observed point rainfall values and the IMD grid rainfall values. The comparison was done using the CORDEX grid values with point rainfall value (station falling within the grid). Similarly, the CORDEX grid value and the IMD grid value were compared. If there are many raingauge station with a grid, only one plot is shown here and for other stations, the plots are shown in ANNEXURE-I. The plots (graphs) plotted are shown below for each.



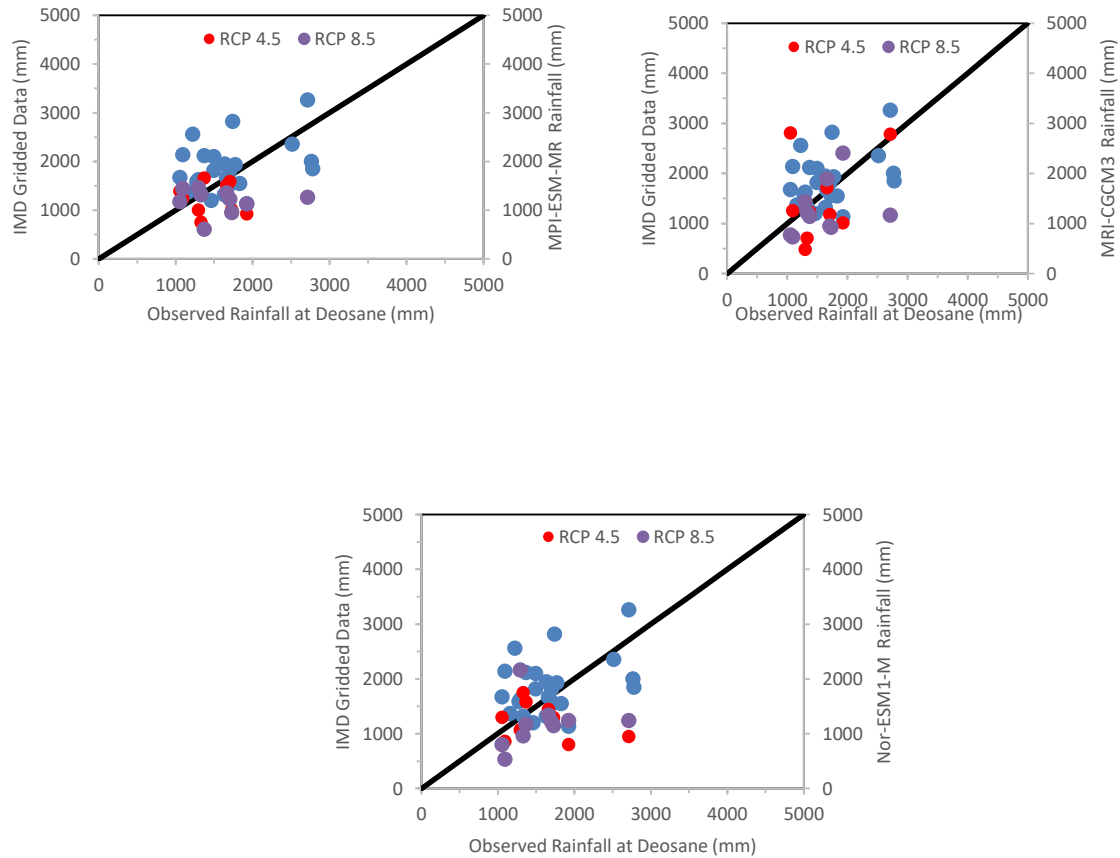


Figure ***. Comparison of Grid Rainfall values of IMD, GCM model with Deosane (Grid-1) Rainfall.

5.3.2 Grid-wise variation of GCM Rainfall

To understand the spatio-temporal variation of the rainfall under selected 9 climate models, the data has been divided into 3 groups, viz., first group is from 2025 to 2050; second group is from 2051-2080; and the third group is from 2081-2099 representing the early century, mid century and end century scenarios. The analysis was carried out using the data of these period. The results are presented below.

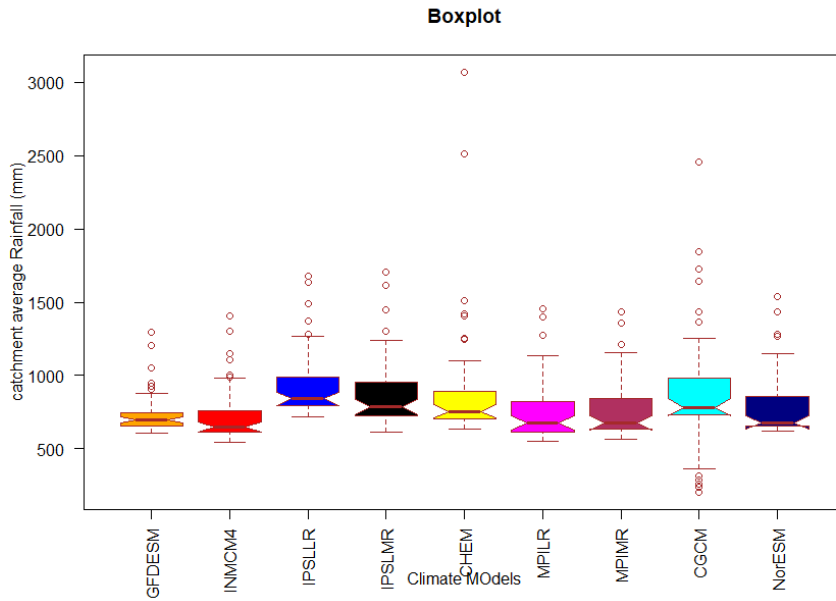


Figure ***: Box plots showing the variation of rainfall across all the grids for each of climate model considered for analysis under RCP 4.5 scenarios during the period 2025 to 2050.

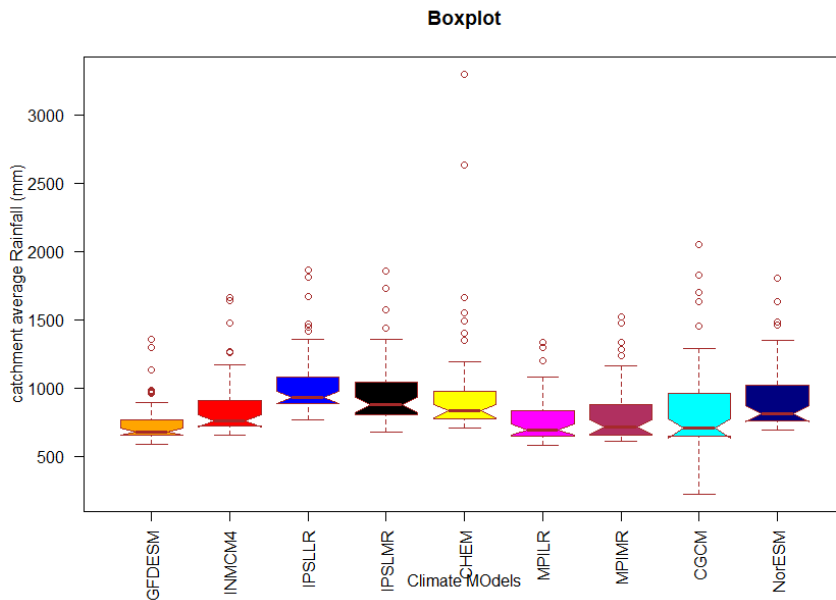


Figure ***: Box plots showing the variation of rainfall across all the grids for each of climate model considered for analysis under RCP 4.5 scenarios during the period 2051 to 2080.

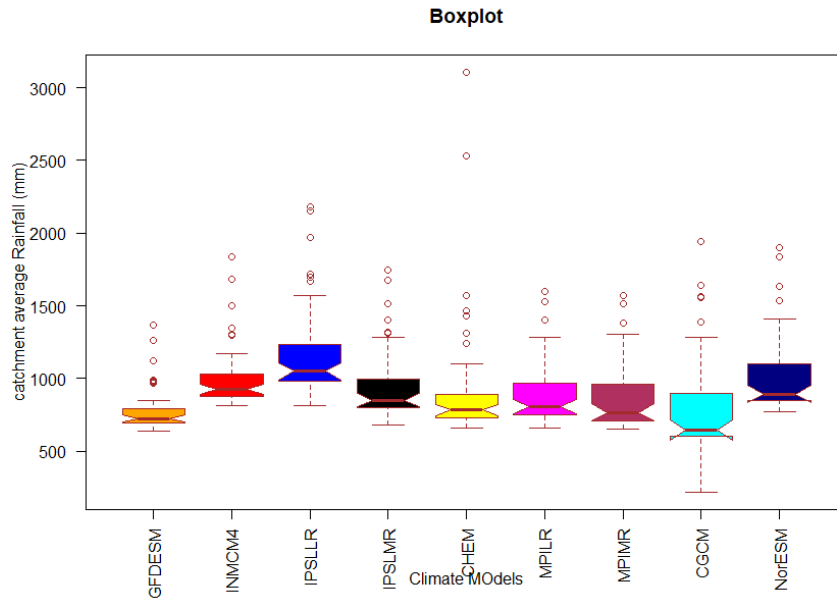


Figure ***: Box plots showing the variation of rainfall across all the grids for each of climate model considered for analysis under RCP 4.5 scenarios during the period 2081 to 2099.

It is observed from these figures that, the highest rainfall is observed in MICRO-ESM-CHEM model and lowest in MPI-CGCM3 model across 3 time groups. The lowest median values is observed by INMCM4 during the 2025-50, GFDL-ESM2M model during 2051-2080 and MPI-CGCM3 model during 2081-2099. Whereas the highest median value is observed in IPSL-ESM-LR model. In order to see how the rainfall predicted by the GCM models is varying across all the grids, a heat map is developed for the period under consideration and presented in Figure ***, Figure ***, and Figure **. It is observed from these plots that, the MPI-CGCM3 has predicted very low rainfall values, i.e., less than 500 mm for the grids 42 to 47. Whereas other models have predicted greater than 500 mm for the same grids in the catchment. Further it is noticed that, the predicted highest rainfall amount are the grid 16 and grid 17 by all the models considered for analysis for all the 3 groups.

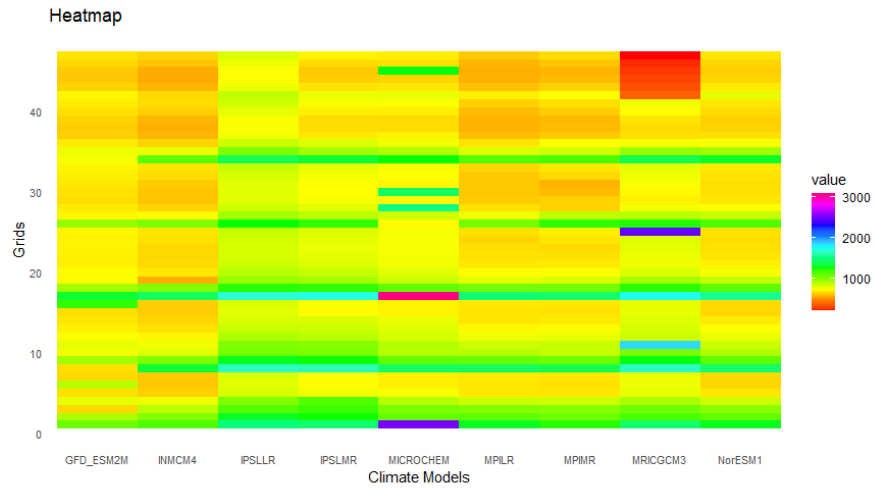


Figure ***: plot showing the grid-wise variation of rainfall for each of climate model considered for analysis under RCP 4.5 scenarios during the period 2025 to 2050.

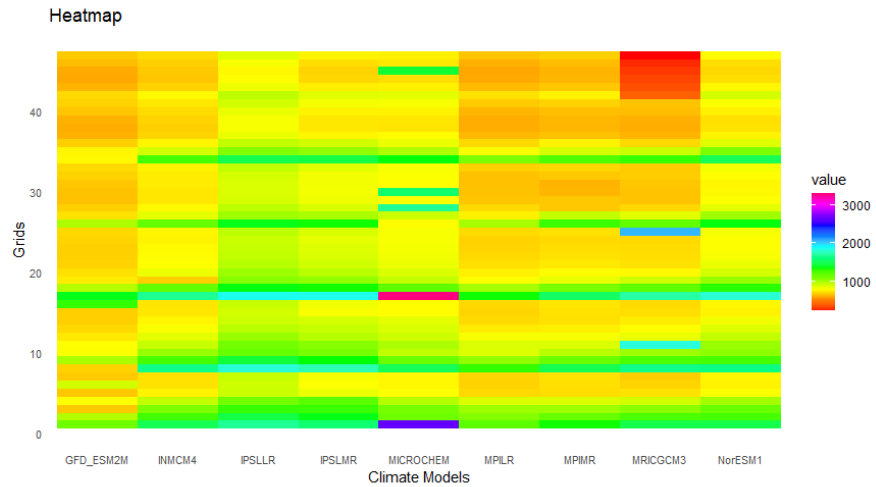


Figure ***: plot showing the grid-wise variation of rainfall for each of climate model considered for analysis under RCP 4.5 scenarios during the period 2051 to 2080.

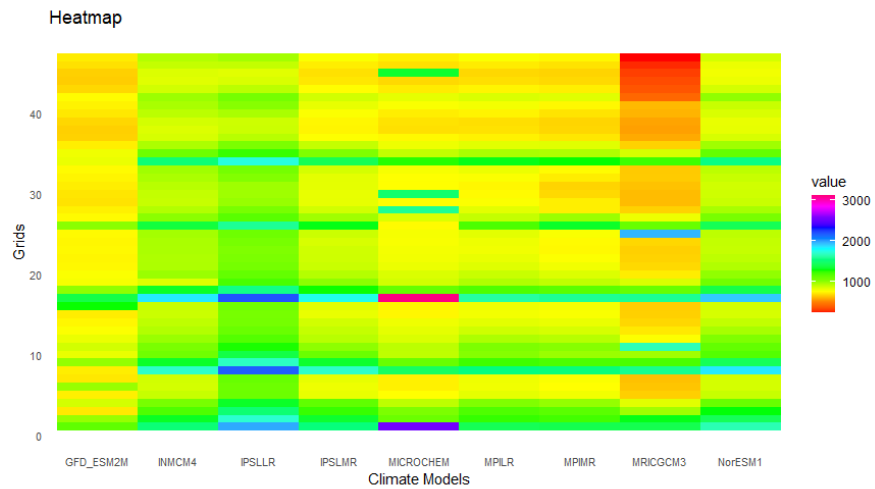


Figure ***: plot showing the grid-wise variation of rainfall for each of climate model considered for analysis under RCP 4.5 scenarios during the period 2081 to 2099.

Analysis carried out for RCP 8.5 reveals that, the maximum and minimum rainfall values were predicted by MPI-CGCM3 model in all the 3 time groups. The minimum medial value is observed in GFDL-ESM2M.

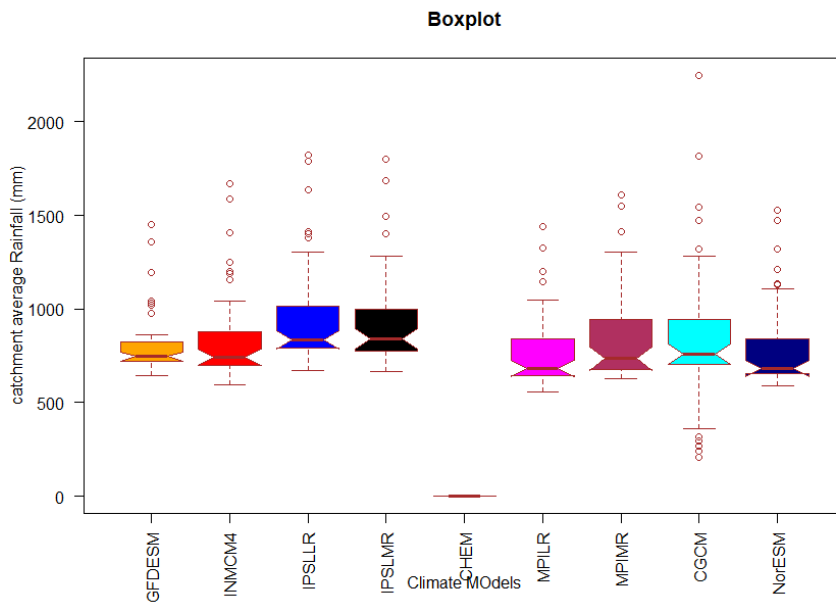


Figure ***: Box plots showing the variation of rainfall across all the grids for each of climate model considered for analysis under RCP 8.5 scenarios during the period 2025 to 2050.

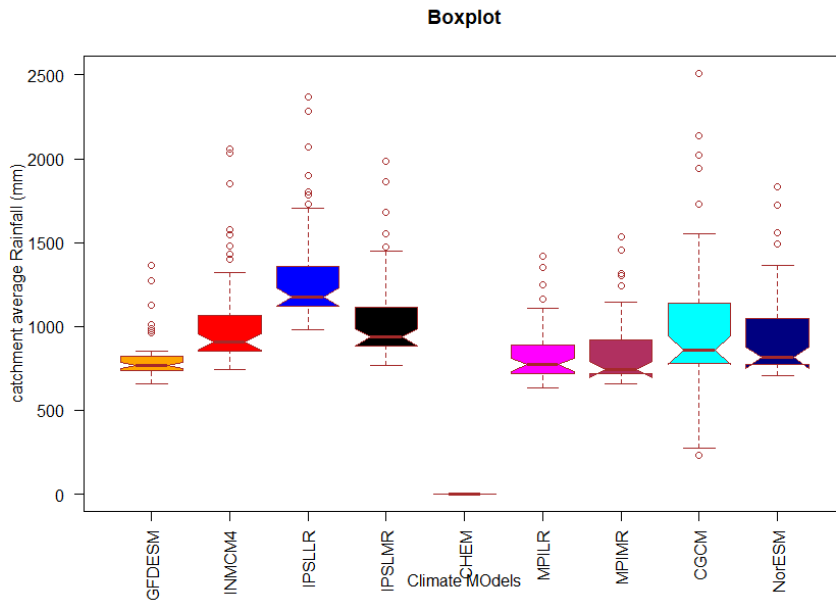


Figure ***: Box plots showing the variation of rainfall across all the grids for each of climate model considered for analysis under RCP 8.5 scenarios during the period 2051 to 2080.

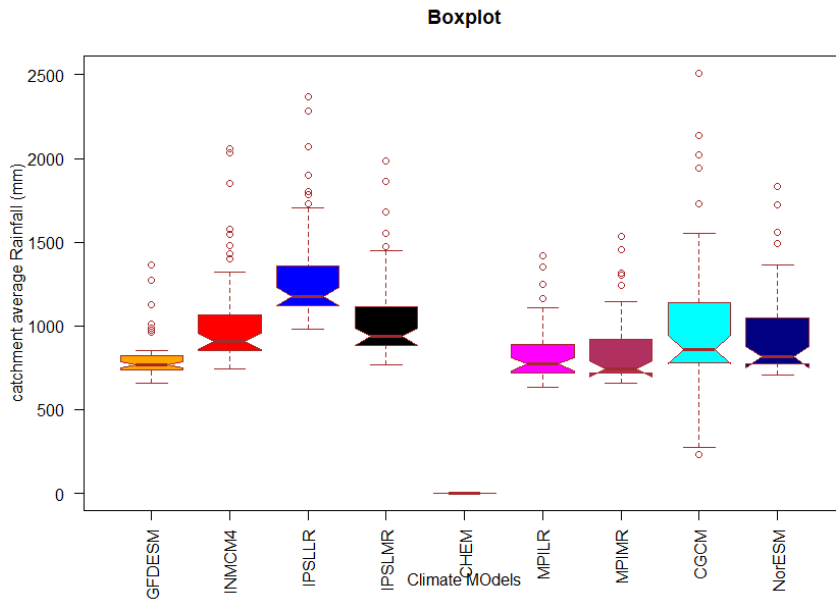


Figure ***: Box plots showing the variation of rainfall across all the grids for each of climate model considered for analysis under RCP 8.5 scenarios during the period 2081 to 2099.

The grid-wise variation under RCP 8.5 is more prevalent and is seen that, all most all models have predicted the higher rainfall totals (annual) for grid no 16, 17, 26 and 34, and the minimum by the MPI-CGCM3 models for grids 42 to 47.

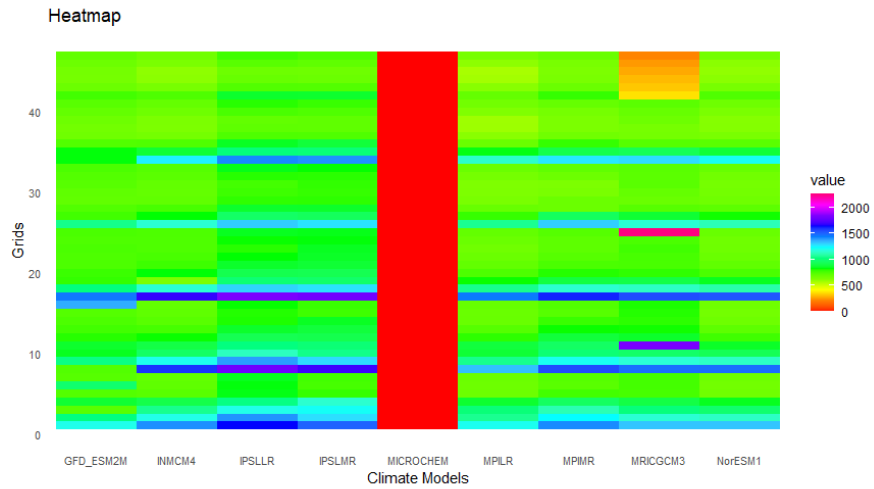


Figure ***: plot showing the grid-wise variation of rainfall for each of climate model considered for analysis under RCP 4.5 scenarios during the period 2025 to 2050.

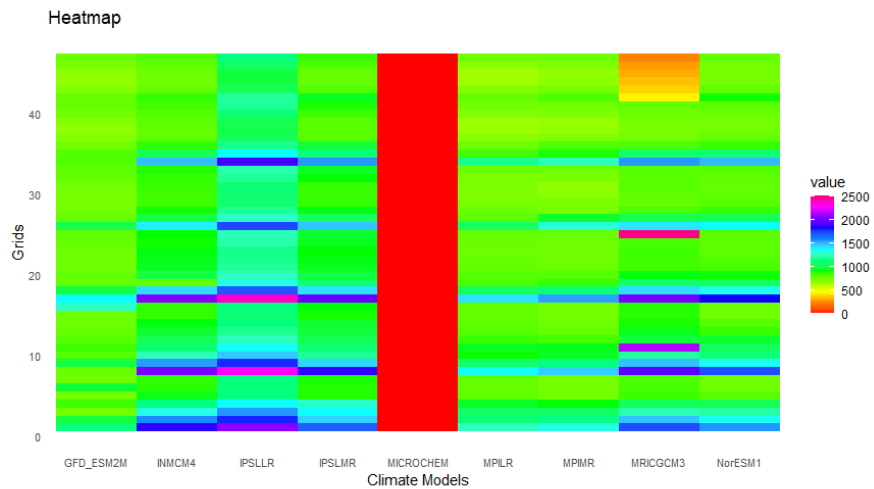


Figure ***: plot showing the grid-wise variation of rainfall for each of climate model considered for analysis under RCP 4.5 scenarios during the period 2051 to 2080.

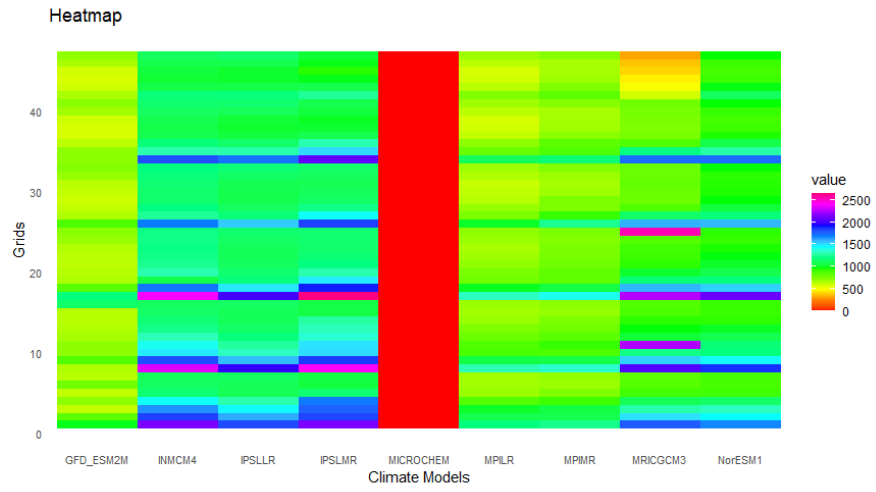


Figure ***: plot showing the grid-wise variation of rainfall for each of climate model considered for analysis under RCP 8.5 scenarios during the period 2081 to 2099.

5.3.3

6.0. APPLICATION OF SWAT MODEL TO ESTIMATE THE YIELD

While interacting with the official of WRD Nashik, it is informed that, it is decided to estimate the water yield in the basin in three division as shown in Figure 12. Keeping this in view, it is decided to use this configuration. The description of the SWAT model along with the application of model in the following section.

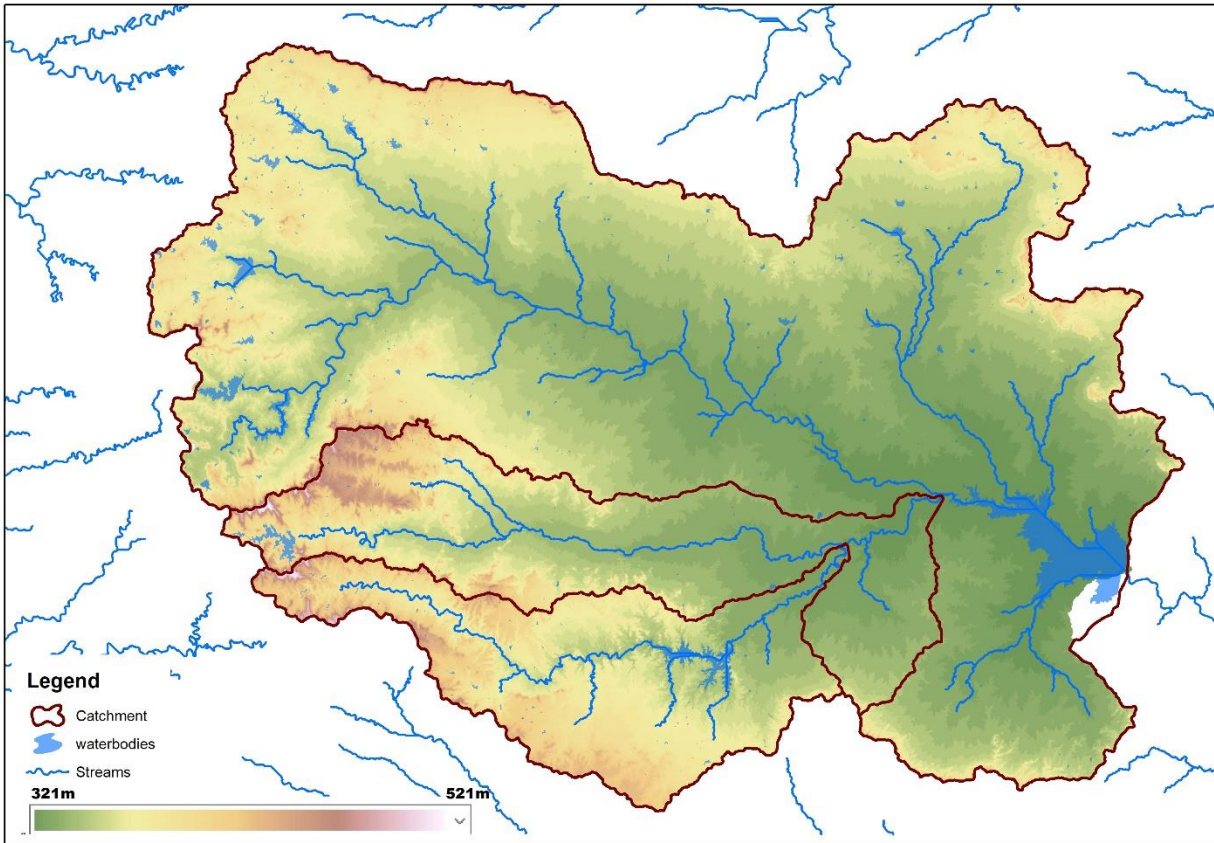


Figure 12: The Jayakwadi Catchment with proposed sub-basin for analysis

6.1 Description of SWAT Model

The SWAT model is a watershed scale continuous-time model with a daily time step. SWAT is capable of simulating long-term yields for determining the effect of land-management practices (Arnold and Allen, 1999). There are many components of SWAT including hydrology, weather, soil temperature, crop growth, nutrients, pesticides, sediment yield, and agricultural management practices (Chanasyk and others 2003). The hydrological components of SWAT are based on the water balance equation applied to water movement through soil;

$$SW_t = SW_o + \sum_{i=1}^t (R_{day} - Q_{surf} - E_a - w_{seep} - Q_{gw})$$

- SW_i = Soil water content at time t;
 SW_o = Initial soil water content;
 t = time (in days)
 R_{day} = amount of precipitation on day i
 Q_{surf} = amount of surface runoff on day i
 E_o = amount of evapotranspiration on day i
 W_{seep} = water percolation to the bottom of the soil profile on day i
 Q_{gw} = amount of water returning to eh groundwater on day i.

This equation takes into account several different processes- precipitation, surface runoff, ET, recharge and soil water storage. The Soil conservation Service (SCS) curve number (CN) equation is used to estimate surface runoff. This method was developed from many years of streamflow records from agricultural watersheds in many part of United States. CN is a function of soil group, land cover complex and antecedent moisture conditions. The curve number method was adopted in the SWAT model because it (i) is used widely through out the world; (ii) has been tested on watersheds of varying sizes, and (iii) required only easily available input data. The SCS curve number method uses two equations for runoff. The first relates runoff to rainfall and retention parameter as;

$$Q = \frac{(R-0.2S)^2}{R+0.8S}, R > 0.2 S$$

Where,

- Q = daily surface runoff (in mm);
 R = daily rainfall (in mm);
 S = retention parameter, the maximum potential difference between rainfall and runoff (in mm) starting at the time the storm begins.

The second equation relates retention parameter to curve number as;

$$S = 25.4 \left(\frac{1000}{CN} - 10 \right)$$

Where

CN = curve number ranging from $0 \leq CN \leq 100$

A complete description of the SCS curve number method is explained by Neitsch and others (2005). The SCS curve number is a measure of the infiltration characteristics of a soil. In general, soils are divided into four major classes of infiltration and runoff characteristics

1. Low runoff potential and high infiltration rate even when thoroughly wetter. These soils mainly consist of excessively drained sand and gravel. These soils have a high water transmission rate.
2. Moderately infiltration rate when thoroughly wetted. These soils mainly consist of well-drained find-to-moderately fine textures. They have a moderate water transmission rate.

3. These soils have a slow infiltration rate when thoroughly wetted. These soils mainly have a layer that impedes downward movement of water and have a slow water transmission rate.
4. These soils have a high runoff potential and very slow to no infiltration when thoroughly wetted. They mainly consist of clay soils that have high swelling potential, soils that have a permanent water table, and soils that have a clay-pan or a clay layer near the surface. These soils have a very slow water transmission rate.

The curve number also depends on the antecedent soil moisture condition. The SCS defines three antecedent soil moisture conditions: I- dry (wilting point), II- average moist, and III-wet. The moisture condition I curve number is the lowest value the daily curve number can be in dry conditions. The standard values of curve number show in SCS table for various soils and land cover conditions are based on the antecedent soil moisture condition II. The standard values for curve number can be adjusted for drier or wetter antecedent conditions using the following equations;

$$CN_1 = CN_2 - \frac{20X(100 - CN_2)}{(100 - CN_2 + \exp[2.533 - 0.0636(100 - CN_2)])}$$

$$CN_3 = CN_2 \exp[0.00673(100 - CN_2)]$$

Where

CN ₁	= moisture conditions I curve number,
CN ₂	=moisture conditions II curve number,
CN ₃	=moisture condition III curve number

SWAT allows the user to select between two methods for calculating the retention parameter. The traditional method is to allow the retention parameter to vary with soil profile water content. An alternative method added in SWAT 2005 allows the retention parameter to vary with accumulated plant ET. The alternative method was added because use of the traditional method base on soil moisture often resulted in over prediction of runoff in shallow soils. By calculating daily CN as a function of plant ET, the value is less dependent on soil storage and more dependent on antecedent climate. The daily retention parameter as a function of plant ET can be calculated with this equation

$$S = S_{prev} + E_o * \exp\left(\frac{-cncoef - S_{prev}}{S_{max}}\right) - R_{day} - Q_{surf}$$

Where

S	= retention parameter for a given day (in mm)
S _{prev}	= retention parameter for the previous day (in mm)
E _o	= potential evapotranspiration for the day (mm/day)
cncoef	= weighting coefficient used to calculate the retention coefficient for daily curve number calculations dependent on plant ET;
S _{max}	= maximum value the retention parameter can achieve on any given day (mm)
R _{day}	= rainfall depth for the day (mm)

Q_{surf} = surface runoff (mm)

The initial value of the retention parameters is defined as

$$S = 0.9 S_{\text{max}}$$

The daily curve number value adjusted for moisture content is calculated by the following equation

$$CN = \frac{25400}{(S + 254)}$$

Where, CN = curve number on a given day
 S = retention parameter calculated for the moisture content of the soil on that day

SWAT uses typical curve number for various soils with moisture condition II, and a set of slope of 5 percent. These data were obtained from the SCS engineering Division 1986 document. To adjust the curve number to different slopes, William (1995) came up with the following equation

$$CN_{2S} = \frac{(CN_3 - CN_2)}{3} [1 - 2 \exp(-13.86 slp)] + CN_2$$

Where, CN_{2s} = moisture condition II curve number adjusted for the slope
 CN_3 = moisture condition III curve number for default 5 percent slope
 CN_2 = moisture condition II curve number for default 5 percent slope
 slp = average percent slope of the sub-watershed

Model Data Structure and Input

SWAT is a comprehensive model that requires a diversity of information. The first step in setting up a SWAT watershed simulation is to partition the watershed into subunits. SWAT allows several different subunits to be defined within a watershed. The first level of subdivision is the sub-watersheds. Sub-watersheds possess a geographic position in the watershed and are related to one another spatially. For example, outflow from upstream sub-watershed may enter downstream sub-watershed. The sub-watershed delineation is defined by surface topography so that the entire area within a sub-watershed flows to the sub-watershed outlet. The land area in a sub-watershed may be divided into HRUs. These portions of a sub-watershed possess unique land use/management/soil attributes. The number of HRUs in a sub-watershed is determined by the threshold value for land use and soil delineation in a sub-watershed. The delineation of HRUs within the sub-watershed is determined using ARCSWAT built-in-tools. The use of HRUs generally simplifies a simulation run because all similar soil and land use areas are lumped into a single response unit. The user can define the amount of lumping depending on the details required for a particular study.

The water balance of each HRU in SWAT is represented by four storage volumes; precipitation, soil profile (0-6.5 ft), shallow aquifer (typically 6.5 to 65 ft) and deep aquifer (>65ft). Flows, sediment yield and nonpoint source loading from each HRU in a sub-watershed area summed, and the resulting flow and loads are routed through channels, ponds and (or) reservoirs to the watershed outlets. The soil profile is sub-divided into multiple layers that may have differing soil-water processes including infiltration, evaporation, plant uptake, lateral flow and percolation to lower layers. The soil percolation component of SWAT uses a storage routing technique to predict flow through each soil layer in the root zone. Downward flow occurs when field capacity (the water content to which a saturated soil drains under gravity) of a soil layer is exceeded and the layer below is not saturated. Percolation from the bottom of the soil profile recharges the shallow aquifer. When the temperature in a particular layer is equal to or below 48° F, no percolation is allowed from that layer. Lateral subsurface flow in the soil profile is calculated simultaneously with percolation. Groundwater flow contribution to total streamflow is simulated by routing a shallow aquifer storage component to the stream.

Input data for SWAT can be defined at different levels of details-Watershed, Sub-watershed, or HRU, watershed level inputs are used to model processes throughout the watershed. For example, for a watershed-level simulation, the method selected to model potential ET will be used in all HRUs in the watershed. There are three main watershed level input files:

1. Watershed configuration file (fig.fig): the watershed configuration file contains information used by SWAT to simulate processes occurring within the HRU/sub-watershed and to route the streamflow and constituent loads through the channel network of the watershed.
2. The master watershed file (File,cio): The master watershed file contains information related to modeling options, climate inputs, databases, and output specification. Information in this file includes number of calendar years simulated, beginning year of simulation, the beginning and ending Julian day of simulation, and weather and rain station information. This file also contains links to files needed for the watershed definition and delineation, as well as links to the files holding the precipitation and temperature information needed for the simulation
3. The basin input file (basin.bsn): General watershed attributes are defined in the basin input file. These attributes control a diversity of physical processes at the watershed level. The attributes initially are automatically set to 'default' values. Examples of attributes in the basin.bsn file are specification of the method used for estimating ET, initial soil water storage, and surface runoff lag time, and other parameters used in the SWAT simulation on the watershed scale. Users can use the default values or change them to better reflect conditions in a specific watershed.

Sub-watershed or HRU-level input files are used to identify unique processes to specific sub-watersheds or HRUs. There are many different types of sub-watersheds and HRU-scale data files used in the SWAT watershed simulation. A set of these sub-watershed and HRU-scale data files

er assigned to each sub-watershed and HRU in the watershed. Some of the more commonly used sub-watershed or HRU-level data files are;

1. The sub-watershed general input file(*.sub) contains information related to a diversity of features within the sub-watershed to which it is assigned. Data in the (*.sub) file can be grouped into the following categories: sub-watershed size and location; specification of climatic data used within the sub-watershed; the amount of topographic relief within the sub-watershed and its effect on the climate; properties of tributary channels within the sub-watershed; variables related to climate change; the number of HRUs in the sub-watershed; and the names of HRU input files.
2. The HRU general input file (*.hru) contains information related to features within a HRU. Data contained in the HRU input file can be grouped into the following categories: topographic characteristics, water flow, erosion, land cover, and depression storage areas.
3. The HRU management file(*.mgt) contains information related to land and water management practices taking place within the system. This file also contains input data for planting, harvest, irrigation applications, fertilizer application, pesticide applications and tillage operation
4. The soil input file (*.sol) defines the physical properties of the soils in the watershed. These properties govern the movement of water and air through the profile and have a major effect on the cycling of water within the HRU.

SWAT MODEL PARAMETES

The conceptual rainfall-runoff models are developed to simulate the catchment behavior. Number of mathematic equations is used to describe the hydrological processes occurring on the surface of the catchment. Some of the hydrological processes can be represented by the results obtained through conducting experiments and some are approximated by representing it as a model parameter. Such parameters can be obtained through matching the known variables while modeling the time series. The SWAT model also has number of parameters which are to be obtained through the calibration of the model with the measured rainfall and runoff. In the present section, the number of parameters used describes the runoff processes and their influence on the processes is described.

Table : Description of SWAT Input parameters used for calibration.

Sl No	Parameter Name	Description	Unit	Input file name	How the parameter is stored in input file
1	CN	Curve Number		*.mgt	The existing parameter value is multiplied by (1+ a given value)

2	SOL_AWC	Soil Available Water Storage Capacity		*.sol	The existing parameter value is multiplied by (1+ a given value)
3	Sol_K	Soil Hydraulic Conductivity	mm/hr	*.sol	The existing parameter value is multiplied by (1+ a given value)
4	ALPHA_B F	Baseflow Alpha Factor		*.gw	Default parameter is replaced by a given values
5	GW_DELAY	Groundwater delay time	days	*.gw	Default parameter is replaced by a given values
6	REVAPM N	Threshold water in shallow aquifer	mmH ₂ O	*.gw	Default parameter is replaced by a given values
7	GW_REVAP	Revap Coefficient	mmH ₂ O	*.gw	Default parameter is replaced by a given values
8	SHALLST	Initial Depth of water in the Shallow Aquifer		*.gw	Default parameter is replaced by a given values
9	RCHRG_DP	Deep aquifer percolation factor		*.gw	Default parameter is replaced by a given values
10	EPCO	Plant uptake compensation factor		*.hur	Default parameter is replaced by a given values
11	ESCO	Soil evaporation compensation factor		*.hur	Default parameter is replaced by a given values
12	SURLAG	Surface runoff lag coefficient	hrs	*.bsn	Default parameter is replaced by a given values
13	SLSUBBS N	Average Slope length	m	*.hru	Default parameter is replaced by a given values
14	SOL_Z	Maximum rooting depth	mm	*.sol	Default parameter is replaced by a given values

CN : Curve Number as defined by the SCS.

SOL_AWC : Available Water Storage Capacity

SOL_K : represents saturated soil hydraulic conductivity of the top soil layer. This values are used in separating the amount of water entering the soil and that does not infiltrate and flow as

direct runoff. Higher the value of SOL_K means more water is entering into the soil and lower values implies that the soils are not permeable.

ALPHA_BF : is the baseflow recession constant.

GW_DELAY : is the delay time or drainage time of the overlaying geologic formation (days). It is used to define the travel time from soil layer to the shallow aquifer. Higher the value of GW_DELAY represent the slower movement of water from soil layer to the aquifer and lower values represent the otherwise.

REVAPMN: represents the amount of water transferring from the shallow aquifer to the unsaturated zone to meet the demand of evapotranspiration. This is significant where the saturated zone is not far below and the deep rooted plants are grown. REVAP is allowed only if the water stored in the shallow aquifer is more than the threshold value. This threshold value is REVAPMN.

GW_REVAP: represents the portion of water which is entering into soil zone from shallow aquifer in response to the deficiencies. This is influenced by the type of soil, plants grown over the sub-watershed.

RECHRG_DP: this represents the amount of water leaving the deepest soil layer to the aquifer. Higher the value, gives more recharge and visa-versa.

ESCO : This parameter represents the amount of water extracted from the soil to meet the evaporation demand. As SWAT model meets the evaporative demand from different soil layer (top 10 mm as 1st layer and next 100 mm as the next layer and so on). The parameter ESCO allows the user to modify the layer so as to meet the evaporation demand. Lower the value of ESCO, higher the extraction of water from lower layer so is the evaporation.

EPCO : If upper layer of the soil do not have the enough soil moisture to meet the demand of the evaporation, then the model is made draw water from the lower layers. In order to activate this phenomena, the EPCO parameter is used. If the EPCO value is higher (maximum value is 1), then the model allows more of the demand is met from the lower layer. If the value is close to 0.0, then model allow lower depth variation (the demand is met from the upper layer only).

SURLAG: this parameter represent the amount of surface runoff released to the main channel. Any decrease in the value of SURLAG, it hold more water in store, and increase the delay in release of surface water . This will smoothen the stream flow hydrograph simulated in the reach/stream

SOL_Z : represents the depth the root of the plant/crop grown within the soil depth. Higher the density, more will be the evaporation and vice versa. If no value is specified, then it assumes the depth of the soil as the root depth

6.2. Development of SWAT Model for Jayakwadi Catchment

The DEM of 30 m resolution was used to delineate the catchment upto Jayakwadi with two other catchment outlet as proposed by the WRD officials. The Landuse data of IWMI of 2016 with 450

m resolution was used. The soil map of 1000m resolution from NBSSLUP was used for the study. Using these information, 861 sub-basin and 861 HRU's are created for the entire basin.

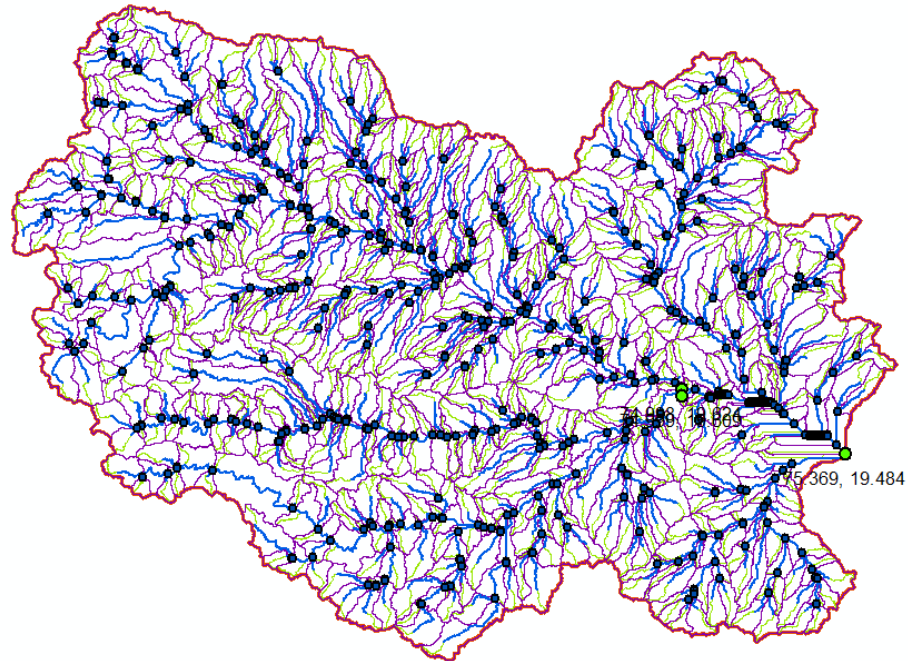


Figure 16: The Jayakwadi catchment and it sub-catchment as conceived in the SWAT model

As per the Recommendation of the department, the SWAT model has been set-up dividing the entire catchment in 3 portions. The model set-up under the SWAT environment is as shown below

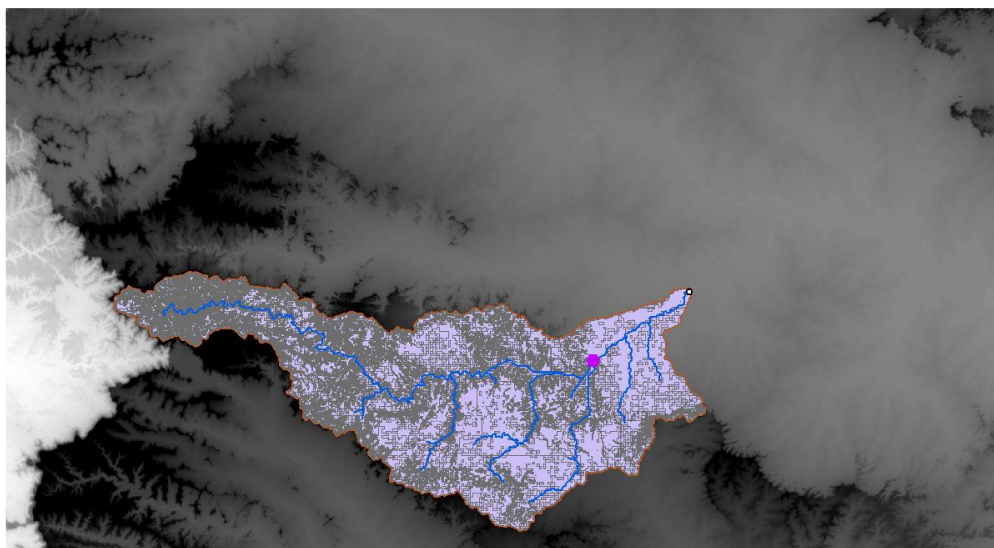


Figure 17. The catchment upto Mula Dam in the Jayakwadi Catchment is considered as one-sub basin.

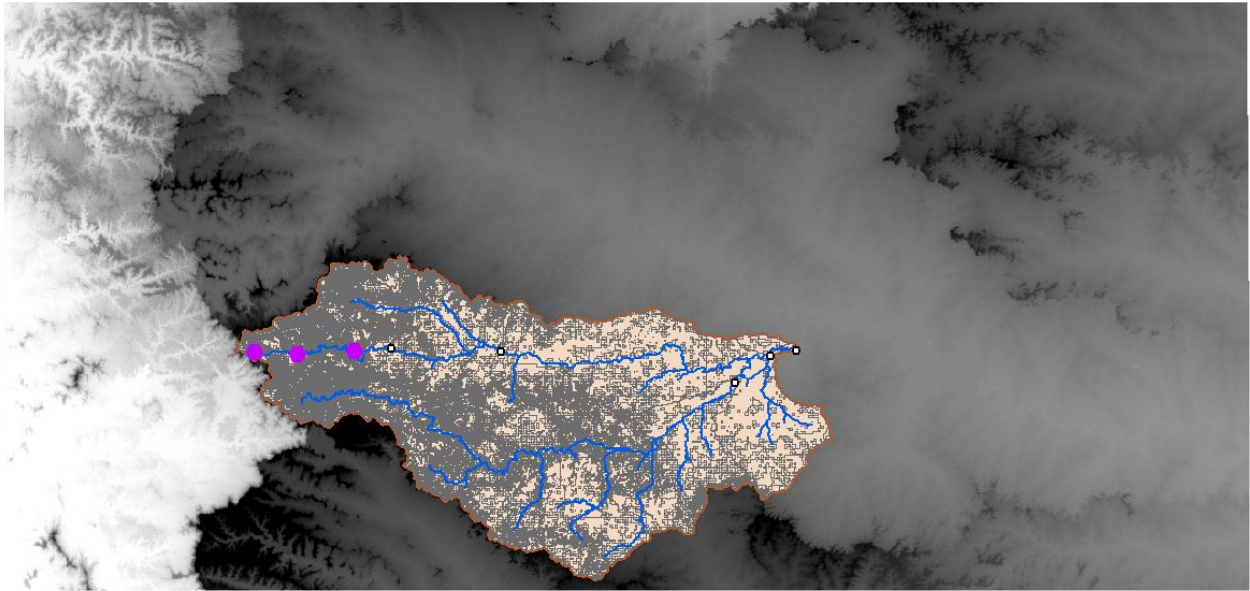


Figure 18. The catchment upto Newasa stream gauge station including Ghatagar, Bhandardara and Nilwande Dam in the Jayakwadi Catchment is considered as separate sub basin.

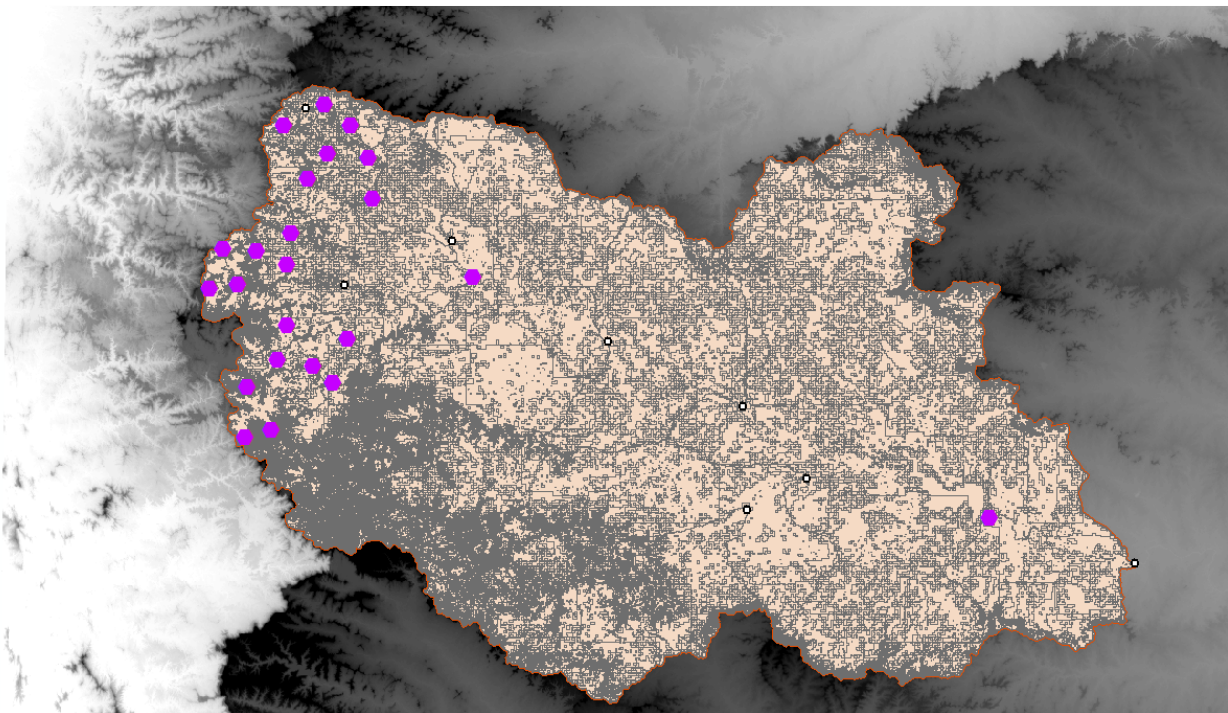


Figure 19. The catchment upto Jayawadi dam including all the upstream dams excluding the dams in the other two sub-basin are considered as separate sub basin.

6.3 Analysis of Mula Catchment

The Mula Reservoir of Upper Godavari Basin in India (Figure ***). It is located at Latitude of 19°21'30'' and Longitude of 74°34'30'', and is 8.04 km upstream of Rahuri, Ahmednagar District, Maharashtra State, India. The project was completed in 1972 on the Mula river, which later meets the Pravara, a major tributary of the Godavari. The catchment area of the project is about 2275 km². It receives an average rainfall of 5080 mm in the hilly region and 508 mm in the Lower Catchment. The gross storage capacity of the reservoir is 788.08 MCM at MWL with live storage of 660.40 MCM. The purposes served by this reservoir are irrigation, domestic, and industrial supply. The total area irrigated under this project is 82,920 ha.

The reservoir data such as elevation-area-capacity, daily water levels, storages, inflow and all the outflows are collected from the Division office at Dam site for the analysis. The Elevation-Area and Elevation-Capacity curve are shown in Figure (****). The mean inflows and outflow measured at dam are shown in Figure***.